

**A Novel System for Monitoring *in vivo* Cell  
Signaling Pathways Involved in Early  
Embryonic Patterning**

Louise Rooney  
2016

Submitted in partial fulfillment of the requirements for the degree of  
Masters of Science in Cell and Molecular Bioscience

*Supervisor: Peter Pfeffer*

Early developmental events, such as the arrangement of the head-tail axis, are fundamentally driven by cell signalling cascades. Such incidents are regulated in a highly complex manner by promoters and inhibitors at many levels of the cascade. This complexity makes it difficult to understand where and when certain signalling occurs, and what effects additional factors have on the signalling system. Nodal signalling, executed by intracellular Smad2/3 signal propagation, is thought to induce the anterior-posterior and head-tail patterning of the early mouse embryo. Target gene outputs of this signalling are fine-tuned by a vast array of modulators; TGB $\beta$  co-receptors, extracellular ligand and receptor inhibitors, DNA binding cofactors, and intracellular enhancers and inhibitors. The endogenous target genes of this system cannot be used as a measure of signalling as they themselves feedback on the original system and others, creating diverse signals. In this body of work, we have distilled the Nodal signalling cascade to a single variable by creating a fluorescent genetic reporter to semi-quantitatively measure Smad signalling during early embryonic development. Reporter constructs contain Smad binding elements, a minimal promoter and fluorescent protein elements. Various sensitivity Smad binding elements were created to respond to different thresholds of signalling. Fluorescent microscopy and flow cytometry were used to verify responsiveness of reporter constructs, tested first in a mouse embryonic fibroblast line and subsequently in transgenic embryos. This study will provide an understanding of how extracellular cues dictate gene expression during early embryonic formation. The knowledge acquired from this work may have implications in dairy cattle and human fertility.



# Contents

Contents .....	4
Table of Figures .....	8
1 Introduction.....	11
1.1 TGF $\beta$ Signalling.....	12
1.1.1 TGF $\beta$ Co-receptors .....	14
1.1.2 Convertase action on Nodal.....	15
1.1.3 Extracellular Inhibitors of Nodal/Activin Signalling.....	15
1.2 Smad Proteins.....	17
1.2.1 Smad molecular composition.....	17
1.2.2 Smad-Receptor Interactions.....	18
1.2.3 Smad-Transcriptional Mediator Interactions.....	20
1.2.4 Smad Inhibitors .....	22
1.2.5 Accessory Proteins in Smad Signaling.....	22
1.3 Early murine embryogenesis .....	23
1.3.1 Nodal signalling in early mouse embryo development .....	27
1.4 Research Question.....	29
2 Methods.....	31
2.1 DNA cloning.....	32
2.1.1 SBE adapter/insert and vector design.....	32
2.1.2 SBE4x adapter preparation.....	34
2.1.3 SBE4x adapter annealing .....	35
2.1.4 Generation of SBE16x-HSP-GFP .....	35

2.1.4 Generation of Tomato element .....	35
2.1.5 Vector restriction.....	36
2.1.6 Vector Dephosphorylation.....	38
2.1.7 Ligation.....	38
2.1.8 Agarose gel .....	38
2.1.9 Agarose gel slice digestion .....	39
2.1.10 Transformation.....	39
2.1.11 Miniprep protocol.....	40
2.1.12 Midiprep protocol.....	40
2.1.13 Glycerol stock preparation .....	41
2.1.14 PCR protocol.....	41
2.2 NIH 3T3 transcriptome analysis .....	42
2.3 Cell culture .....	43
2.3.1 NIH 3T3 Cell Culture .....	43
2.3.2 Thawing of cells.....	43
2.3.3 Passaging of Cells.....	44
2.3.4 Freezing of cells.....	44
2.3.5 Transfection of NIH 3T3 cells with Lipofectamine 2000 and 3000.....	44
2.4 Fluorescent Microscopy.....	45
2.5 Flow cytometry.....	45
2.6 Creation of transgenic mouse line containing SBE16x-SCP-GFP construct .....	48
2.6.1 Genotyping mice .....	49
2.6.2 Production and analysis of transgenic mice .....	50
3 Results .....	51

3.1 Design strategy of a Nodal/Activin signaling reporter.....	52
3.2 Construct generation .....	52
3.2.1 Generation of vectors containing various Smad binding affinity sites driving GFP translation.....	52
3.2.2 Generation of SBE16x-HSP-GFP vector.....	57
3.2.3 Generation of vectors containing various Smad binding affinity sites driving TOM translation.....	57
3.3 Indication of Nodal/Activin signaling components in 3T3 cells.....	62
3.4 In vitro results .....	64
3.4.1 Response of SBE0x-, 4x- and 8x-SCP-GFP transfected NIH 3T3 cells to increasing concentrations of Activin .....	64
3.4.2 Response of SBE16x-SCP-GFP transfected NIH 3T3 cells to increasing concentrations of Activin .....	67
3.4.3 Optimisation of Activin incubation period.....	69
3.4.4 Effect of inhibitor SB431542 on fluorescent reporter system.....	70
3.4.5 Response of cells transfected with SBE16x-HSP-GFP to increasing concentrations of Activin .....	71
3.4.6 Response of various Smad sensitivity constructs driving TOM via SCP to increasing concentrations of Activin .....	73
3.4.7 Co-transfection of PmaxGFP and SBE0x-, 4x-, 8x- or 16x-SCP-TOM.....	77
3.4.8 Co-transfection of SBE8x-SCP-GFP and SBE16x-SCP-TOM .....	82
3.5 In Vivo results .....	84
4 Discussion.....	90
5 Recipes.....	96
5.1 LB Broth and LB Agar.....	97

5.1.1 LB Broth.....	97
5.1.2 LB Agar.....	97
5.2 Alkaline Lysis Solutions .....	97
5.2.1 Alkaline Lysis Solution I .....	97
5.2.2 Alkaline Lysis Solution II.....	98
5.2.3 Alkaline Lysis Solution III .....	98
5.3 Injection buffer .....	98
5.4 Proteinase K buffer .....	99
6 Supplementary material .....	100
6.1 Wizard SV Gel Clean-Up System protocol .....	101
6.2 Takara Mighty Mix Protocol-at-a-Glance.....	103
6.3 Invitrogen Max Efficiency DH5 $\alpha$ transformation protocol.....	104
6.4 Qiagen Miniprep protocol.....	107
6.4 NIH 3T3 Culture method .....	109
6.5 Lipofectamine Transfection Protocols.....	110
6.5.1 Lipofectamine 2000 Protocol.....	110
6.5.2 Lipofectamine 3000 Protocol.....	112
6.6 Supplementary embryo microscopy images .....	113
7 References .....	115

# Table of Figures

Figure 1 Heteromeric combination of TGF $\beta$ superfamily receptors.....	13
Figure 2 Schematic overview of the Nodal signalling pathway. ....	16
Figure 3 Overall structure of Smad-3 MH1 bound to a Smad binding element. ....	18
Figure 4 Schematic overview of the Smad-dependent TGF $\beta$ signalling pathway. ....	20
Figure 5 Cleavage events and generation of a morula and blastula in mice. ....	23
Figure 6 Post implantation events in the mouse embryo. ....	24
Figure 7 Extra-embryonic ectoderm patterning in AVE development. ....	25
Figure 8 Mouse embryo gastrulation.....	26
Figure 9 Nodal signalling positions the anterior-posterior axis of the embryo. ....	28
Figure 10 SBE4x binding element insert design. ....	33
Figure 11 Cloning strategy for multimerisation of SBE.....	34
Figure 12 Cloning strategy creating a tomato element.....	36
Figure 13 Parental vector, RAstat12x-SCP-GFP.....	37
Figure 14 PCR reaction mix and cycling conditions. ....	42
Figure 15 Florescence spectral graph, Detection efficiency table and florescence normalized to fluorophore intensity table.....	47
Figure 16 Cytometer Parameters. ....	48
Figure 17 Restriction strategy for preparation of vector for pronuclear injection. ....	49
Figure 18 Primer locations on SBE4x-SCP-GFP vector. ....	53
Figure 19 Sequence read SBE4x-SCP-GFP against clone chart.....	54
Figure 20 SBEnx-SCP-GFP sequencing reads aligned to reference clone charts. ....	57
Figure 21 Primer locations on SBE16x-SCP-TOM.....	58
Figure 22 Sequencing read SBE16x-SCP-TOM against clone chart showing sequencing errors. ....	58
Figure 23 SBEnx-SCP-TOM sequencing reads aligned to reference clone charts. ....	62



Figure 24 Expression profiles of Smad signaling constituents and housekeeping genes in NIH 3T3 cells.....	63
Figure 25 Gating strategy used to determine number of and fluorescent output of GFP expressing cells.....	65
Figure 26 Geometric mean of GFP <sup>+</sup> cells transfected with SBE0x-, 4x- and 8x-SCP-GFP constructs treated with increasing concentrations of Activin for 48 hours. ....	66
Figure 27 Average number of GFP <sup>+</sup> cells transfected with SBE0x-, 4x- and 8x-SCP-GFP constructs treated with increasing concentrations of Activin for 48 hours. ....	66
Figure 28 Geometric mean of GFP <sup>+</sup> cells transfected with SBE16x-SCP-GFP and incubated with increasing concentrations of Activin for 48 hours.....	68
Figure 29 Number of GFP <sup>+</sup> SBE16x-SCP-GFP transfected cells. ....	68
Figure 30 Fluorescent microscopy images of NIH 3T3 cells transfected with SBE16x-SCP-GFP and treated with 1.00, 10.00 or 100.00 ng/ml activin. ....	69
Figure 30 Experiment to determine optimal time length for Activin incubation.....	70
Figure 31 Inhibitory action of SB431542 on SBE16x-SCP-GFP Smad signaling reporter system. ....	71
Figure 32 Response of cells transfected with SBE16x-HSP-GFP to increasing concentrations of Activin treatment. ....	72
Figure 33 Gating strategy used to determine number of and fluorescent output of TOM expressing cells.....	74
Figure 34 Geometric mean of cells transfected with SBE0x- 4x- 8x- and 16x-SCP-TOM constructs which lie in TOM <sup>+</sup> gate. ....	76
Figure 35 Average number of cells in TOM <sup>+</sup> gate.....	76
Figure 37 Fluorescent microscopy images of NIH 3T3 cells transfected with SBE16x-SCP-TOM and treated with 1.00, 10.00 or 100.00 ng/ml activin. ....	77
Figure 36 Gating strategy for co-transfection of NIH 3T3 cells with both GFP and TOM containing vectors. ....	78

Figure 37 Number of TOM <sup>+</sup> cells (A) and number of TOM <sup>+</sup> cells as a percentage of GFP <sup>+</sup> TOM <sup>+</sup> cells (B) co-transfected with PmaxGFP and SBE0x-, 4x-, 8x- and 16x-SCP-TOM and treated with varying concentrations of Activin. ....	80
Figure 38 Dot plots showing response of cells co-transfected with PmaxGFP and SBE16x-SCP-TOM to increasing concentrations of Activin treatment. ....	81
Figure 39 Dot plots showing response of cells co-transfected with SBE8x-SCP-GFP and SBE16x-SCP-TOM to increasing concentrations of Activin treatment. ....	83
Figure 40 Agarose gel of pronuclear injection offspring genotyping.....	84
Figure 41 Microscopy images of embryonic day 6 embryos 1 and 2.....	86
Figure 42 Microscopy images of embryo number 10 (tg) transgenic for SBE16x-SCP-GFP at embryonic day 8.5. ....	87
Figure 43 Microscopy images of embryo number 12 (wt) at embryonic day 8.5. ....	88
Figure 44 Agarose gel image of embryo genotyping results.....	89

## 1 Introduction

## 1.1 TGF $\beta$ Signalling

The transforming growth factor- $\beta$  (TGF $\beta$ ) superfamily is a large group of regulatory proteins expressed in most cell types which are involved in embryogenesis, development, cell differentiation and immune system regulation (Herpin, Lelong, and Favrel 2004). Family members include TGF $\beta$  proteins, bone morphogenic proteins (BMPs), Activin/Nodal, glial-derived neurotrophic factors (GDNFs), and Müllerian inhibiting substance (MIS) (Burt 1992; Weiss and Attisano 2013). These groupings are determined by related function and downstream signalling. For example, BMP signalling plays critical roles in neural, heart, cartilage and postnatal bone formation (D. Chen, Zhao, and Mundy 2004) and MIS causes the regression of the Mullerian ducts in male embryogenesis (Lee and Donahoe 1993), both of which signal through Smads 1, 5 and 8. Nodal and Activin induce early embryonic axis formation and signal through Smads 2 and 3.

Due to their similar effector functions, Nodal and Activin signalling are often referred to as Nodal/Activin. This nomenclature grouping is due to the activation of the Nodal signalling pathway requiring the binding of Nodal and Activin to Activin-like receptors (A. F. Schier and Shen 2000). Nodal signalling is essential for specification of the body axis during gastrulation, and also for mesoderm signalling through a complex of TGF $\beta$  receptors and Smad2 and Smad3.

TGF $\beta$  family members, of which there are more than 60, are polypeptides which induce cellular responses during growth and differentiation. This high number of ligands is the result of the need for precise developmental patterns, achieved by distinct ligand expression regulation (Feng and Derynck 2005). TGF $\beta$  factors act through combinations of specific heteromeric receptor complexes comprising two type I and two type II transmembrane serine/threonine kinases at the cell surface. Seven type I and five type II

receptors have been identified (Feng and Derynck 2005), see Figure 1. Functional receptor complexes containing combinations of type I and II receptors allow for selectivity and diversity in both ligand binding and intracellular signalling. Indeed, many ligands may activate the same receptor, however distinct ligand expression patterns and a small number of receptor combinations allow for signalling specificity.

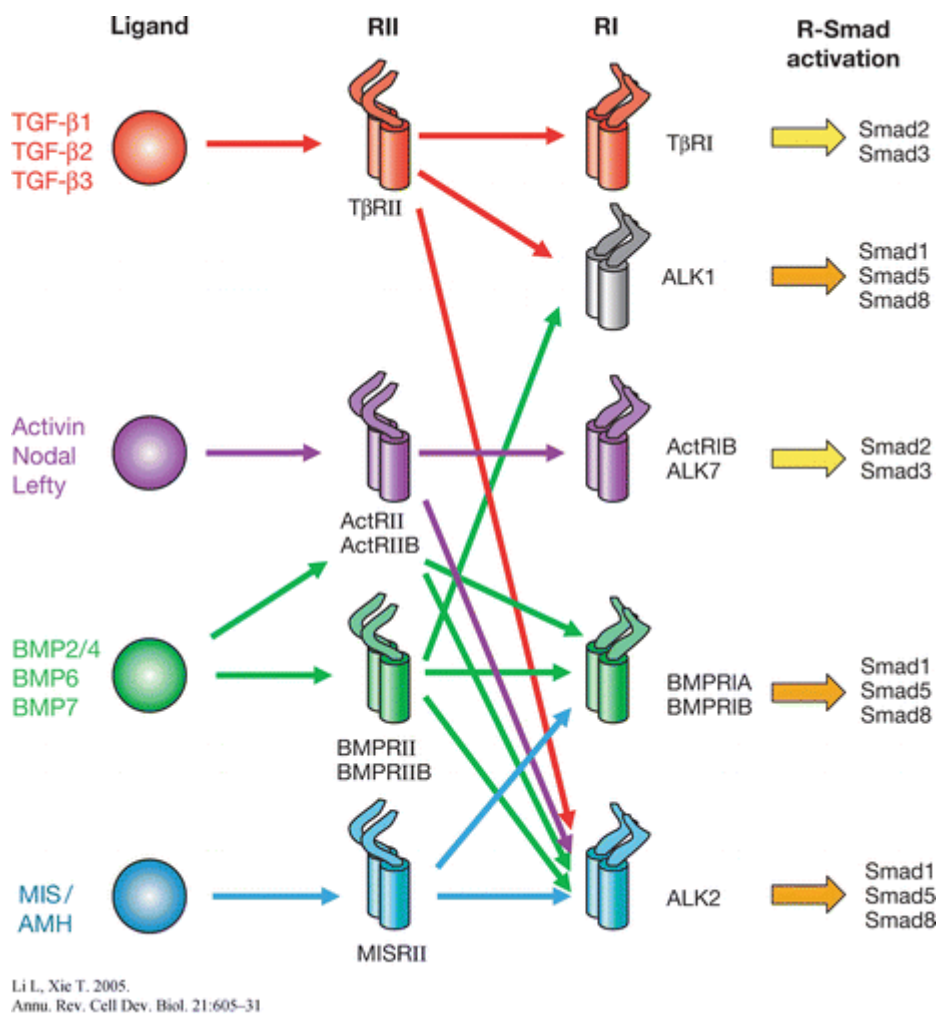


**Figure 1 Heteromeric combination of TGFβ superfamily receptors.** TGFβ ligands bind specific combinations of TGFβ receptors. For example, Nodal/Activin binds the type I receptor ActRII/ALK7 (ActRIC) and the type II receptor ActRII/ActRIIB. Image from *Specificity and versatility in TGF-β signalling* 2005 Xin-Hua Feng<sup>1</sup> and Rik Derynck *Annual Review of Cell and Developmental Biology*.

The two receptor types, I and II, are structurally similar transmembrane serine/threonine kinases. Type I receptors have a Gly/Ser-rich “GS sequence” sequence upstream of their kinase domain (Feng and Derynck 2005) which Type II receptors do not. Ligand binding induces formation of a stable, complete complex consisting of four subunits (two receptors of each type) and allows phosphorylation of the type I GS sequence by the type II receptor kinases. This phosphorylation activates the type I receptor kinase which subsequently phosphorylates R-Smad proteins intracellularly through the L45 region of the type I receptor interacting with the L3 loop of the Smad protein (Derynck and Zhang 2003a; Schmierer and Hill 2005; J. Massagué 1998).

### 1.1.1 TGF $\beta$ Co-receptors

The mouse EGF-CFC (epidermal growth factor-Cripto1/FRL1/Cryptic) co-receptor Cripto is an extracellular molecule which mediates the binding of ligands to signal-transducing receptors (Shen and Schier 2000). EGF-CFCs are tethered to the cell membrane by C-terminal glycosyl-phosphatidylinositol (GPI) linkage. Cripto interacts with the TGF $\beta$  receptors ALK4 (AcvRIB, type I receptor) and ALK7 (AcvRIC, type II receptor) via its conserved CFC motif to enable Nodal binding to the ALK/ActRIIB receptor complex (Reissmann et al. 2001; C.-Y. Yeo and Whitman 2001) and therefore enhancing signal propagation. Activin, which acts in a similar way to Nodal, does not require Cripto to bind to the TGF $\beta$  receptor (Cheng et al. 2004). Studies of Cripto mutants have shown that Cripto is necessary for primitive streak and mesoderm induction (Ding et al. 1998).

### 1.1.2 Convertase action on Nodal

Nodal mRNA translation results in generation of an immature, precursor form of Nodal (pro-Nodal) which is subsequently cleaved by the convertase proteins Furin and Pace4 forming mature Nodal (Ben-Haim et al. 2006). These convertases are expressed in the extraembryonic visceral endoderm and ectoderm and the trophectoderm, respectively, where they act on pro-Nodal to generate active Nodal protein (Beck et al. 2002).

### 1.1.3 Extracellular Inhibitors of Nodal/Activin Signalling

Lefty and Cerberus-like are the two most widely studied inhibitors of Nodal signalling. Lefty antagonises Nodal by competing with Nodal for binding to the EGF-CFC co-receptor Cripto (Cheng et al. 2004) and the type II TGF $\beta$  receptors ActRIIA and ActRIIB (Sakuma et al. 2002). Studies into loss of function of Lefty show a strong induction of the endoderm and mesoderm, which suggests an upregulation of the Nodal pathway (Agathon, Thisse, and Thisse 2001). Lefty expression is induced by Nodal and its expression pattern follows that of Nodal both spatially and temporally in a classical feedback mechanism (Hamada et al. 2002).

Cerberus-like is a cysteine knot protein which binds Nodal and blocks signal propagation through interference with Nodal:TGF $\beta$  receptor interaction (Belo et al. 2000; Perea-Gomez et al. 2002). Unlike lefty, Cerberus-like expression does not follow Nodal's expression, and is instead mainly limited to the anterior visceral endoderm from where it inhibits Nodal signalling, thus allowing anterior neural development to occur (Shawlot, Deng, and Behringer 1998; Stanley et al. 1998). Lefty and Cerberus-like act together in the

extraembryonic endoderm to limit Nodal signalling in the epiblast, and therefore mesoderm formation to the posterior side of the embryo (Perea-Gomez et al. 2002).

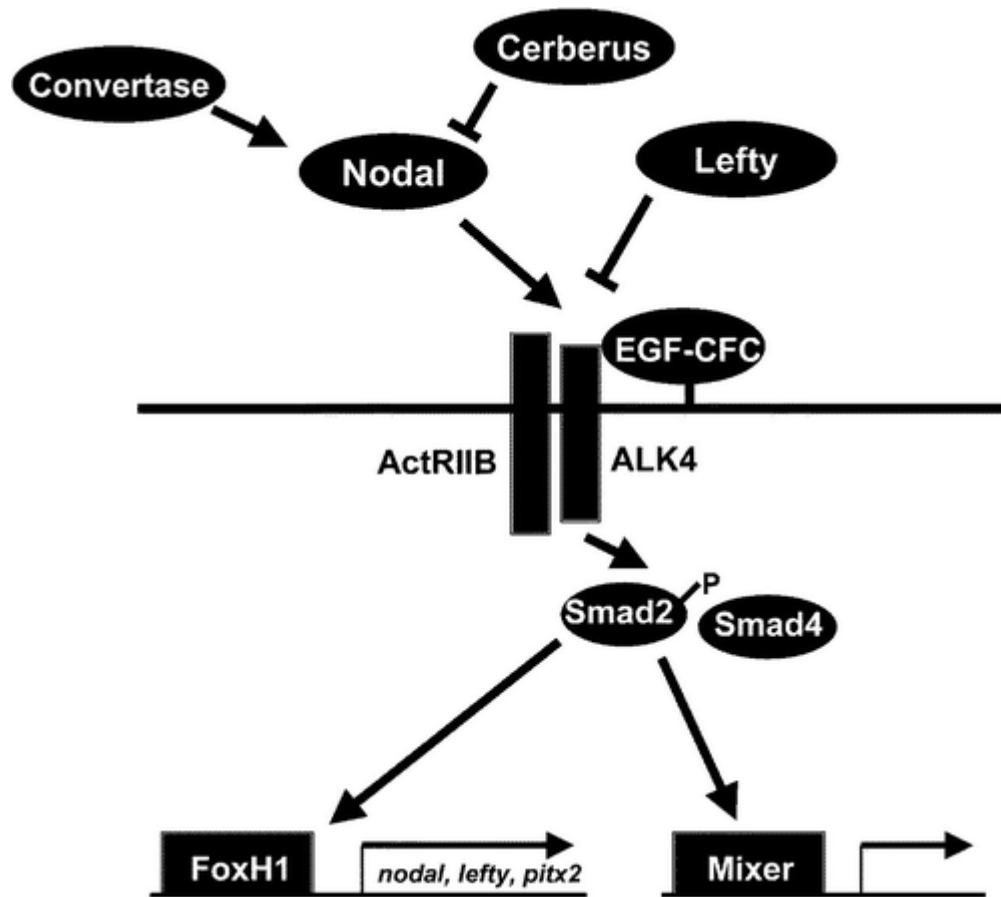


**Figure 2 Schematic overview of the Nodal signalling pathway.** Signalling is initiated by the activation of TGF $\beta$  receptors (ActRIIB and ALK4 (AcvRIB)) by Nodal ligands. Nodal is cleaved from pro-Nodal to Nodal extracellularly by the convertases Furin and Pace4. Cerberus antagonises Nodal and Nodal signalling is inhibited by lefty. Image from *Nodal Signalling in Vertebrate Development* 2003 Alexander F. Schier *Annual Review of Cell and Developmental Biology*.

SB431542 is a potent ALK5 (T $\beta$ RI), ALK4 (ActRIB) and ALK7 (AcvRIC) kinase activity inhibitor which acts by inhibiting phosphorylation of Smad3. The inhibitor's activity is selective for Nodal and Activin signalling as SB431542 has no effect on BMP signal transduction (Gareth J. Inman et al. 2002).



## 1.2 Smad Proteins

Smad proteins are the intracellular effectors of TGF $\beta$  signalling. They orchestrate the activation or repression of specific gene networks. Smads are classified into three subgroups; regulatory (R)-Smads (Smad1, Smad2, Smad3, Smad5 and Smad8/9) (J.-W. Wu et al. 2001), the common Smad (co-Smad, Smad4) which interacts with R-smads to mediate transduction of TGF $\beta$  signalling (Y. Shi et al. 1997) and inhibitory Smads (Itoh et al. 2001).

### 1.2.1 Smad molecular composition

R-Smads and Smad4 each comprise two globular, polypeptide domains, connected by a linker domain (Yigong Shi and Massagué 2003). The N-terminal domain, also known as Mad Homology – 1 (MH1) domain, is largely conserved between the R-Smads and the co-Smad, Smad4. Containing a DNA-binding motif, the MH1 domain interacts with DNA by base-specific binding in a  $\beta$ -hairpin structure as seen in Figure 3 (Y. Shi et al. 1998a). The C-terminal domain (MH2) is conserved between all Smad groups and contains the Gly/Ser rich sequence, which becomes phosphorylated by an activated type I TGF $\beta$  receptor, and functions as the protein interacting area of the Smad protein. The C-terminal domain contains an L3 loop which is a 17-amino acid region that mediates and specifies Smad-TGF $\beta$  receptor interactions (Lo et al. 1998). The linker domain, a flexible structure comprising binding sites for additional factors, is divergent between groups. (Joan Massagué, Seoane, and Wotton 2005; Yigong Shi and Massagué 2003; J.-W. Wu et al. 2001).

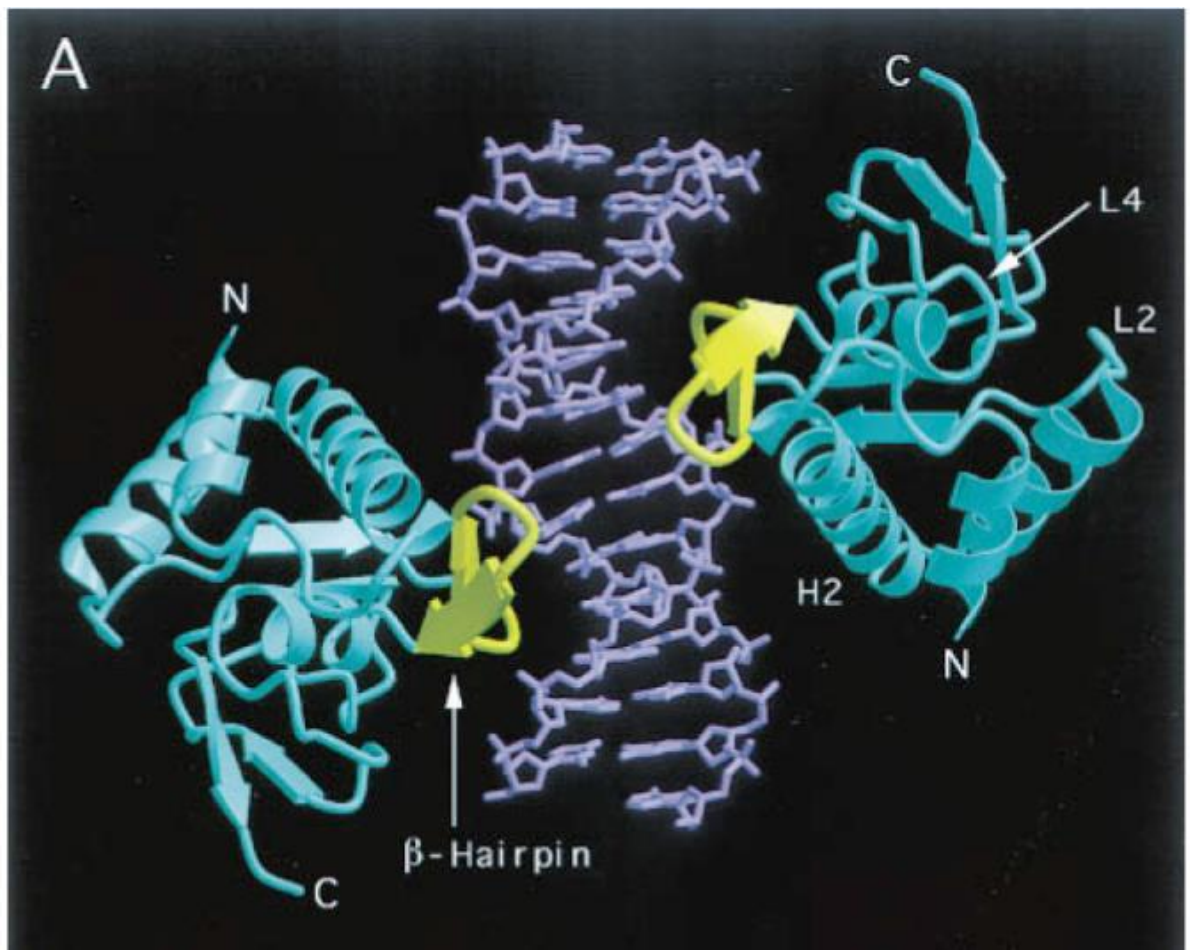


**Figure 3 Overall structure of Smad-3 MH1 bound to a Smad binding element.** MH1 domain is coloured in cyan and the DNA in purple. The beta hairpin is coloured in yellow. Image from Crystal Structure of a Smad MH1 Domain Bound to DNA: Insights on DNA Binding in TGF-Beta Signalling Shi et al Cell.

### 1.2.2 Smad-Receptor Interactions

Ligand binding induces formation of a stable, complete complex consisting of four TGF $\beta$  receptor subunits, including two receptors of each type, which allows phosphorylation of the type I GS sequence by type II receptor kinases. As explained in *1.3 TGF $\beta$  signalling*, activation of type I receptor kinase phosphorylates R-Smads. Recruitment of R-Smads to the receptor complex occurs through an interaction between the L45 domain of the type I TGF $\beta$  receptor and the L3 domain of the R-Smad protein (Y. G. Chen et al. 1998). This

interaction allows the activated type I TGF $\beta$  receptor to phosphorylate the C terminal Gly/Ser unit of the R-Smad, and induce protein conformational changes. Type I receptor-mediated phosphorylation of the Smad MH2 domain decreases the Smad protein's affinity for its cytoplasmic anchors such as SARA (see *1.4.5 Accessory Proteins in Smad Signaling*) and increases affinity for nuclear factors (Yigong Shi and Massagué 2003; Xu and Massague 2004; Tsukazaki et al. 1998). R-Smads' subsequently dissociate from the membrane bound type I TGF $\beta$  receptor and generate a trimeric protein complex of two R-Smads and a Smad-4 (R-Smad phosphorylation creates a binding site for Smad-4) which then translocate to the nucleus, as visualised in Figure 4 (J. W. Wu et al. 2002). Smad 2 and 3 are recruited to, and are phosphorylated by, the type I receptor T $\beta$ RI and the type II receptor ActRIB. Smads 1, 5 and 8 are intracellular signaling substrates for the receptors BMP-RIA, BMP-RIB, ALK-1 (AcvRI) and ALK-2 (AcvRII A and B) (Feng and Derynck 2005). Dephosphorylation of Smad proteins by the phosphatase PPM1A/PP2C $\alpha$  in the nucleus (Lin et al. 2006) initiates the return of the protein to the cytoplasm. Smad proteins are thus in a state of constant cytoplasmic-nuclear shuttling which allows for continual sensing of TGF $\beta$  receptor activation (G. J. Inman, Nicolas, and Hill 2002).

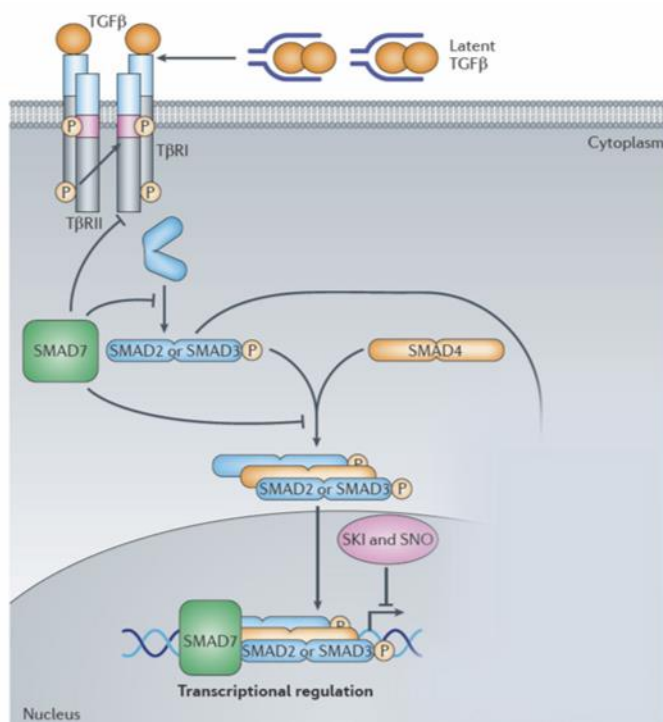


**Figure 4 Schematic overview of the Smad-dependent TGFβ signalling pathway.** Extracellular ligands induce heteromeric complex formation between specific TGFβ receptors. Type II receptors phosphorylate type I receptors then subsequently phosphorylate intracellular Smad proteins which propagate the signal. Smad 7, an inhibitor Smad, obstructs Smad signalling. Image adapted from *Targeting the TGFβ signalling pathway in disease* Rosemary J. Akhurst & Akiko Hata *Nature Reviews Drug Discovery*

### 1.2.3 Smad-Transcriptional Mediator Interactions

Stimulation of targeted transcriptional initiation occurs through complex interactions between Smads and ligand-responsive promoter elements in conjunction with additional transcription factors. Smad proteins interact with the coactivators CBP/p300 and FoxH1 (FAST-1), enhancing the inherent transcriptional activity of Smad binding elements (C. Y. Yeo, Chen, and Whitman 1999a; Topper et al. 1998; Feng and Derynck 2005). The Smad DNA binding site is known as the Smad Binding Element (SBE) with the sequence 5-GTCT-3' (Keeton et al. 1991; Dennler et al. 1998b; Westerhausen, Hopkins, and Billadello

1991). The MH1 domain of Smad3 binds this SBE via a  $\beta$  hairpin structure. Hydrogen bonds bind the two guanine residues of the SBE to the MH1 domain of Smad3. (Y. Shi et al. 1998a). Smad2 interacts with DNA through Smad 4, as it is unable to bind DNA due to a sequence modification in its MH1  $\beta$  hairpin domain. (Derynck and Zhang 2003a; Y. Shi et al. 1998a). Dennler et al went on to investigate the increased transcriptional activation in the presence of multiple SBEs, first found in the PAI-1 gene promoter region, demonstrating that 9 repeats of the sequence 5-AGGCCAGACA-3' resulted in optimal activation (Dennler et al. 1998b). Dennler's methodologies have been successfully adapted recently in Warmflash and colleagues' work exploring the nuclear localisation of Smad2/4 *in vitro*, upon ligand stimulation (Warmflash et al. 2012).

Smad proteins bind other transcription factors on DNA resulting in a modulation of transcription. These factors can be further regulated by additional signalling pathways increasing the complexity and versatility of TGF $\beta$  signalling.

FoxH1 is a forkhead transcription factor which binds Smad2/4 complexes at DNA binding sites in response to Activin/Nodal signalling (X. Chen et al. 1997a). In these complexes, Smad2 interacts with FoxH1 via a Smad interaction motif while Smad4 binds DNA (Randall et al. 2004; Labbé et al. 1998). This DNA binding association mediates Activin/Nodal signalling and regulates transcription during anterior primitive streak, endoderm and mesoderm formation in mice, as described in *1.3 Early murine embryogenesis* (Yamamoto et al. 2001; Hoodless et al. 2001).

CBP/p300 is a co-activator which increases target gene expression by localising transcription factors to the RNA polymerase II complex (Janknecht, Wells, and Hunter 1998). R-Smads interact with CBP/p300 directly through their MH2 domain (Topper et al. 1998). For this interaction to occur, the R-Smad must be in their activated state, i.e. their C-terminal GS must be phosphorylated. Smad4 stabilises this interaction (Feng et al.

1998). Histone acetyltransferase activity of CBP/p300 increases gene expression by modifying chromatin structure, indeed, acetylated histones are characteristic of transcriptionally active chromatin (Ogryzko et al. 1996).

## 1.2.4 Smad Inhibitors

Smad 6 and 7 are inhibitory Smads (I-Smads). These Smad proteins inhibit TGF $\beta$  signal propagation by competitively associating with type I TGF $\beta$  receptors and therefore interfering with receptor mediated R-Smad recruitment and phosphorylation (Hayashi et al. 1997). Smads 1 and 5 induce Smad 6 expression, and Smad 3 induces Smad 7 expression. Therefore, through a classic negative feedback mechanism, TGF-  $\beta$  signaling induces an inhibitory feedback loop by inducing I-Smad expression. Additionally, Smad 6 and 7 inhibit TGF $\beta$  signaling by mobilising SmurfE3 ubiquitin ligases to type I receptors, resulting in their proteasomal degradation and therefore limitation of R-Smad activation (Ebisawa et al. 2001).

## 1.2.5 Accessory Proteins in Smad Signaling

SARA, a FYVE domain containing protein, is required for efficient recruitment and activation of R-Smads. Localised at the plasma membrane, SARA interacts with both the type I TGF $\beta$  receptor and the MH2 domain of Smad2 and 3, thus controlling subcellular localisation of Smad2 (Tsukazaki et al. 1998). C-terminal phosphorylation of Smad results in its dissociation from SARA. SARA mutations that mis-localise Smad2 inhibit TGF $\beta$  responses, highlighting the importance of appropriate R-Smad recruitment to the TGF- $\beta$  receptor complex (Tsukazaki et al. 1998).

Dab2 (Disabled-2) is an accessory protein that interacts with the T $\beta$ RII/T $\beta$ RI receptor complex and stabilises its interaction with R-Smads (Hocevar et al. 2001). Additionally, Dab2 interacts with AP-2 -the clathrin adapter- and clathrin, and may be linked to clathrin mediated endocytosis of activated TGF $\beta$  receptor complexes (Hocevar et al. 2001).

### 1.3 Early murine embryogenesis

After fertilisation of the murine egg, cellular cleavage events take place within a protective shell called the zona pellucida, producing a solid ball of cells - the morula (see Figure 5). Compaction follows cleavage, a process in which the cells of the embryo increase both in size and surface area contact with one another, and become polarised (Sutherland, Speed, and Calarco 1990). The next stage in development is the formation of the blastocyst, a hollow ball comprised of two distinct groups of cells; the trophoblast and the inner cell mass. These cell groups originate from the outer and inner morula cells, respectively. The trophoblast will become extra-embryonic structures while the inner cell mass will give rise to the embryo (Gardner 1983; Johnson and Ziomek 1981).

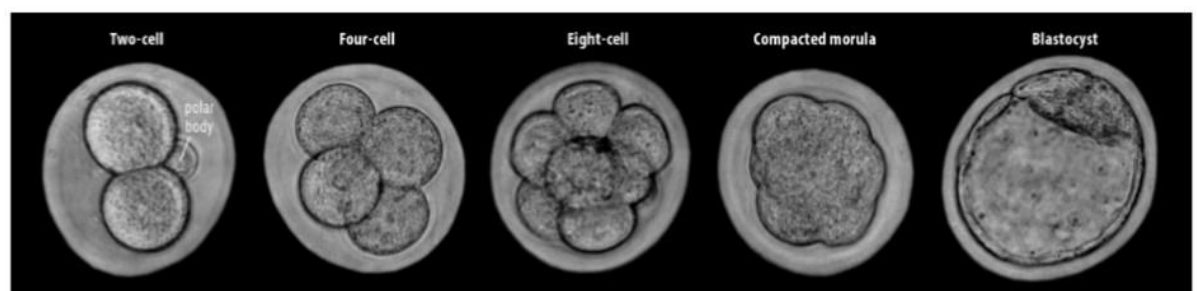


**Figure 5 Cleavage events and generation of a morula and blastula in mice.** Image from *Principles of Development* 2007 Wolpert et al.

Between embryonic days 3.5 and 4.5, the inner cell mass differentiates into two groups of cells: the lower layer, which is in contact with the fluid filled blastocoel, is the primitive endoderm and those cells above become the epiblast (see Figure 6). The primitive endoderm will become extra-embryonic membranes and the epiblast will become the embryo proper (Gardner 1983). At this stage (embryonic day 4.5), the embryo “hatches” from the zona pellucida and implants into the uterine wall. As seen in Figure 6, *panels B and C*, post-implantation, the epiblast elongates and becomes cup-shaped, while the primitive endoderm expands to surround the epiblast (the visceral primitive endoderm) and the mural trophoctoderm (the parietal primitive endoderm) (Stanley et al. 1998).

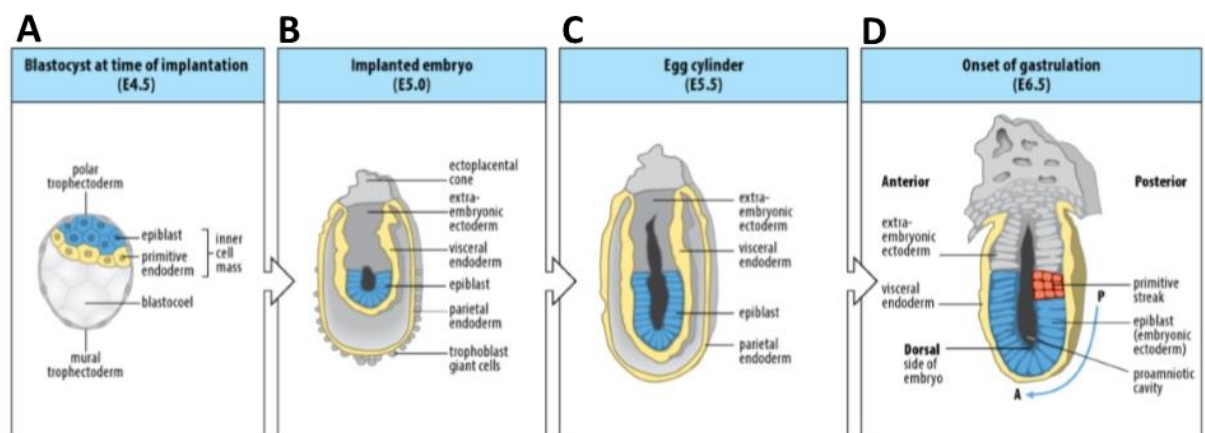


**Figure 6 Post implantation events in the mouse embryo.** Panel A: the blastocyst is comprised of a hollow ball of cells, the trophoctoderm, and an aggregation of cells, the inner cell mass. At implantation, the inner cell mass differentiates into two types of cells; the primitive endoderm and the epiblast. Panels B and C: the polar trophoctoderm forms extra-embryonic tissue (ectoplacental cone and extra-embryonic ectoderm) while the mural trophoctoderm becomes trophoblast giant cells. The epiblast lengthens and develops a hollow internal cavity (proamniotic cavity) which gives the embryo a cup shaped form. The primitive endoderm becomes both the visceral and parietal endoderm, covering the elongating egg cylinder. Panel D: formation of the primitive streak at the posterior side of the epiblast indicates the beginning of gastrulation. The primitive streak extends anteriorly towards the bottom of the egg cylinder (arrow). Image from *Principles of Development* 2007 Wolpert et al.



Around embryonic day 5, Nodal is ubiquitously expressed in the epiblast. This TGF $\beta$  signalling induces formation of the anterior visceral endoderm (AVE) in synergy with inhibitory signals from the extraembryonic ectoderm (Figure 7). AVE formation is subsequently limited to the distal most tip of the visceral endoderm (Rodriguez et al. 2005; Brennan et al. 2001). The AVE expresses a unique cohort of molecular markers including Cerebus-like 1 and Lefty1 (Beddington and Robertson 1999) which are required to limit Nodal signalling to the posterior side of the developing embryo, facilitating formation of the primitive streak (Perea-Gomez et al. 2002) as explained in *1.3.1 Nodal signaling in early mouse embryo development*.

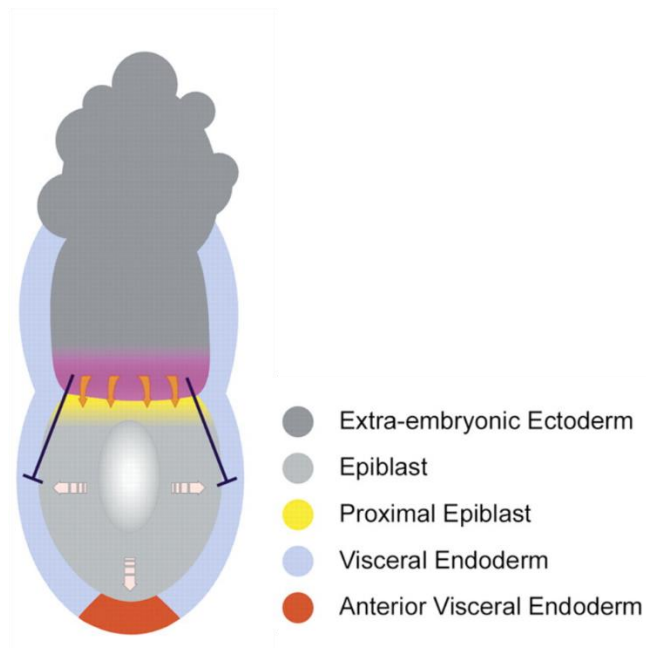


**Figure 7 Extra-embryonic ectoderm patterning in AVE development.** At embryonic day 5, Nodal is ubiquitously expressed in the epiblast (light pink arrows). In addition to this, AVE inhibition signals are expressed in the extra-embryonic ectoderm (inhibitory arrows). This complex of signalling results in the formation of AVE to be limited to the distal tip of the visceral endoderm. Image adapted from *Induction and migration of the anterior visceral endoderm is regulated by the extra-embryonic ectoderm* Rodriguez et al 2005.

At embryonic day 6.5 (Figure 6, *D*), gastrulation is initiated and the primitive streak appears. Epiblast cells converge at the posterior side of the embryo and ingress under the surface of the epiblast (Bellairs 1986). Once underneath, the epiblast cells spread out laterally between the epiblast surface and the visceral endoderm and become the mesoderm (see Figure 8, *panel 1*) (Tam and Beddington 1987). The primitive streak lengthens towards the bottom of the egg cylinder and the node develops at the anterior end (Figure 8, *panel 2*). The node subsequently gives rise to the notochord, which forms the head process (Lawson, Meneses, and Pedersen 1991).

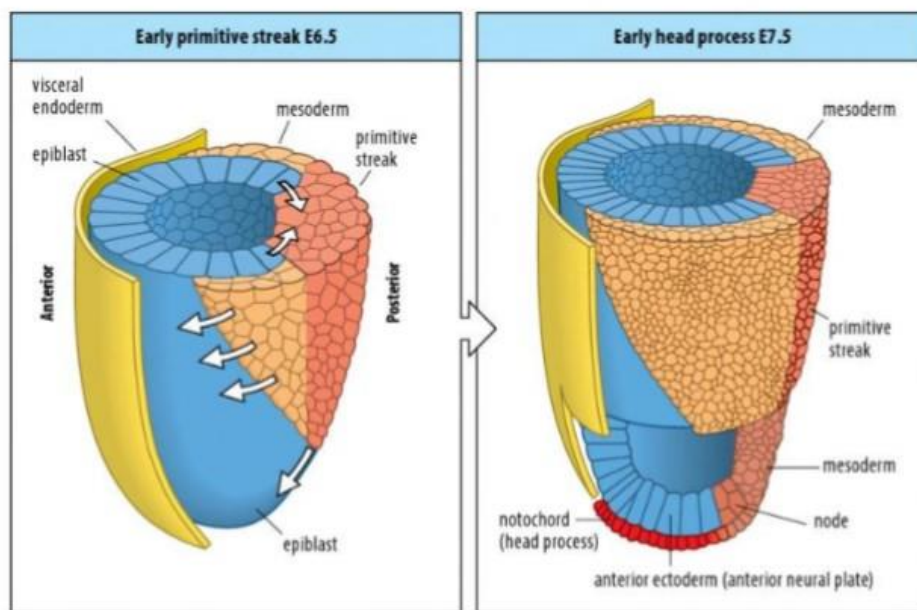


**Figure 8 Mouse embryo gastrulation.** During gastrulation, epiblast cells migrate between the epiblast and the visceral endoderm, becoming the primitive streak, then migrate laterally forming the mesoderm. The node of the embryo first develops on the posterior side of the embryo, then moves toward the bottom of the egg cylinder. Image from *Principles of Development* 2007 Wolpert et al.

### 1.3.1 Nodal signalling in early mouse embryo development

During gastrulation, Nodal precisely controls patterning and positioning of the anterior-posterior and left-right axis, and formation of mesoderm and endoderm (A. F. Schier and Shen 2000). Nodal is expressed in the epiblast and converted into its functional state by convertases produced in the extraembryonic endoderm, as illustrated in Figure 9 (also see chapter 1.2.2 *Convertase action on Nodal*). The expression of Nodal is maintained by autoregulation (Brennan et al. 2001). Nodal signaling in the epiblast induces Nodal expression and subsequently Smad signaling in the visceral endoderm which results in target gene expression (such as Cer1, Lefty1, Foxa2 and Nodal itself) (Brennan et al. 2001). Inhibitors of Nodal signaling (Cer1 and Lefty1, the generation of which are stimulated by Nodal itself) in the visceral endoderm eventually restrict Nodal signaling to the proximal and posterior epiblast where the primitive streak subsequently forms (Perea-Gomez et al. 2002) as seen in Figure 9, also see chapter 1.2.2 *Extracellular Inhibitors of Nodal/Activin Signalling*.

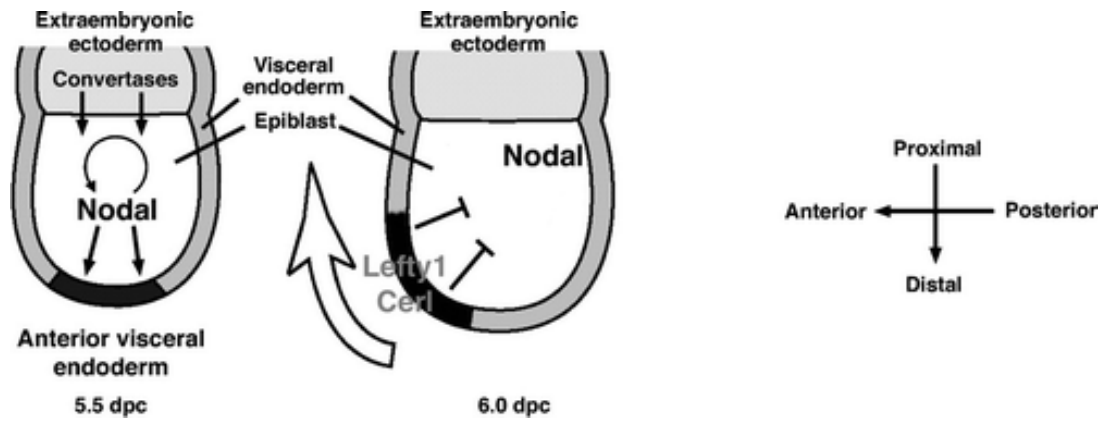


**Figure 9 Nodal signalling positions the anterior-posterior axis of the embryo.** Nodal is produced in the epiblast and converted from pro-Nodal to Nodal by convertases expressed by the extraembryonic ectoderm. At embryonic day 5.5 Nodal is ubiquitously expressed in the epiblast, where it induces production of its inhibitors *Cer1* and *Lefty1*. These inhibitors then limit Nodal expression to the posterior area of the epiblast, initiating the anterior-posterior axis differentiation (day 6.0). Image from *Nodal Signalling in Vertebrate Development* 2003 Alexander F. Schier *Annual Review of Cell and Developmental Biology*.

Nodal is inhibited by Lefty1 and antagonised by Cerebus-like, as seen in Figure 2, also see 1.2.2 *Extracellular Inhibitors of TGF $\beta$  Signalling* (A. F. Schier and Shen 2000; Piccolo et al. 1999). Downstream signalling is mediated by additional transcription mediators such as FoxH1 transcription factor and Mixer transcriptional activators (see Figure 2 and 1.3.3 *Smad-Transcriptional Mediator Interactions*) (A. F. Schier and Shen 2000; Alexander F. Schier 2003a).

## 1.4 Research Question

Early developmental processes, such as the arrangement of the head-tail axis, are fundamentally driven by cell signaling cascades. Such events are regulated in a highly complex manner by promoters and inhibitors at many levels of the cascade. This complexity makes it difficult to understand where and when certain signaling events occur and what the effects of additional factors have on the system.

The TGF $\beta$  system, activated via Nodal binding and executed through Smad signaling, induces the head-tail patterning of the early embryo. Target gene outputs of this signaling are fine-tuned by a vast array of modulators; TGF $\beta$  receptor cofactors, alternative ligands, TGF $\beta$  receptor inhibitors, DNA binding cofactors, up regulators, enhancers, inhibitors and repressors. Indeed, the endogenous target genes of this system cannot be used as a measure of signaling as they themselves feedback on the original system and others, creating diverse signals. In this project, we aim to create a multi-fluorophore genetic reporter which distills the Nodal/Activin signaling system to a single variable to semi-quantitatively investigate Smad signaling during early development

Various levels of Smad signaling were directly measured by multiple fluorescent signals via constructs containing Smad binding elements, a minimal promoter and fluorescent protein elements. Combinations of varying numbers of Smad binding elements were used to create constructs which respond to different thresholds of signalling. Fluorescent microscopy and flow cytometry was used to verify responses of NIH 3T3 cells transfected with fluorescent Smad reporter construct to various concentrations of Activin stimulation.

Subsequently, a transgenic mouse line was created to visualise where Nodal/Activin signaling occurs during gastrulation. We aim to create a fluorescent genetic Smad signaling reporter system in which constructs containing differing sensitivity Smad binding elements

drive transcription of colour coded fluorescent proteins to investigate where, when and to what degree Smad signaling occurs in early murine embryonic development.

This study will provide an understanding of how extracellular cues dictate gene expression during early embryonic formation. Knowledge acquired from this work may have implications in stem cell research, and dairy cattle and human fertility.

## 2 Methods

## 2.1 DNA cloning

A collection of fluorescent genetic reporters were created by DNA cloning mechanisms. Firstly, the RAstat12x element from the parental vector RAstat12x-SCP-GFP was excised and replaced with a SBE4x element, generating SBE4x-SCP-GFP. A multimerisation technique was used to generate SBE8x- and SBE16x-SCP-GFP vectors from the SBE4x-SCP-GFP vector. Removal of the SBE4x element from SBE4x-SCP-GFP generated SBE0x-SCP-GFP, a vector used as a negative control and to assess enhancer-independent transcription of GFP in our reporter system.

A SBE16x-HSP-GFP element was created by replacing the SCP element of SBE16x-SCP-GFP with a HSP element.

To create SBE0x-, 4x-, 8x- and 16x-SCP-TOM vectors, GFP elements were excised from SBE0x-, 4x-, 8x- and 16x-SCP-GFP and replaced with tdTomato elements (TOM).

Using these strategies, we have created an assembly of vectors containing various sensitivity Smad binding elements, driving both GFP and TOM.

### 2.1.1 SBE adapter/insert and vector design

Dennler et al 1998 found that the sequence AG(C/A)CAGACA is repeated 3 times in the PAI-1 promoter in a region that was shown to mediate TGF $\beta$  signaling. When cloned in multiple repeats into a transcriptional reporter system, Dennler et al saw a substantial increase in TGF $\beta$ -mediated induction (Dennler et al. 1998a). Here we have applied Dennler's AGCCAGAC sequence to create a Smad binding element (SBE) insert which was designed with 4 repeats of a double SBE as seen in Figure 10 below.





**Figure 10 SBE4x binding element insert design.** Four Smad binding CAGA boxes, designed based on work by Dennler et al 1998, flanked by restriction sites SpeI and XbaI.

Repeats were linked by 4 adenine bases or 3 adenine bases and a thymine base. Overlapping sticky ends were designed compatible to the site of interest. These restriction sites can insert within SpeI and XbaI sites bidirectionally, however, reverse insertion renders restriction sites uncleavable. Multimerisation of SBEs was achieved by cutting a recipient vector at the XbaI site and inserting additional SBEs as seen below in Figure 11. This allowed for constructs of various numbers of SBE repeats and therefore sensitivities to be created.

Vectors were designed to incorporate minimal plasmid bacterial replication mechanisms, an insulator region to isolate experimental transcriptional events (SBE and SCP driving transcription of GFP) from additional transcriptional machinery in surrounding area, a minimal promoter and a poly A tail. The promoter is a Super Core Promoter (SCP) which contains a TATA box, and initiator, a motif ten element and a downstream promoter element (Juven-Gershon, Cheng, and Kadonaga 2006). This promoter was chosen as it does not induce transcriptional activation without upstream promoter enhancer activity. It is therefore sufficient for fluorescent protein transcription initiation when Smad binding elements are engaged with Smad2-4 or 3-4 heterodimers, without inducing enhancer-independent transcription which would be seen as 'background' fluorescence.

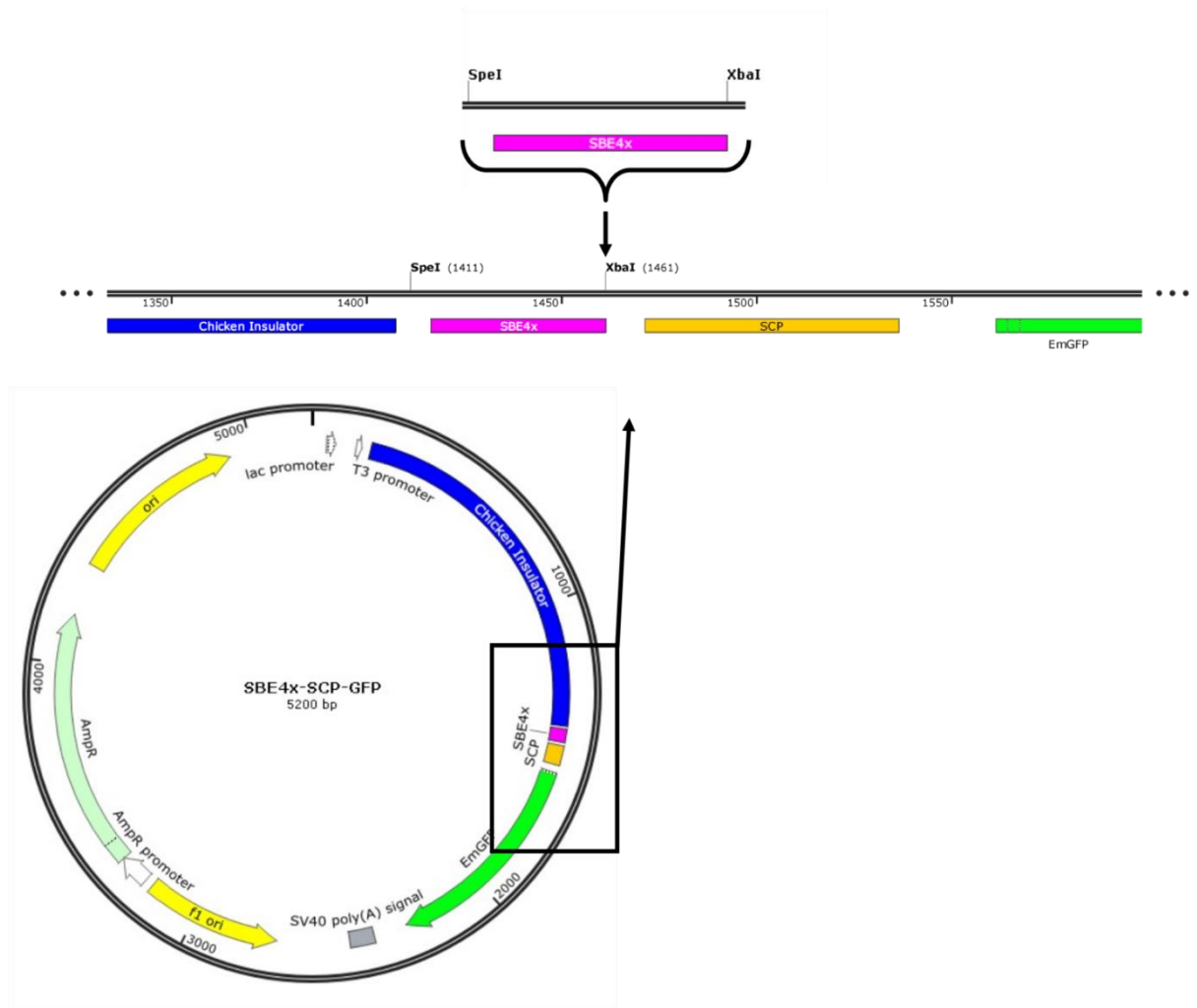


**Figure 11 Cloning strategy for multimerisation of SBE.** Multimerisation of the SBE4x was achieved by butting the SBE4x-SCP-GFP vector with *XbaI*, and ligating in an additional SBE4x element to create SBE8x-SCP-GFP. This methodology was also used to create SBE16x-SCP-GFP. Image created using SnapGene.

### 2.1.2 SBE4x adapter preparation

The 3' and 5' oligos of the SBE4x adapter (Sigma, NZ) were phosphorylated in separate solutions containing; 10  $\mu$ l ddH<sub>2</sub>O, 1  $\mu$ l of 1 mM oligo stock, 2.5  $\mu$ l PNK buffer (Roche, Australia), 2.5  $\mu$ l ATP (Roche, Switzerland), 2  $\mu$ l 10 U/ $\mu$ l T4 polynucleotide kinase (Thermo Scientific, NZ), which were incubated for 1 hour at 37°C. 1  $\mu$ l of 0.5 M EDTA was added to the solution and the mix was

incubated at 70°C for 10 minutes to inactivate the polynucleotide kinase. Incubating the mix at a high temperature under low salt conditions retains separation of compatible oligo DNA strands.

### 2.1.3 SBE4x adapter annealing

Equimolar concentrations of phosphorylated 3' and 5' oligos in PNK buffer (Roche, Switzerland) were mixed, incubated for 5 minutes in an 80 °C water bath to keep the oligo strands apart and allowed to slowly cool to room temperature to allow formation of correctly aligned oligo duplexes. Phosphorylated adapters were generated at 20 pmol/μl.

### 2.1.4 Generation of SBE16x-HSP-GFP

To investigate the efficiency and activity of an alternative promoter, a SBE16x-HSP-GFP vector was generated. The Super Core Promoter (SCP) was removed from SBE16x-SCP-GFP and replaced with a Heat Shock Promoter (HSP), a well-studied, less stringent, inducible eukaryotic promoter (Amin, Ananthan, and Voellmy 1988).

### 2.1.4 Generation of Tomato element

A tomato fluorescent protein element flanked by NcoI and NotI was generated by creating oligos illustrated in Figure 12 (B) and amplifying a preexisting tomato sequence flanked by sites not compatible with the target vector. After PCR cycling in conditions described in 2.2.13 *PCR Protocol*, Tomato product was isolated by gel electrophoresis and the WIZARD Gel Clean kit (2.2.8 *Agarose gel slice digestion* and 6.1 *Wizard SV Gel Clean-Up System protocol*). The Tomato product was cut with BsaI and NotI (generating NcoI and NotI – to be compatible with target site), and subsequently

ligated into SBE0x-, 4x-, 8x-, and 16x-SCP vectors (see 2.2.6 *Ligation*) of which the GFP fragment had been removed by NcoI and NotI restriction, gel electrophoresis and WIZARD Gel Clean kit.

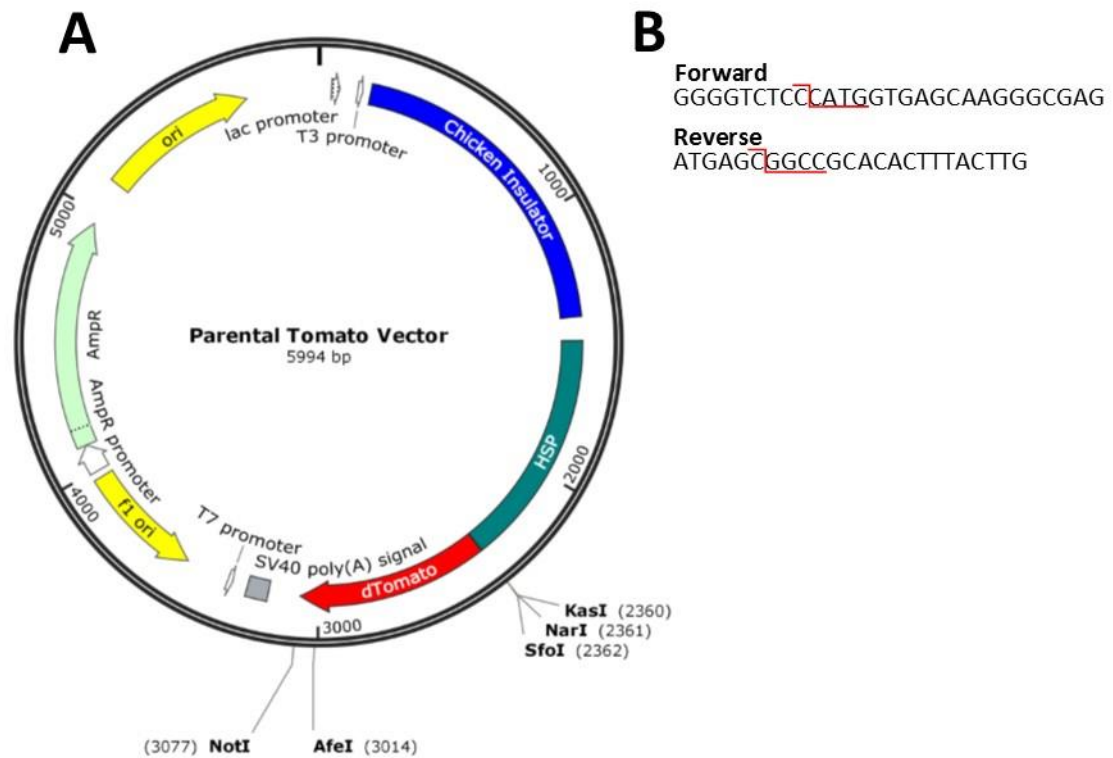


**Figure 12 Cloning strategy creating a tomato element.** A tomato element flanked by NcoI and NotI was created by designing oligos which consist of a clamp followed by NcoI or NotI sites. This allowed a tomato element, flanked by restriction sites compatible to target vector, to be generated from reference tomato element flanked by incorrect restriction sites. (A) reference vector containing tomato elements flanked by incorrect restriction sites, (B) Oligo design. The Forward oligo contains a NcoI sites and the reverse contains a NotI site, both contain clamp regions.

## 2.1.5 Vector restriction

A parental vector, RAsat12x-SCP-GFP Figure 13 containing the chicken insulator, SCP, GFP and minimal bacterial plasmid constituents, was used to create SBE4x-SCP-GFP. The RAsat elements are flanked by SpeI and XbaI and therefore these elements can be excised and replaced

with the SBE4x insert (also flanked by SpeI and XbaI), creating SBE4x-SCP-GFP. In a 20  $\mu$ l reaction containing 15  $\mu$ l of ddH<sub>2</sub>O and 2  $\mu$ l of 10x buffer H (Roche, Switzerland), 1  $\mu$ g of RAstat12x-SCP-GFP was digested by 10 units of SpeI (10U/ $\mu$ l) and XbaI (10U/ $\mu$ l) enzymes (Roche, Switzerland).

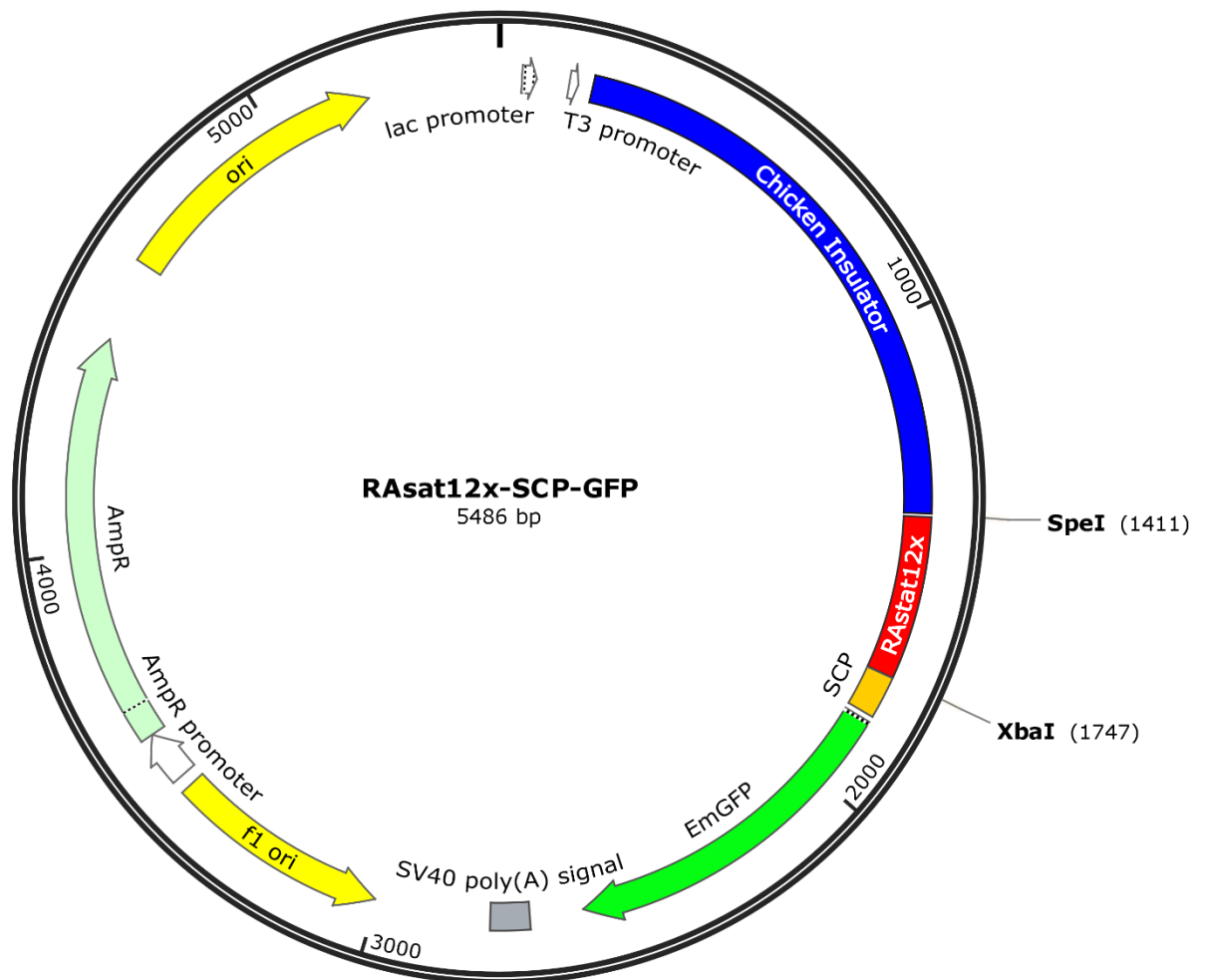


**Figure 13 Parental vector, RAstat12x-SCP-GFP.** This vector was used as a parental vector. RAstat12x element was excised and replaced with SBE4x creating SBE4x-SCP-GFP.

## 2.1.6 Vector Dephosphorylation

The restricted vector was dephosphorylated to remove the 5' phosphate group so as to prevent self-ligation. 24 µl ddH<sub>2</sub>O, 5 µl of 10x CIP buffer (Roche, Switzerland) and 1 µl of 1 U/µl CIP (Roche, Switzerland) was added to the restricted vector solution which was then incubated for 30 minutes at 37°C. The mix was then spun down at 12,000xg (Thermo Scientific Heraeus Pico 17 centrifuge) and 1 µl of CIP was added. After another 30 minutes' incubation at 37°C the reaction was heat inactivated at 75°C for 10 minutes.

The resulting fragments were separated in a 1% agarose gel to isolate target DNA from CIP and off target DNA, and to ensure no reannealing of fragments.

## 2.1.7 Ligation

Vector and adapter were mixed on ice at a 1:1 molar ratio (1 pmol of each) with 2 µl Mighty Mix (Takara Bio Inc, Japan). The mix was incubated at 16 °C overnight. See 6.2 *Takara Mighty Mix Protocol-at-a-Glance*.

## 2.1.8 Agarose gel

To make a 1%, 50 ml gel, 0.5 g of SeaKem LE agarose (Lonza, USA) was dissolved in 50 ml 1x TAE (Tris and EDTA) by heating for 1 – 2 minutes in a microwave. The solution was cooled under running water and poured into a gel case. 50 ml gels were run at 80 V and 80 ml gels were run at 100 V (BioRad PowerPac HC or BioRad PowerPac Basic). To make gels of varying agarose concentrations, amount of LE agarose was altered accordingly (eg, to make a 1.5%, 50 ml gel, 0.75 g of agarose was used).

## 2.1.9 Agarose gel slice digestion

Gels were visualised under UV light and sterile dissection of target DNA bands was undertaken. Gel slices were digested using the Wizard SV Gel and PCR Clean-Up System (Promega, USA). Slices were placed in a 1.5 ml microcentrifuge tube with 10 µl of Membrane Binding Solution per 10 mg of gel slice. The tubes were vortexed and incubated at 65°C until the gel slice was completely dissolved. The dissolved gel mix was transferred into a minicolumn assembly and incubated at room temperature for 5 minutes to allow cooling of the solution and binding of DNA to the minicolumn. The minicolumn assembly was centrifuged at 16,000 xg for 1 minute and flowthrough discarded. The minicolumn was washed with two washes of 700 µl and 500 µl of membrane wash solution. After each wash the minicolumn was centrifuged at 16,000 xg for 1 and 5 minutes, respectively. The flowthrough was discarded after each centrifugation and the minicolumn was allowed to stand for 1 minute to allow evaporation of any residual ethanol from the wash solution. The minicolumn was transferred to a 1.5 ml microcentrifuge and 30 µl of nuclease-free water was added. The minicolumn was allowed to stand for 1 minute at room temperature and was then centrifuged at 16,000xg for 1 minute. DNA was stored at -20°C. See *6.1 Wizard SV Gel Clean-Up System protocol*.

## 2.1.10 Transformation

25 µl of MAX efficiency E. coli DH5α competent cells (Thermofisher, NZ) were transformed with 2 µl of ligation mix (see *2.8 Ligation*) according to the product transformation protocol. See *6.3 Invitrogen Max Efficiency DH5α transformation protocol*.

## 2.1.11 Miniprep protocol

Transformed DH5 $\alpha$  competent cells were grown on an LB agar + ampicillin plate (see 5.1.2 *LB Agar*) overnight at 37°C. Single colonies were picked from this plate and grown in 3 ml LB broth + ampicillin (see 5.1.1 *LB Broth*) overnight at 37°C, shaking at 300 RPM. 1 ml of this culture was transferred into a 1.5 ml microcentrifuge tube for miniprep and centrifuged at 11,000 RPM for 1 minute. Supernatant was removed and discarded. 100  $\mu$ l of Alkaline Lysis Solution I (5.2.1 *Alkaline Lysis Solution I*) was added and the mix was vortexed until the pellet was dissolved. 200  $\mu$ l of Alkaline Lysis Solution II (5.2.2 *Alkaline Lysis Solution 2*) was then added and the solution was mixed by inverting the microcentrifuge tube 5 times. 200  $\mu$ l of Alkaline Lysis Solution III at 4°C (5.2.3 *Alkaline Lysis Solution III*) was added to the tube and the solution was mixed by flicking the microcentrifuge tube 3 times. The mix was then centrifuged (16,000 xg, 4 minutes, 4°C). Resulting supernatant was transferred to a fresh 1.5 ml microcentrifuge tube and 1 ml of 100% EtOH was added. The mix was vortexed briefly and subsequently centrifuged (16,000xg, 4 minutes, 4°C). Supernatant was removed and the remaining pellet was rinsed with 700  $\mu$ l 70% ethanol. The 70% ethanol was removed and the DNA pellet was left to air dry for 3 minutes. The DNA pellet was reconstituted in 30  $\mu$ l of dd-H<sub>2</sub>O containing 10  $\mu$ l TE and 1  $\mu$ l RNase-A and incubated at 37°C for 30 minutes.

## 2.1.12 Midiprep protocol

Midipreps were prepared with the QIAGEN Plasmid Midi Kit (QIAGEN, Netherlands). Refer to QIAGEN Plasmid Midi Quick-Start Protocol (see 6.4 *Qiagen Miniprep protocol*/DNA). DNA content was measured on a Nanodrop ND-1000 Spectrophotometer.



### 2.1.13 Glycerol stock preparation

150 µl of autoclaved 100% glycerol (Sigma, USA) was mixed with 850 µl of culture from midi preps (see 6.4 *Qiagen Midiprep Protocol*) and vortexed briefly. The mix was flash frozen in dry ice with ethanol and stored at -80°C.

### 2.1.14 PCR protocol

PCR was performed using an Eppendorf VapoProtect PCR machine under the conditions described in Figure 14.

### Reaction set up

Total Volume 25  $\mu$ l

10x Roche FASTAQ Reaction Buffer	2.5 $\mu$ l
dNTP	2.5 $\mu$ l
Primers 20 mM each	0.5 $\mu$ l
Roche FASTAQ DNA Polymerase	0.2 $\mu$ l
ddH <sub>2</sub> O	17.8 $\mu$ l
Diluted sample	1.0 $\mu$ l

### PCR Cycling conditions

Step	Temp	Time	Cycles
Initial denaturation	95°C	5 min	1
Denaturation	94 °C	30 sec	35
Annealing	60°C	30 sec	
Extension	72°C	45 sec	
Finish	72°C	5 min	

**Figure 14 PCR reaction mix and cycling conditions.**

## 2.2 NIH 3T3 transcriptome analysis

To investigate circadian clock gene expression, Menger et al compared the transcriptome of forskolin-stimulated NIH 3T3 cells with SCN2.2 cells and rat suprachiasmatic nucleus in their work *Circadian Profiling of NIH3T3 Fibroblasts: Comparison with Rhythmic Gene Expression in SCN2.2 Cells and the Rat SCN* (Menger et al. 2007). Microarray data from these experiments was deposited in the National Center for Biotechnology Information's (NCBI) Gene Expression Omnibus database. Time point 1 (0 hr stimulation) data of NIH 3T3 cells (platform GPL81, accession number GSM132958) of Menger's body of work was used here to investigate expression of Smad signaling

pathway constituents. Expression of the ubiquitously expressed Acta (Actin) gene was compared to Nodal/Smad signaling components to illustrate presence of these elements in NIH 3T3 cells.

## 2.3 Cell culture

Cell culture was conducted in an Alphatech (Alphatech, Czech Republic) laminar flow hood with a 0.2 µm HEPA filter. Both the laminar flow hood and all instruments entering the hood were sterilized with 70% ethanol before and after use. Cells were grown and maintained in a 37°C/ 5% CO<sub>2</sub> water jacket incubator (VWR International, USA). Plastic ware for tissue culture was purchased from Thermofisher (USA) and Corning (USA).

### 2.3.1 NIH 3T3 Cell Culture

Mouse embryonic fibroblast NIH 3T3 cells were obtained from Victoria University and maintained in DMEM media containing 10 % new-born calf serum (ICB Bio, NZ) and 1 % Penicillin Streptomycin (Life Technologies, USA). The pH of media was monitored by the colour of the phenol red in the media which was subsequently changed when required. See *6.5 NIH 3T3 culture method*.

### 2.3.2 Thawing of cells

Cell stocks were stored in liquid nitrogen (-196 °C) in freeze media (complete growth media supplemented with 5% DMSO (Sigma, USA)). After removal from storage, cells were rapidly warmed until just thawed. Cells were not left to incubate in freeze media to prevent DMSO toxicity. Once thawed, cells in freeze media were mixed into 10 ml of growth media and centrifuged at 180 x g for 3 minutes in an Eppendorf centrifuge 5810R. The resulting supernatant was removed and the cells were re-suspended in 10 ml of growth media and re-plated into cell culture flasks.

### 2.3.3 Passaging of Cells

Cells were passaged with 37°C 0.25% Trypsin (Life Technologies, USA) in EDTA (BDH, UK) after being washed with 37°C growth media. When cells were at around 80% confluence they were passaged, and plated at a seeding density of 1:6 of the original culture.

### 2.3.4 Freezing of cells

Cells were frozen at  $1-3 \times 10^6$  cells per cryovial in a freeze medium of 20% Foetal Bovine Serum (ICB Bio, NZ) 2.5% Penicillin Streptomycin (Life Technologies, USA) and 10% DMSO (Sigma, USA) in DMEM media (Life Technologies, USA). First cells were placed in a “Mr Frosty” box in -80°C overnight to freeze cells at 1°C per hour. This slow freezing prevents ice crystal formation and subsequent damage to cells. Twenty-four hours later, cryovials were transferred to a liquid nitrogen dewar for long term storage.

### 2.3.5 Transfection of NIH 3T3 cells with Lipofectamine 2000 and 3000

Cells were transfected using Lipofectamine 2000 or 3000 reagent (Thermofisher Scientific, USA) according to the manufacturer’s protocols (*6.5.1 Lipofectamine 2000 Protocol* and *6.5.2 Lipofectamine 3000 Protocol*).

## 2.4 Fluorescent Microscopy

Transfected cells were photographed using an Olympus IX53 microscope with an Olympus DP73 camera, Olympus TH4-200 white light and LumenDynamics X-Cite Series 120 Q mercury light. CellSense software (Olympus, NZ) was used for photography.

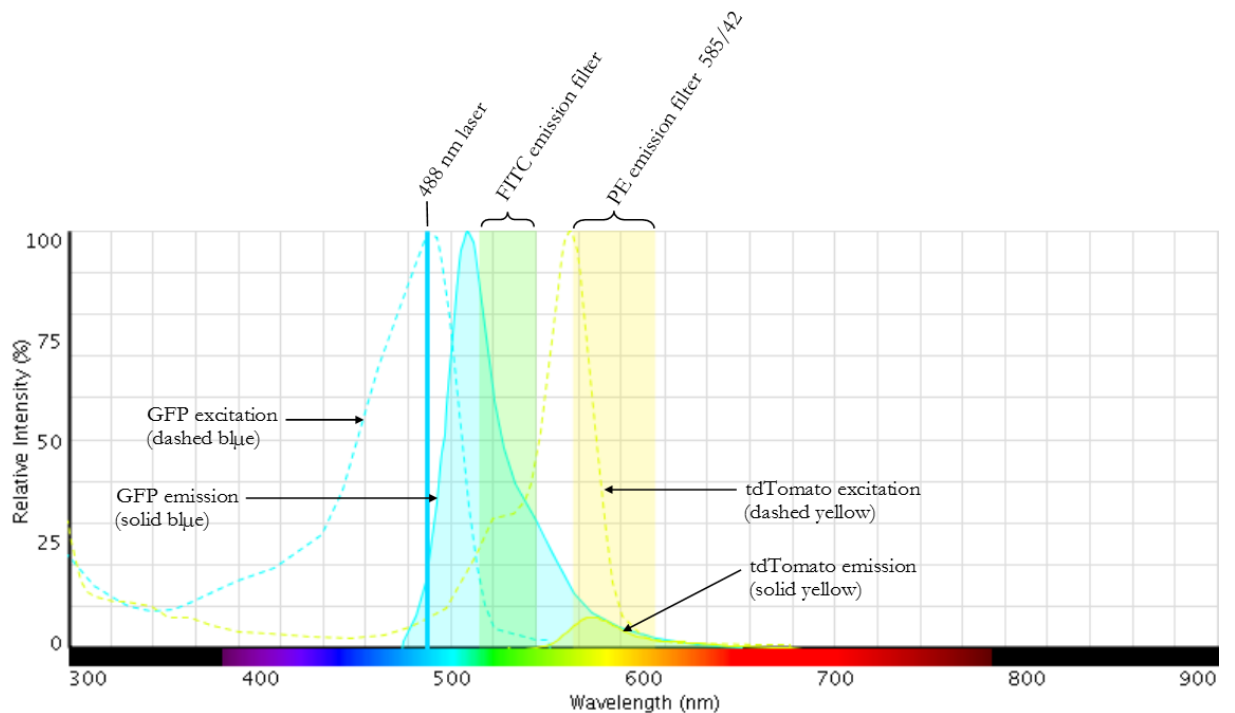
## 2.5 Flow cytometry

Transfected cells were lifted from adherent growth surfaces (12-48 well plates, Thermofisher, USA) with 37°C 0.25% Trypsin (Life Technologies, USA) in EDTA (BDH, UK). Cells were centrifuged to remove Trypsin and resuspended in FACS buffer (2% new-born calf serum (ICB Bio, NZ) in PBS).

Cells were analysed on a Canto II flow cytometer and data was examined and interpreted using FLOWJO 7.6.1 software (Tree Star, Ashland, OR, USA) or Flowing Software (Cell Imaging Core, Turku Centre for Biotechnology, Finland). The Canto II cytometer is limited in its capacity to detect red fluorescence emission. The cytometer has three lasers; 405 nm, 488 nm and 633 nm. As illustrated in Figure 15 (yellow dotted line), the excitation peak of tdTomato lies at about 580 nm, meaning that the 633 nm laser would not excite tdTomato fluorescent protein. We therefore used the 488 nm laser to excite both GFP and TOM fluorescent proteins and used two filters; the FITC 530/30 and the PE 585/42, to collect emission data of GFP and TOM, respectively. Amount of excitation of tdTomato was limited by the excitation spectra (yellow dotted line) which is at 488 nm, and subsequently, a small peak of tdTomato emission is induced (solid yellow). The detection efficiency table, (B) in Figure 15, shows the amount of emission (based on excitation by the 488 nm laser) collected by the FITC and PE filters. Table (C) shows the amount of fluorescence collected normalized to percentage of excitation spectra that is being excited at 488 nm and to relative fluorescence intensity of the fluorophores. For example; 100% of GFP excitation spectra is induced by the 488 nm laser. This was multiplied by 56,000, the fluorophore intensity coefficient (Shaner, Steinbach, and Tsien 2005) and the result was multiplied by 35% (0.35, the amount of GFP

emission collected by the FITC filter) to arrive at a number that represents the amount of fluorescence normalized to fluorophore intensity. Fluorophore intensity coefficient of tdTomato is 138,000 (Shaner, Steinbach, and Tsien 2005).

## A Fluorescence spectra table



## B Detection efficiency

Fluorophore / Filter	FITC	PE
tdTomato	0.7%	63.8%
GFP (emerald GFP)	35.0%	6.4%

## C Florescence collected by FITC and PE filters normalized to fluorophore intensity

Fluorophore / Filter	FITC	PE
tdTomato	77	7043
GFP (emerald GFP)	19600	3584

**Figure 15** Florescence spectral graph, Detection efficiency table and florescence normalized to fluorophore intensity table. (A) Fluorescence spectral graph showing GFP and TOM (tdTomato) excitation and emission. Solid blue line at 488 represents the 488 nm laser used on the BD Canto II flow cytometer. Dotted lines show excitation of GFP (blue) and TOM (yellow). Solid blue and yellow areas represent GFP and TOM emission respectively, when excited by the 488 nm lazer. The FITC emission filter

was used to collect GFP emission data, and the PE emission filter was used to collect TOM emission data.

(B) Spillover table showing percentage of GFP and TOM emission collected by the FITC and PE filters. Both Graph and table were generated using the ThermoFisher Scientific Fluorescence SpectralViewer tool.

(C) Table showing amount of florescence emission collected normalized to percentage of excitation spectra induced by the 488 nm laser and fluorophore intensity.

Figure 16 shows the voltage settings for experiments run in this body of work. These were determined by running sample tubes, collecting forward and side scatter data, and altering voltages accordingly to generate data in which cells of interest are visualized appropriately.

Parameter	Voltage
FSC	170
SSC	400
GFP	230
PE	300

**Figure 16 Cytometer Parameters.** Forward scatter (FSC), side scatter (SSC), GFP and PE data were collected.

## 2.6 Creation of transgenic mouse line containing SBE16x-SCP-GFP construct

After confirming reporter activity of the SBE16x-SCP-GFP, we created a transgenic mouse line. The SBE16x-SCP-GFP vector was cut with XhoI and SalI (restriction sites illustrated in Figure 17) and the restriction mix was subsequently run on an agarose gel from which the fragment of interest was cut. The gel piece was digested and DNA isolated as described above in 2.2.8 *Agarose Gel Digestion*. The DNA was reconstituted in injection buffer (see 5.3 *Injection Buffer*) This process removed the bacterial component of the vector and prepared the sample for pronuclear injection performed by Ric Broadhurst at AgResearch New Zealand.



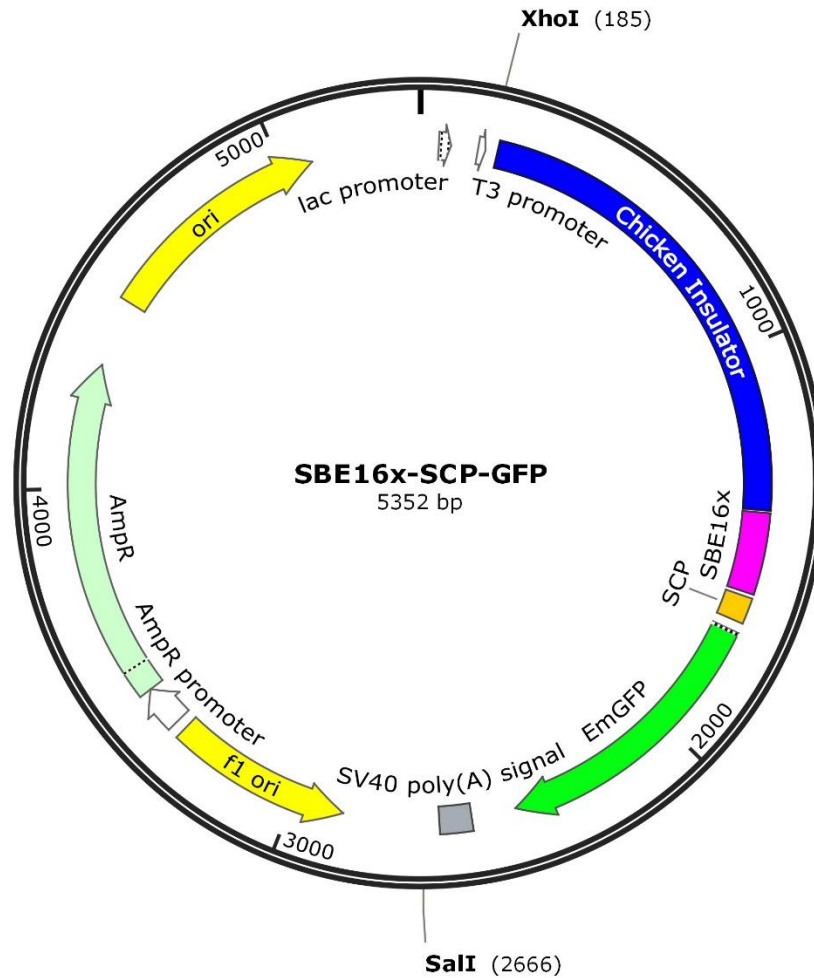


**Figure 17 Restriction strategy for preparation of vector for pronuclear injection.** SBE16x-SCP-GFP was cut with XhoI and SalI to separate bacterial components from region of interest. Image generated using SnapGene.

## 2.6.1 Genotyping mice

Offspring of the pronuclear injection described in 2.6 *Creation of transgenic mouse line containing SBE16x-SCP-GFP construct* were ear-notched and tail clipped at Ag Research. Tail clips were couriered to Victoria where genotyping of offspring was performed. Samples were digested in 200  $\mu$ l Proteinase K buffer (5.4 *Proteinase K Buffer*) containing 0.2 mg/ml Proteinase K for 2 hours in a 55  $^{\circ}$ C thermomixer (900 RPM). Digested samples were diluted at a 1:4 ratio in water and amplified

by PCR according to the protocol described in *2.2.13 PCR Protocol* using GFP primers. PCR products were subsequently run on a gel to determine presence of transgene.

## 2.6.2 Production and analysis of transgenic mice

One male mouse, transgenic for SBE16x-SCP-GFP, was couriered to Victoria University from Ag Research and mated with two wild type Swiss female mice. Conception day (embryonic day 0) was noted by probing for semen plugs in the female vagina, and females were sacrificed at embryonic day 6 (E6) and 8.5 (E8.5). Embryos were harvested and visualized under fluorescent microscopes, then subsequently analysed by PCR for presence of transgenic gene.

### 3 Results

### 3.1 Design strategy of a Nodal/Activin signaling reporter

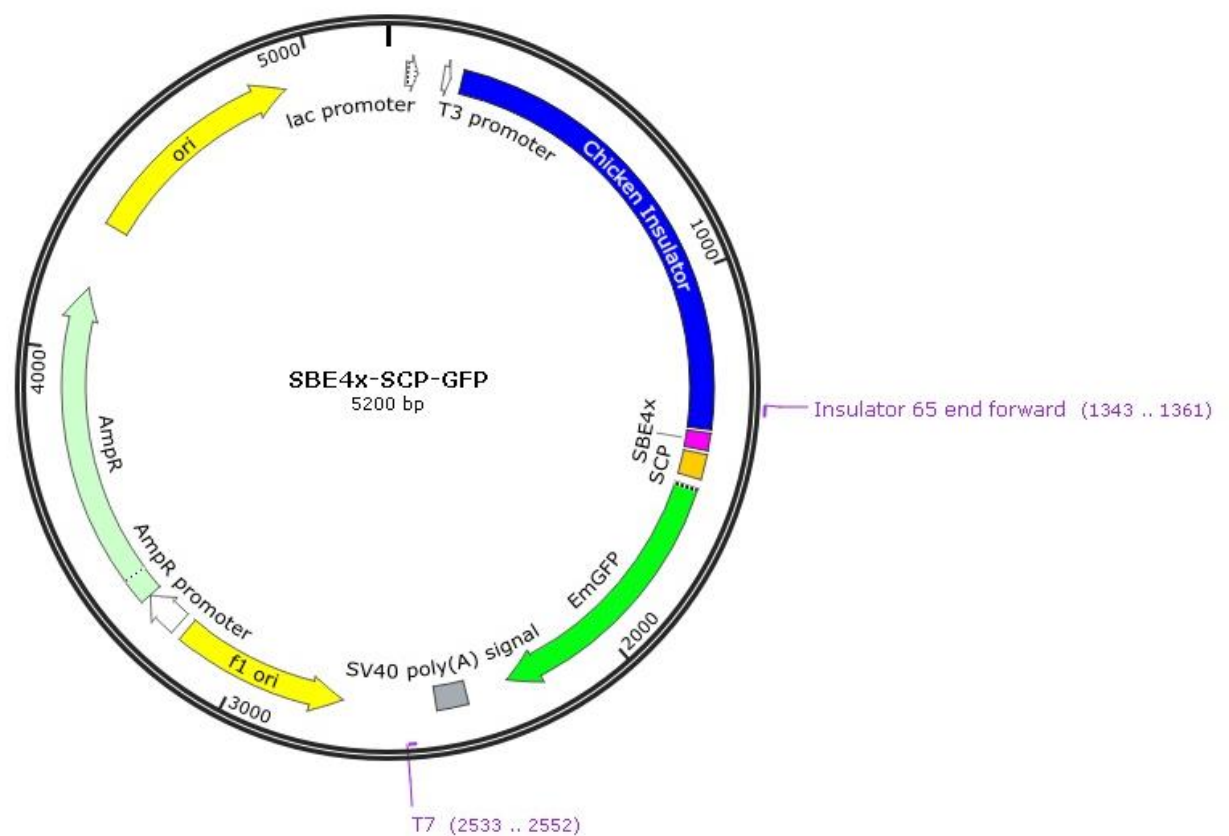
A Smad binding element (SBE) was designed based on Dennler et al's CAGA box 'AGCCAGACA' as this element, adapted from the PAI-1 promoter, was shown to confer TGF $\beta$  and Smad3 signalling. Dennler et al showed that the CAGA box had greater reporter efficacy when multimerised in 12 repeats than 9 repeats, spurring us to design a SBE that could be multimerised to investigate sensitivity of Smad signalling. We designed a 4x repeated CAGA box linked by adenine and thymine regions which we named SBE4x. Oligos were designed as illustrated in *2.1.1 SBE adapter/insert and vector design* and ordered from Sigma, NZ. SBE4x product was generated annealing fragments together and SBE4x was subsequently cloned into recipient vectors (*2.1.1 SBE adapter/insert and vector design*).

### 3.2 Construct generation

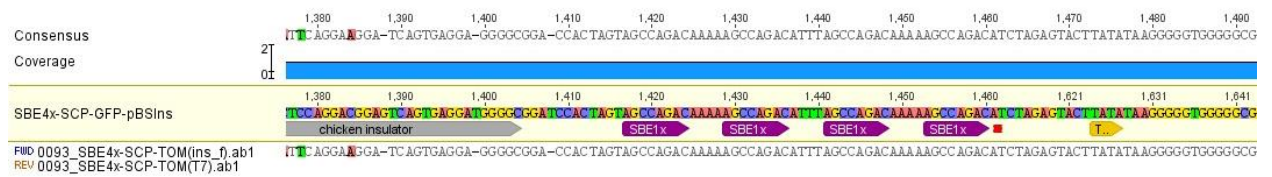
#### 3.2.1 Generation of vectors containing various Smad binding affinity sites driving GFP translation

A SBE4X-SCP-GFP vector was created by the cloning strategy described in *2.2.1 SBE adapter/insert and vector design*. This vector was transformed into DH5a E.coli cells which were grown on agar plates containing ampicillin to select for successfully transformed cells. Colonies grown on this plate were picked and expanded in LB media (3 ml) containing ampicillin and mini-prepped (see *2.2.10 Miniprep protocol*). DNA from minipreps was analysed by restriction digest and agarose gel to visualise fragment sizes. Minipreps containing correct vector (those that had the insert in correct number of times and correct orientation – determined by restriction digest and gel electrophoresis) were subsequently expanded in a larger volume (50 ml) and midi-prepped. Midi prepped sample concentration was determined using a nanodrop spectrometer and aliquoted samples were sent to

Waikato University Sequencing Facility for sequencing. Figure 19 illustrates 100% sequence match between clone chart and sequencing read of the SBE4x-SCP-GFP. This shows that we successfully created a SBE4x element from designed oligos (Figure 10: *SBE4x binding element insert design*) which was inserted into the target vector in the correct orientation. Primers used for this sequencing were insulator 65 end forward and T7, as shown in Figure 18. These primers were chosen as they will sequence through the cloning sites of interest giving information on both the number of SBE repeats and their orientation.

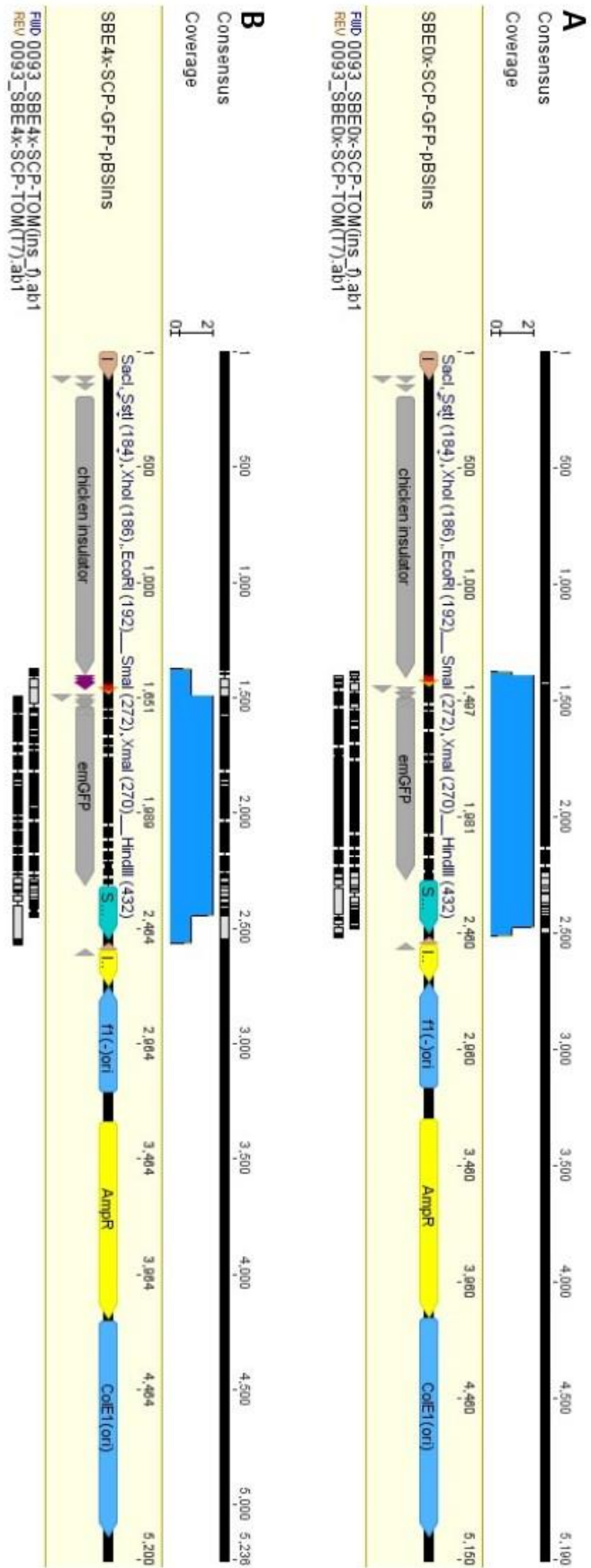


**Figure 18 Primer locations on SBE4x-SCP-GFP vector.** Insulator 65 end forward and T7 primers were used to sequence vectors.



**Figure 19 Sequence read SBE4x-SCP-GFP against clone chart.** Sequence read shows a 100% match between reference clone chart (yellow background) and created vector (bottom line).

Mutlimerisation of the SBE4x segment was generated as explained in 2.2.1 *SBE adapter/insert and vector design*. Through this cloning strategy, SBE8x- and SBE16x-SCP-GFP were generated. SBE0x-SCP-GFP was generated by removing the SBE4x segment from SBE4x-SCP-GFP. Alignments of sequencing results against clone charts of SBE0x-, 4x-, 8x and 16x-SCP-GFP are shown in Figure 20 A-D.



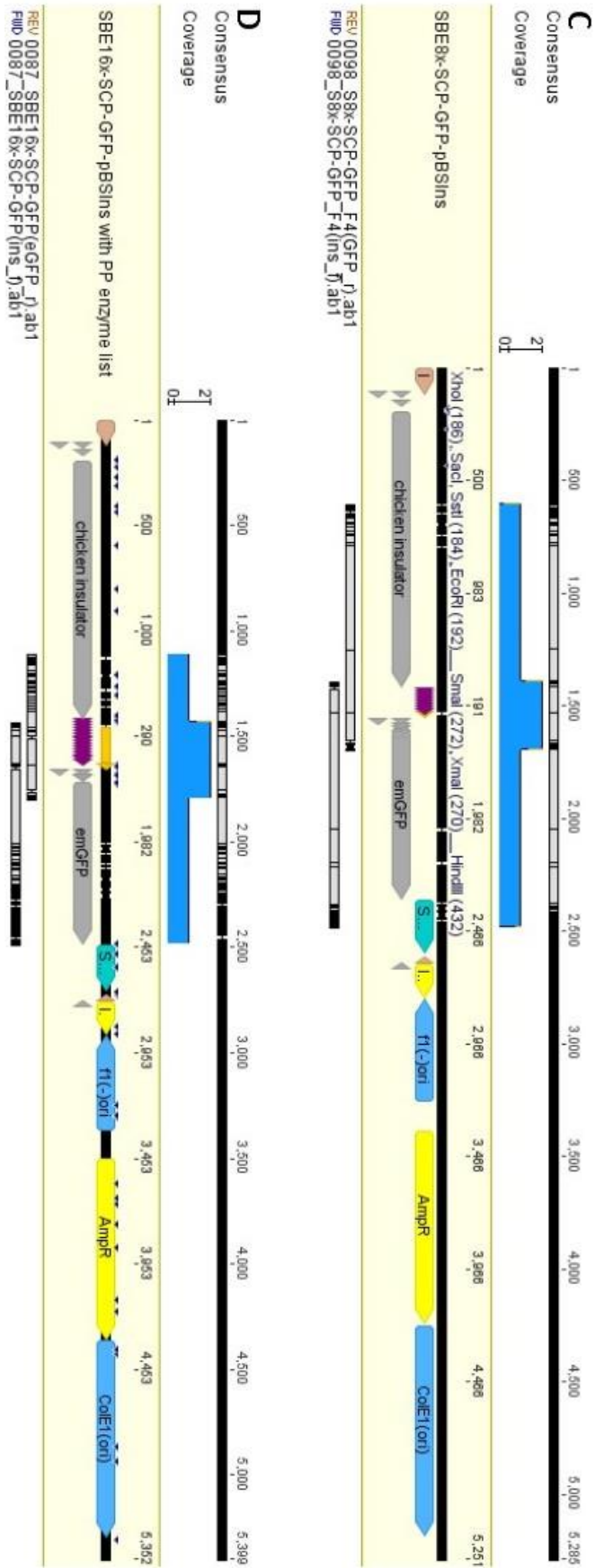




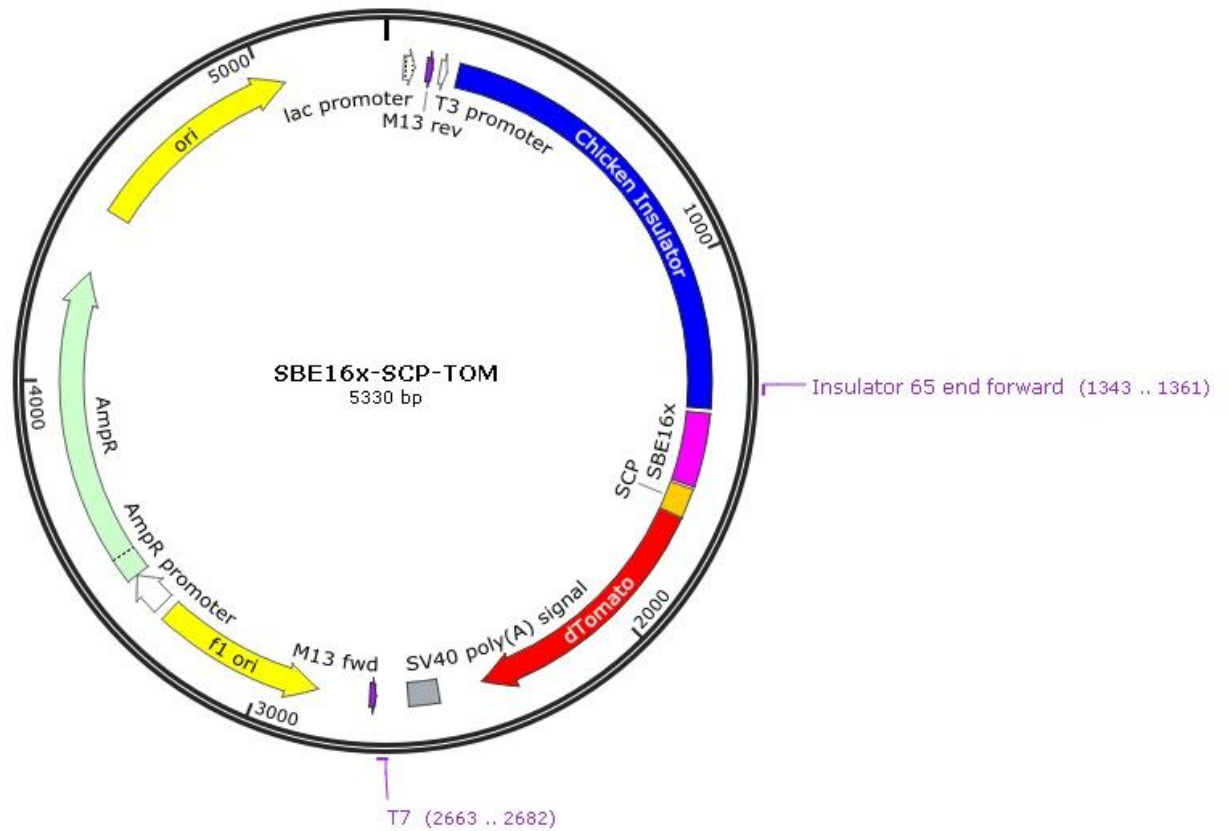
**Figure 20 SBE<sub>n</sub>x-SCP-GFP sequencing reads aligned to reference clone charts.** SBE<sub>8</sub>x- and 16x-SCP-GFP were created by multimerisation of the SBE<sub>4</sub>x element of SBE<sub>4</sub>x-SCP-GFP. SBE<sub>0</sub>x-SCP-GFP was created by “cutting out” the SBE<sub>4</sub>x element from SBE<sub>4</sub>x-SCP-GFP. These sequence alignments show that vectors with various binding elements were created, in correct orientation.

### 3.2.2 Generation of SBE<sub>16</sub>x-HSP-GFP vector

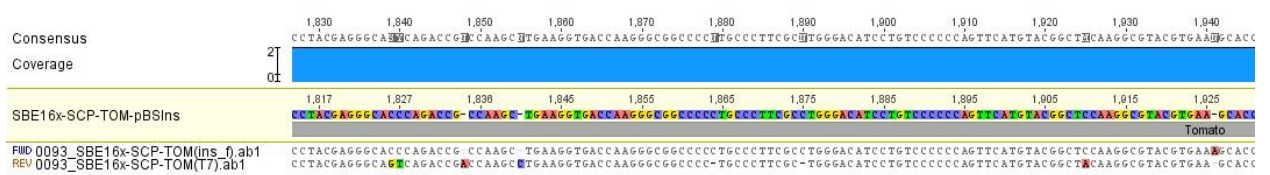
A SBE<sub>16</sub>x-HSP-GFP vector was generated by exchanging the SCP element from SBE<sub>16</sub>x-SCP-GFP for a HSP element excised from RAstat<sub>12</sub>x-HSP-GFP.

### 3.2.3 Generation of vectors containing various Smad binding affinity sites driving TOM translation

SBE<sub>0</sub>x-, 4x-, 8x- and 16x-SCP-TOM constructs were made by creating a tomato element from a reference vector (see 2.2.4 *Generation of tomato element*). GFP elements from SBE<sub>0</sub>x-, 4x-, 8x- and 16x-SCP-GFP were excised and replaced with tomato elements. Sequencing results showed some single base mismatches. These were discounted as SNPs and credited to sequencing errors as only one of the two sequencing reads contained the mistake, as seen in Figure 22. Insulator 65 end forward and T7 primers used for sequencing constructs, location of these primers on construct vectors is illustrated in Figure 21.

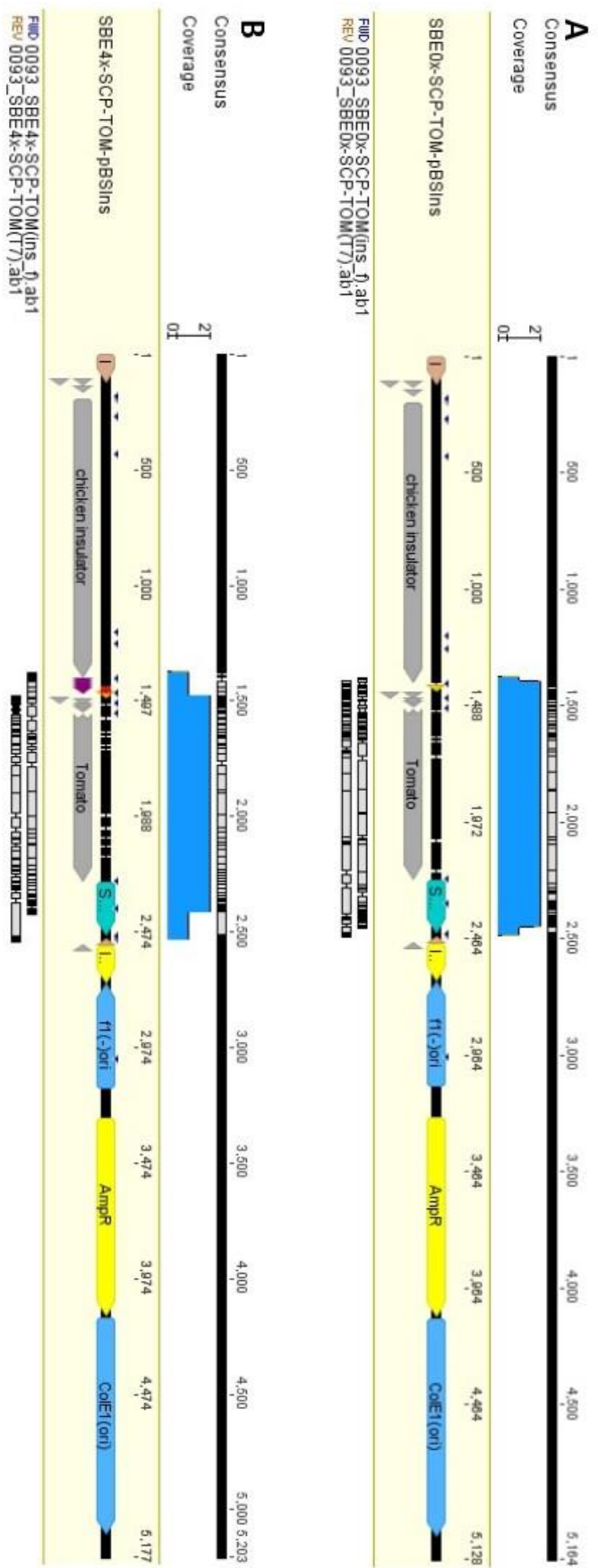


**Figure 21 Primer locations on SBE16x-SCP-TOM.** Insulator 65 end forward and T7 primers were used to sequence vectors to illustrate correct orientation and sequence of the tomato element.



**Figure 22 Sequencing read SBE16x-SCP-TOM against clone chart showing sequencing errors.** Single base errors seen in one sequence and not the other were regarded as sequencing errors, not SNPs.

Figure 23(*A-D*) shows alignments of sequencing results against clone chart for SBE0x-, 4x-, 8x- and 16x-SCP-TOM. Primers insulator forward and T7 were used to sequence through the tomato element.



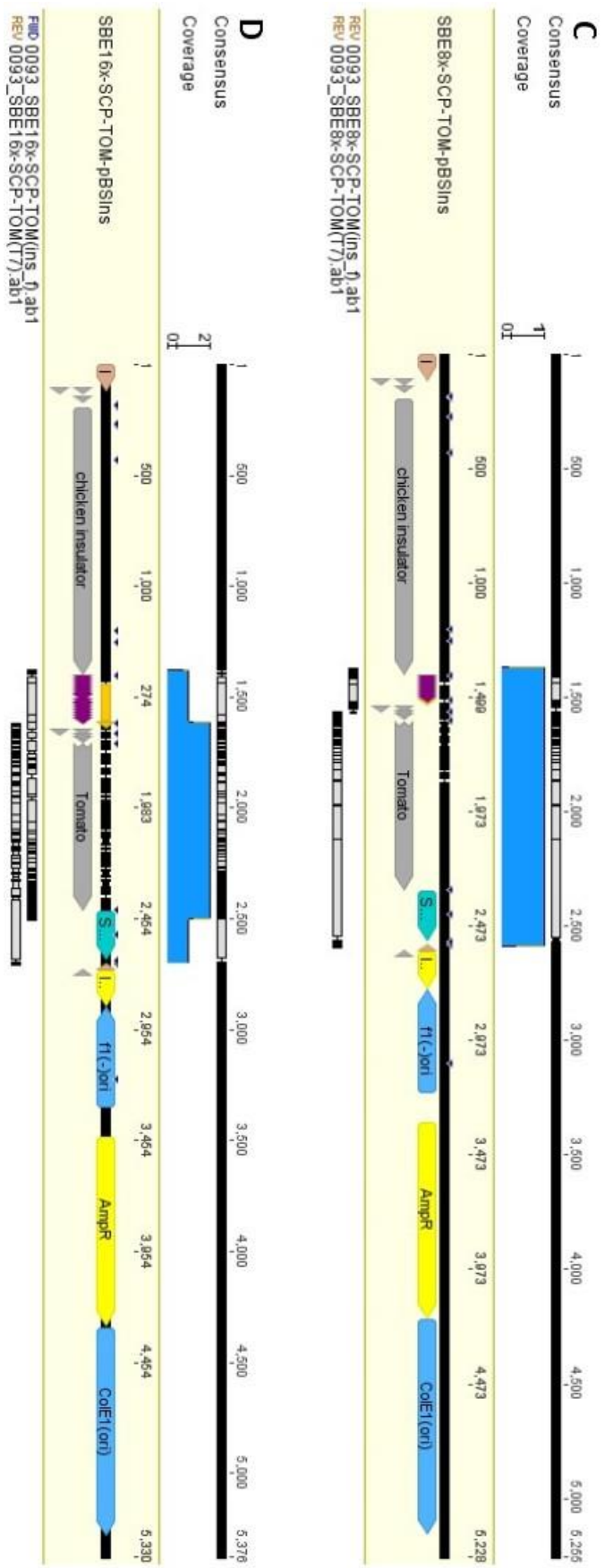


**Figure 23 SBEnx-SCP-TOM sequencing reads aligned to reference clone charts.** SBE0x-, 4x-, 8x and 16x-SCP-TOM were created by removing the GFP element from SBE0x-, 4x-, 8x and 16x-SCP-GFP and replacing it with a tomato element created as described in 2.2.4 *Generation of tomato element*. These sequence alignments show that vectors containing a tomato element containing no SNPs and in the correct orientation were created.

### 3.3 Indication of Nodal/Activin signaling components in 3T3 cells

An appropriate immortalised cell line was required to carry out investigations into fluorescent genetic reporter activity. NIH 3T3 cells were chosen as they are a robust, well characterized and widely used mouse embryonic fibroblast line. Additionally, Dennler et al have reported positive SBE reporter investigations using NIH 3T3 cells (Dennler et al. 1998a). Analysis of Menger et al's *Circadian Profiling of NIH3T3 Fibroblasts: Comparison with Rhythmic Gene Expression in SCN2.2 Cells and the Rat SCN* microarray data indicates that Smad signaling constituents are present in NIH 3T3 cells (Figure 24). Acvr1b Acvr2a and Acvr2b are the Activin TGF $\beta$  receptors which Nodal and Activin bind to induce intracellular secondary signals, Tdgf1 is the gene coding for Cripto, the TGF $\beta$  co-receptor and FoxH1 is a transcription factor required to mediate Smad2 binding to DNA. Acta1 codes for the protein actin which is constitutively expressed in most cell types. Nodal is expressed at low levels in NIH 3T3 cells meaning our reporter signal will represent amount of ligand that cells are incubated in rather than native Nodal expression.

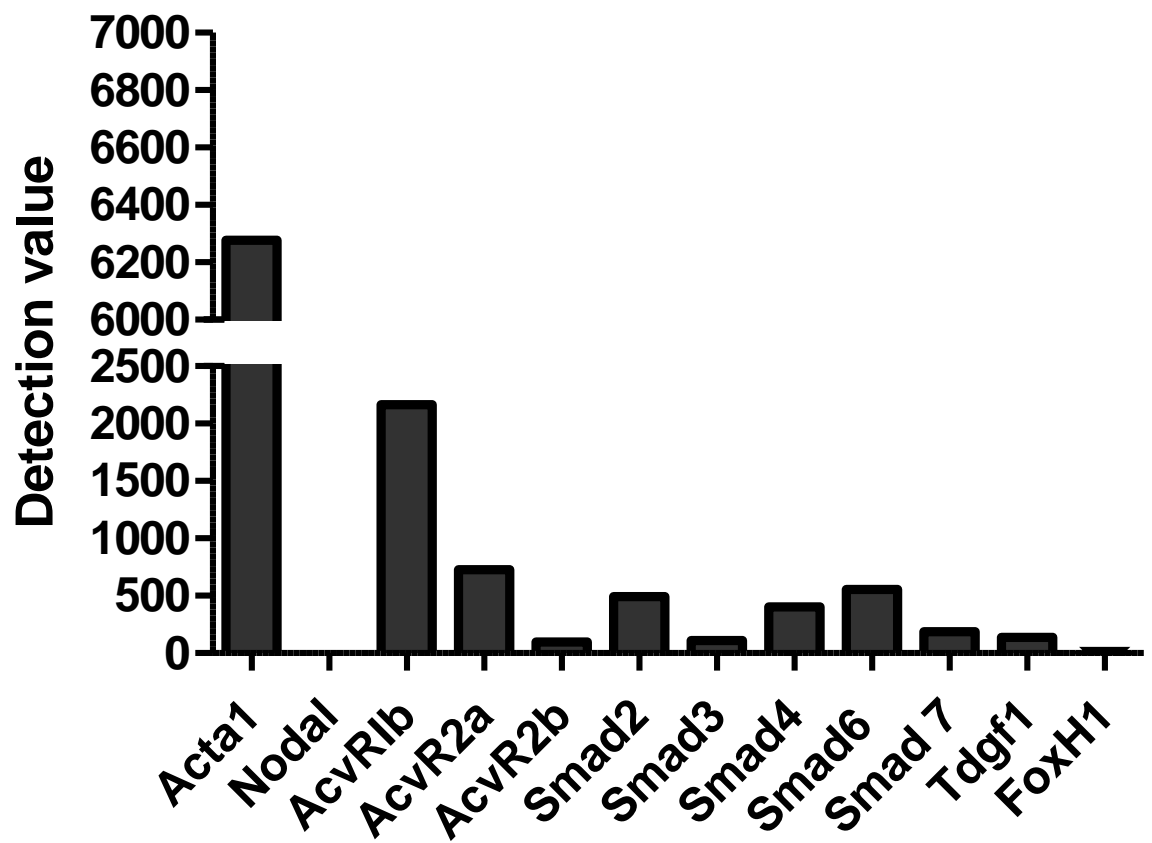


Figure 24 Expression profiles of Smad signaling constituents and housekeeping genes in NIH 3T3 cells. Transcriptome analysis of NIH 3T3 cells indicates the presence Smad signaling components.

### 3.4 *In vitro* results

#### 3.4.1 Response of SBE0x-, 4x- and 8x-SCP-GFP transfected NIH 3T3 cells to increasing concentrations of Activin

To determine response of various sensitivity SBE vectors to increasing concentrations of Activin, we transfected NIH 3T3 cells with SBE0x-, 4x- or 8x-SCP-GFP and subsequently incubated transfected cells with 0.00, 0.01, 0.10, 1.00, 10.00 or 100.00 ng/ml Activin (PeproTech, USA) for 48 hours. These Activin concentrations were chosen as we wanted to illustrate the response of our reporter system to a range of ligand concentrations, and because Dennler et al show a response of Mv-1Lu cells transfected with their CAGA reporter to 20 ng/ml Activin. Considering this, we decided to use a range of activin treatments which incorporated 20 ng/ml. Fluorescent output of our reporter system, and therefore amount of Smad signaling occurring in the cells was visualised by fluorescent microscopy and quantified by flow cytometry. The gating strategy used for collection of GFP positive cells from flow cytometry data is shown below in Figure 25.



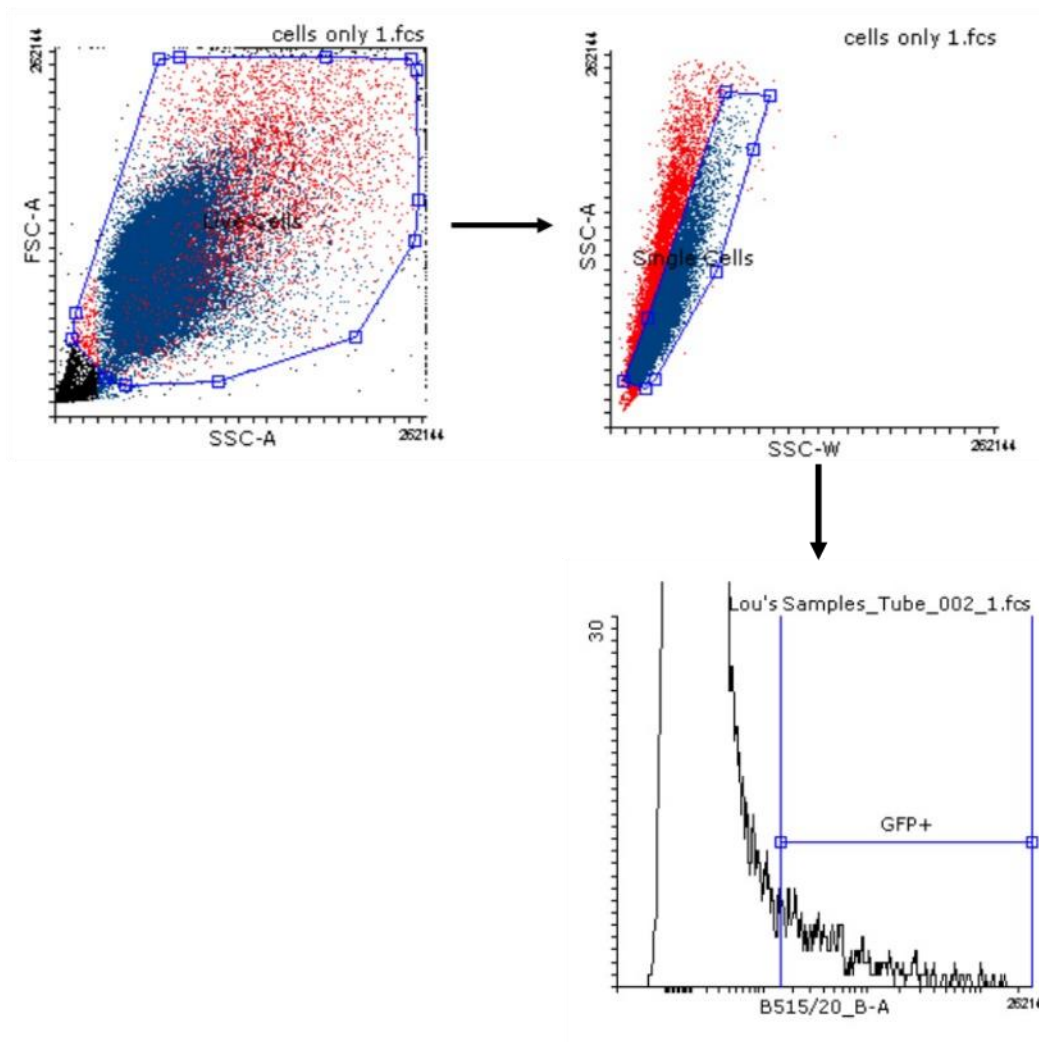


**Figure 25 Gating strategy used to determine number of and fluorescent output of GFP expressing cells.** Live cells were first determined by a gate of cells plotted by forward scatter and side scatter area. Single cells were then determined by gating side scatter area against side scatter width to determine and eliminate doublets. GFP fluorescence was gated for using a histogram. Positive events were gated for based on background and negative signal.

Figure 26 shows that SBE0x-SCP-GFP, SBE4x-SCP-GFP and SBE8x-SCP-GFP do not respond to an increasing concentration of Activin signaling. Background levels of fluorescence are seen between geometric mean of 2000 and 3000 for all 3 constructs at all concentrations of Activin treatment. A trend of increasing number of GFP<sup>+</sup> cells with increasing concentration of Activin

treatment is seen in cells transfected with SBE0x-SCP-GFP, SBE4x-SCP-GFP and SBE8x-SCP-GFP (Figure 27).

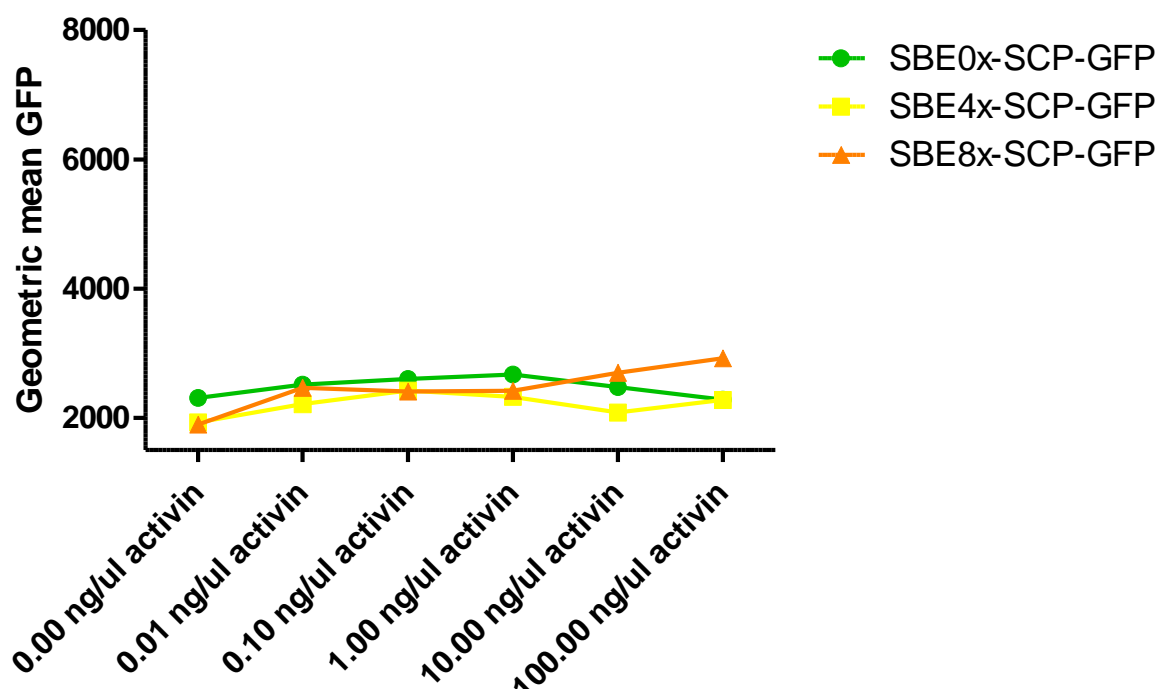


Figure 26 Geometric mean of GFP<sup>+</sup> cells transfected with SBE0x-, 4x- and 8x-SCP-GFP constructs treated with increasing concentrations of Activin for 48 hours. Cells transfected with SBE0x-, 4x- or 8x-SCP-GFP did not respond to any concentrations of Activin treatment. Values given as mean of geometric mean of GFP<sup>+</sup> cells.

	SBE0x-SCP-GFP	SBE4x-SCP-GFP	SBE8x-SCP-GFP
0.00 ng/ul activin	770	355	465
0.01 ng/ul activin	737	333	415
0.10 ng/ul activin	720	249	560
1.00 ng/ul activin	689	309	620
10.00 ng/ul activin	1163	612	908
100.00 ng/ul activin	867	538	1042

Figure 27 Average number of GFP<sup>+</sup> cells transfected with SBE0x-, 4x- and 8x-SCP-GFP constructs treated with increasing concentrations of Activin for 48 hours. An increase in the number of GFP<sup>+</sup> cells is seen in all three transfection groups.

### 3.4.2 Response of SBE16x-SCP-GFP transfected NIH 3T3 cells to increasing concentrations of Activin

After determining that SBE0x-SCP-GFP, SBE4x-SCP-GFP and SBE8x-SCP-GFP do not respond to treatment of increasing Activin concentration, we investigated the response of a higher sensitivity Smad reporter construct, SBE16x-SCP-GFP, to increasing concentrations of Activin signaling. A dose dependent response of both geometric mean of GFP<sup>+</sup> cells and number of GFP fluorescing cells was seen (Figure 28 and Figure 29, respectively). Geometric mean of GFP<sup>+</sup> cells increases from 3035 at 0.00 ng/ml Activin treatment to 5750 at 10 ng/ml and 7441 at 100 ng/ml, an almost 250% increase in fluorescence from background/baseline. Similarly, number of GFP<sup>+</sup> cells increases from 427 at 0.00 ng/ml Activin treatment to 905 at 10 ng/ml and 1098 at 100 ng/ml. Fluorescence microscopy images of NIH 3T3 cells transfected with SBE16x-SCP-GFP are shown in Figure 30. These images visualize the reporter response shown in Figure 28.

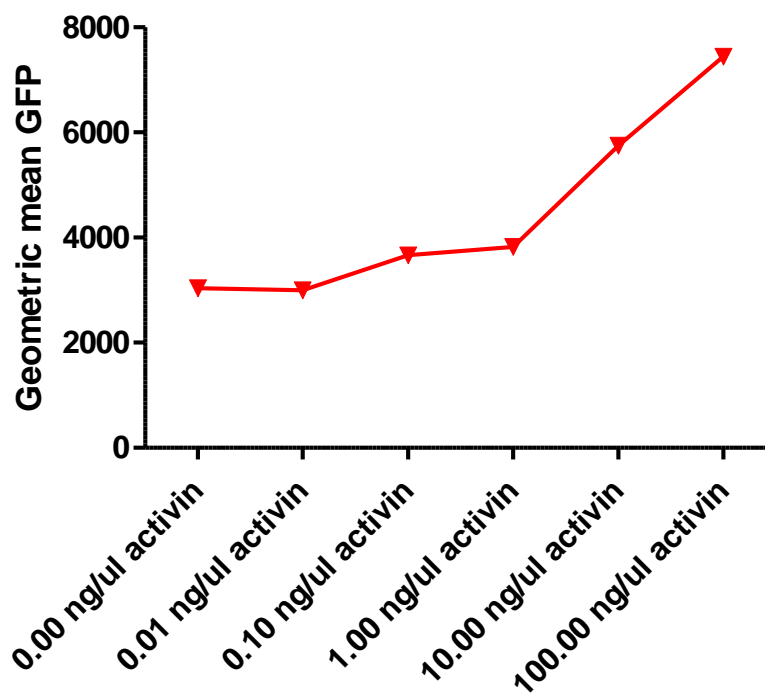


**Figure 28** Geometric mean of GFP<sup>+</sup> cells transfected with SBE16x-SCP-GFP and incubated with increasing concentrations of Activin for 48 hours. An increase in the geometric mean of GFP fluorescing cells was seen with increasing Activin treatment concentrations. Values given as mean of geometric mean of GFP<sup>+</sup> cells.

	SBE16x-SCP-GFP
0.00 ng/ul activin	427
0.01 ng/ul activin	425
0.10 ng/ul activin	441
1.00 ng/ul activin	529
10.00 ng/ul activin	905
100.00 ng/ul activin	1098

**Figure 29** Number of GFP<sup>+</sup> SBE16x-SCP-GFP transfected cells. A Activin treatment dose dependent response in the number of GFP<sup>+</sup> cells is seen.

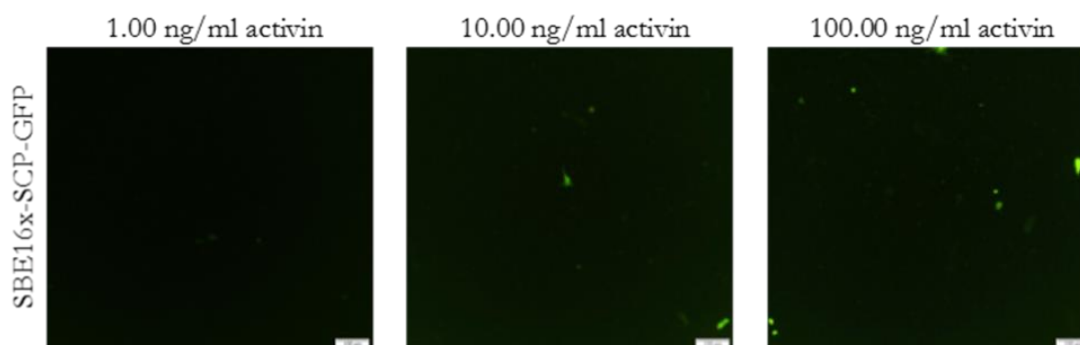


**Figure 30** Fluorescent microscopy images of NIH 3T3 cells transfected with SBE16x-SCP-GFP and treated with 1.00, 10.00 or 100.00 ng/ml activin. An increasing number of GFP fluorescing cells is seen with increasing concentrations of activin treatment.

### 3.4.3 Optimisation of Activin incubation period

To determine optimal Activin incubation time for quantification of fluorescent output, NIH 3T3 cells transfected with PmaxGFP, SBE0x-SCP-GFP or SBE16x-SCP-GFP were incubated with varying concentrations of Activin for 48 or 72 hours. From flow cytometry fluorescence quantification seen in Figure 31, we can determine that 48-hour incubation period yields greater fluorescent response of our signaling reporter system. This is most probably due to “dilution” of the vector with consecutive cell replication. We also found that cell density reached over-confluency after 48 hours of incubation time and that sufficient fluorescence was not seen at lesser time points (data not shown), such as 24 hours.

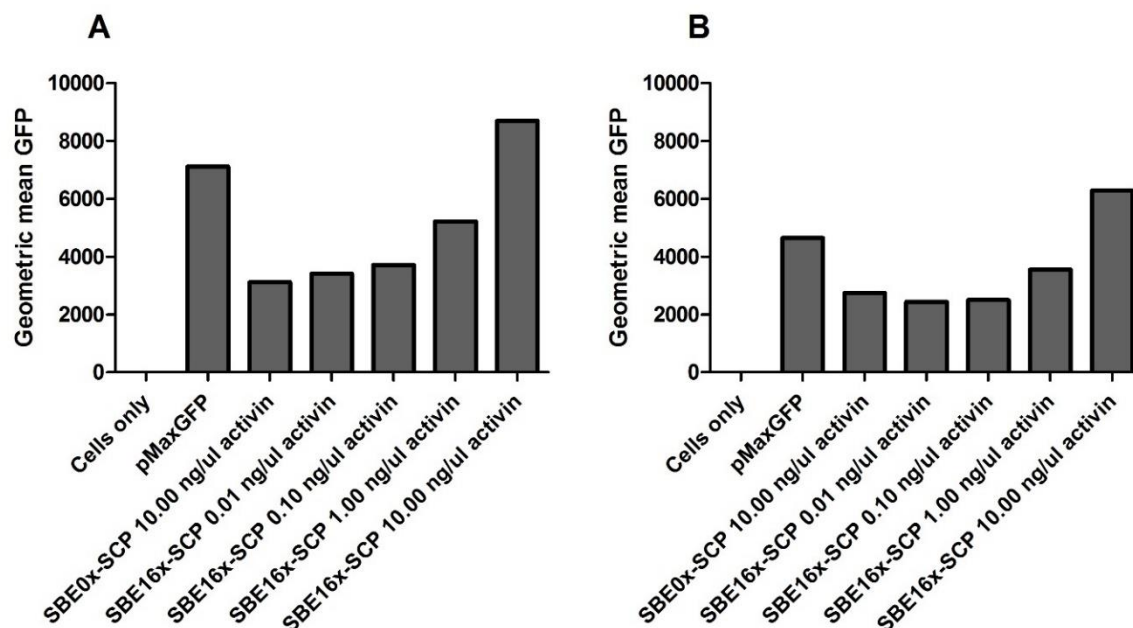


**Figure 31** Experiment to determine optimal time length for Activin incubation. NIH 3T3 cells transfected with PmaxGFP, SBE0x-SCP-GFP or SBE16x-SCP-GFP were treated with various concentrations of Activin and treated for (A) 48-hour incubation time and (B) 72-hour incubation time. Values given as mean of geometric mean of GFP<sup>+</sup> cells.

### 3.4.4 Effect of inhibitor SB431542 on fluorescent reporter system

To illustrate specificity of our Smad signaling reporter system to Activin/Nodal signaling, we demonstrated that treatment of SBE16x-SCP-GFP transfected NIH 3T3 cells with an inhibitor specific for Activin/Nodal TGF $\beta$  receptors (see 1.2.1 *Extracellular Inhibitors of Nodal/Activin Signaling*) reduces both the number of GFP<sup>+</sup> cells and the geometric mean of GFP<sup>+</sup> cells (Figure 32). A 52% percent decrease in the number of GFP<sup>+</sup> cells and a 58% decrease in the geometric mean of GFP<sup>+</sup> cells was seen. While the geometric mean of SBE16x-SCP-GFP GFP<sup>+</sup> cells decreases from 716 to 418, fluorescence does not reduce to the ‘background’ levels of 287 and 274

seen of non-transfected, 'cells only' samples. This may be due to incomplete inhibitor activity, insufficient concentration of SBE431542 inhibitor or dissociation of inhibitor from receptor complex over time.

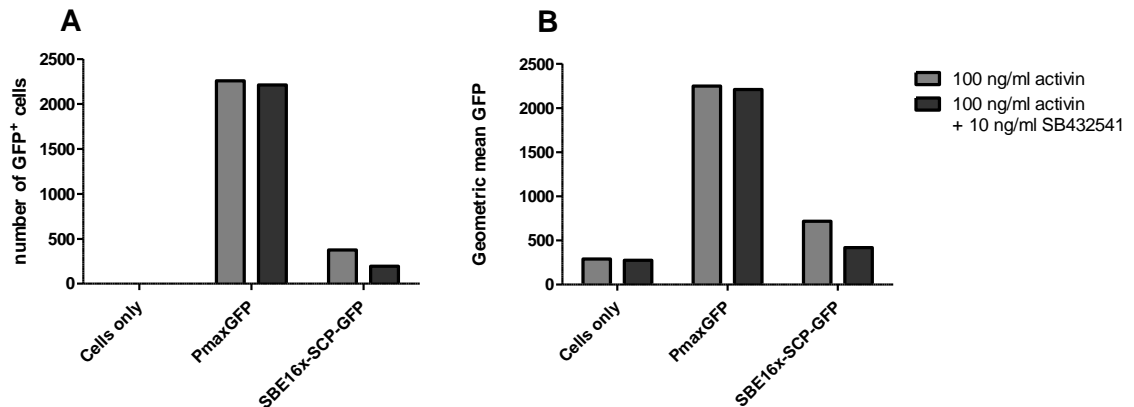


**Figure 32 Inhibitory action of SB431542 on SBE16x-SCP-GFP Smad signaling reporter system.**

Incubation of NIH 3T3 cells transfected with SBE16x-SCP-GFP in media containing 100 ng/ml Activin and 10 ng/ml SB431542 resulted in decreased fluorescent output and decrease in number of fluorescent cells compared to incubation with 100 ng/ml Activin alone. Number of and geometric mean of GFP<sup>+</sup> PmaxGFP transfected cells was not affected by inhibitor treatment. Values given as mean of geometric mean of GFP<sup>+</sup> cells.

### 3.4.5 Response of cells transfected with SBE16x-HSP-GFP to increasing concentrations of Activin

After seeing a dose dependent fluorescent response of SBE16x-SCP-GFP transfected NIH 3T3 cells to increasing concentrations of Activin treatment (Figure 28), we decided to investigate the effect of an additional minimal promoter, the Heat Shock Promoter (HSP). Figure 33 illustrates that a higher level of background/SBE enhancer-independent response is seen in cells transfected with

SBE16x-HSP-GPF compared to those transfected with SBE16x-SCP-GFP. This is seen as the geometric mean of GFP<sup>+</sup> cells is consistently between 3000 and 3500 for sample groups treated with 0.00, 0.01, 0.10 and 1.00 ng/ml Activin. 10.00 ng/ml and 100 ng/ml Activin treatment groups showed a slight increase in geometric mean of GFP<sup>+</sup> cells which may reflect a SBE enhancer-dependent response.

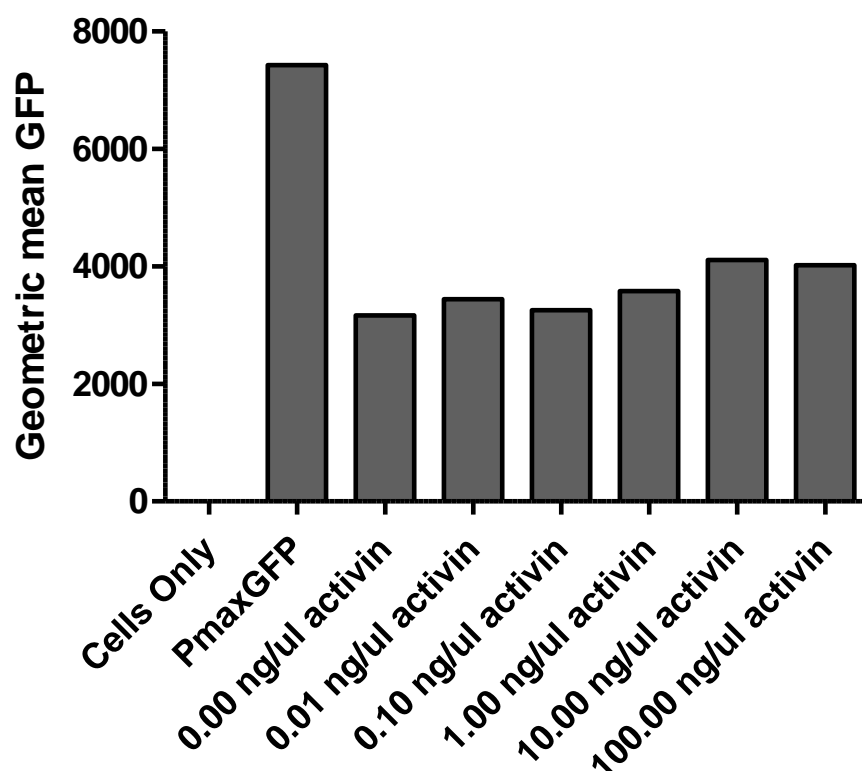


**Figure 33 Response of cells transfected with SBE16x-HSP-GFP to increasing concentrations of Activin treatment.** Little dose-dependent response of NIH 3T3 cells transfected with SBE16x-HSP-GFP to increasing concentrations of Activin treatment is seen. Values given as mean of geometric mean of GFP<sup>+</sup> cells.



### 3.4.6 Response of various Smad sensitivity constructs driving TOM via SCP to increasing concentrations of Activin

With the long-term goal of creating a reporter system containing multiple Smad sensitivity elements driving transcription of different colour fluorescent proteins, we generated SBE0x-, 4x-, 8x- and 16x-SCP-TOM vectors. These may be used in conjunction with reporters driving transcription of different coloured fluorescent proteins, such as GFP, YFP or CFP to create a multi-coloured dose-dependent reporter system. SBE0x-, 4x-, 8x- and 16x-SCP-TOM constructs were transfected into NIH 3T3 cells and treated with increasing concentrations of Activin by the same procedures used for investigating fluorescent response of SBE0x-, 4x-, 8x- and 16x-SCP-GFP to Activin treatments. The gating strategy used for collection of TOM fluorescing cells and geometric mean of TOM<sup>+</sup> cells is illustrated in Figure 34.

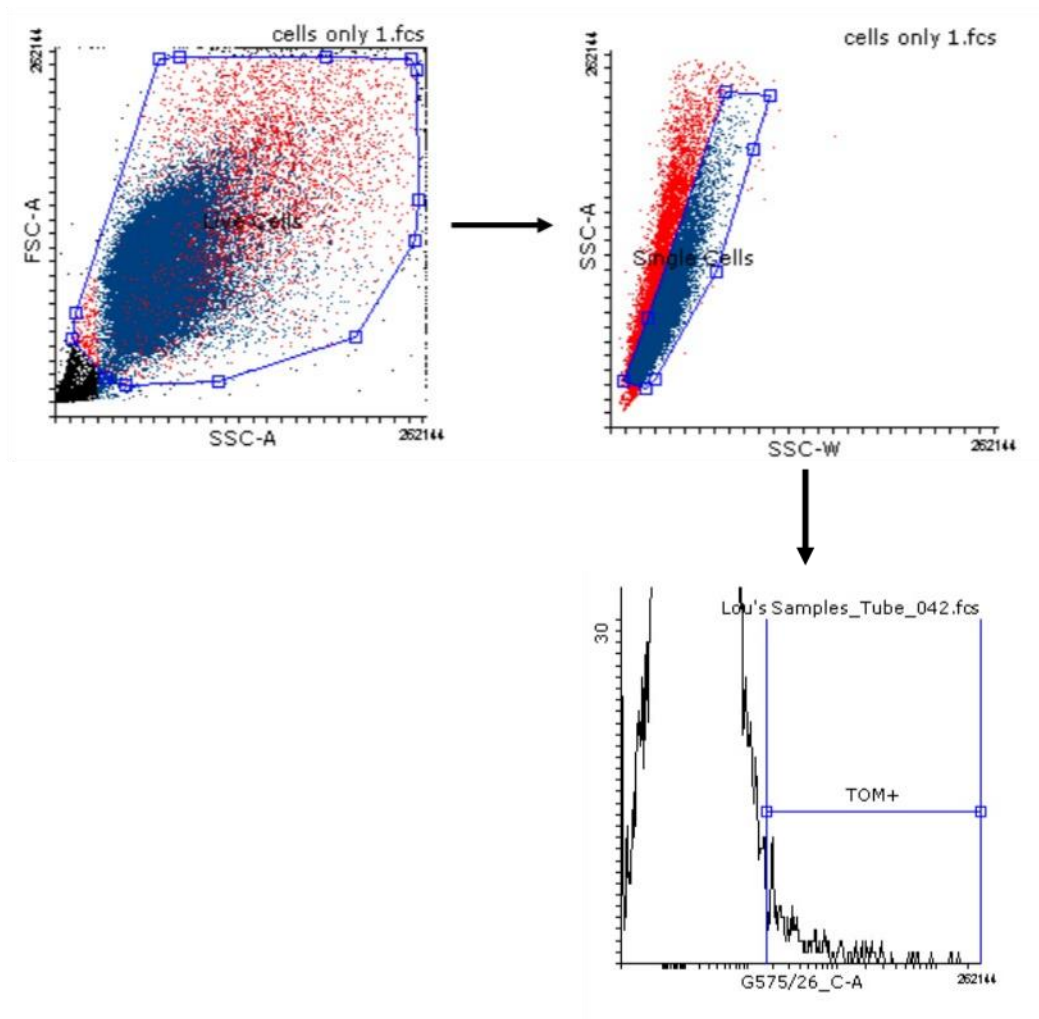


**Figure 34** Gating strategy used to determine number of and fluorescent output of TOM expressing cells. Live cells were first determined by a gate of cells plotted by forward scatter and side scatter area. Single cells were then determined by gating side scatter area against side scatter width to determine and eliminate doublets. TOM fluorescence was gated for using a histogram. Positive events were gated for based on background and negative signal.

SBE0x-SCP-TOM, SBE4x-SCP-TOM and SBE8x-SCP-TOM did not show any dose-dependent response to increasing concentrations of Activin treatment (Figure 35), similar to responses of SBE0x-SCP-GFP, SBE4x-SCP-GFP and SBE8x-SCP-GFP (Figure 26). Background levels of fluorescence are seen between geometric mean of 1000 and 2000 TOM<sup>+</sup> cells in cells transfected with SBE0x-SCP-TOM, SBE4x-SCP-TOM and SBE8x-SCP-TOM. Smad signaling-dependent response is seen in cells transfected with SBE16x-SCP-TOM to high concentrations of Activin

similar to the GFP response of SBE16x-SCP-GFP. An increase from a geometric mean of TOM<sup>+</sup> cells of 1390 with Activin treatment concentration of 0.00 ng/ml to 2341 at 10.00 ng/ml and 3834 at 100.00 ng/ml is seen. Collectively, these results indicate that a high number of SBE repeats, seen here as at least 16, are required for initiation of transcription via a super core promoter and that the SBE16x-SCP-GFP and SBE16x-SCP-TOM constructs respond to incubations with increasing concentrations of Activin in a dose-dependent manner. While the number of TOM<sup>+</sup> cells is relatively consistent between Activin treatment groups, the number of TOM<sup>+</sup> cells fluctuates widely between transfection groups (Figure 36). This is most likely due to inconsistencies in transfectional efficiency. Figure 37 shows fluorescence microscopy images of NIH 3T3 cells transfected with SBE16x-SCP-TOM. These images visualize and reiterate the reporter response of SBE16x-SCP-TOM shown in Figure 35.

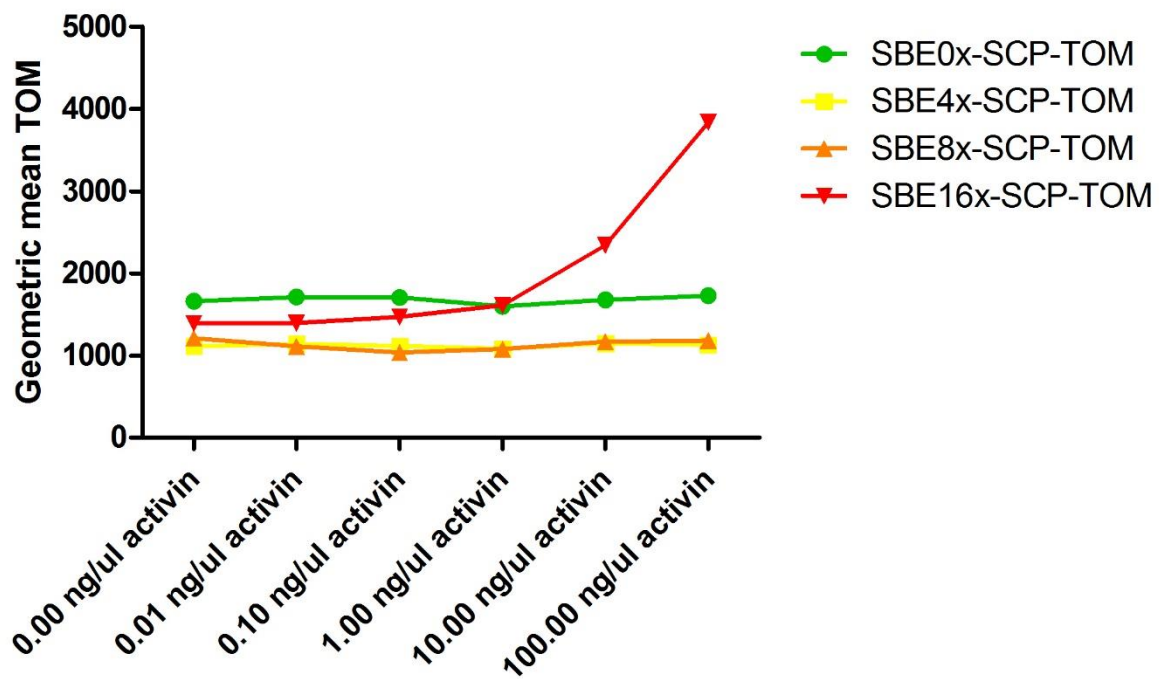
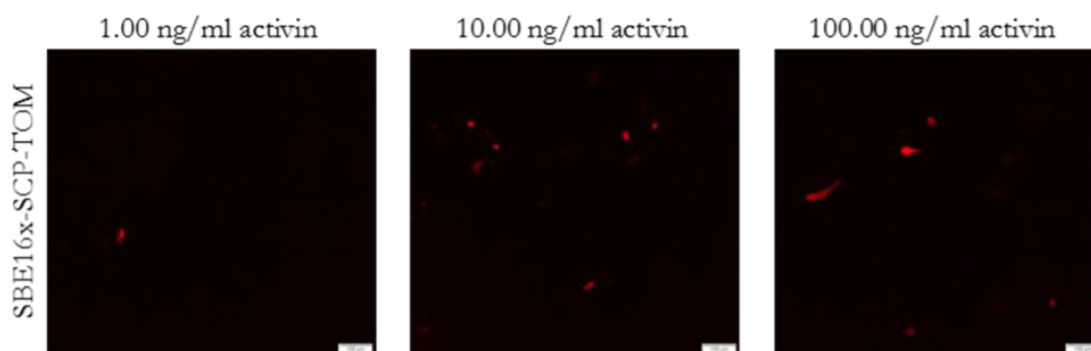


Figure 35 Geometric mean of cells transfected with SBE0x- 4x- 8x- and 16x-SCP-TOM constructs which lie in TOM<sup>+</sup> gate. A dose dependent response to Activin treatment was seen in cells transfected with SBE16x-SCP-TOM but not SBE0x-, 4x- or 8x-SCP-TOM. Values given as mean of geometric mean of TOM<sup>+</sup> cells.

	SBE0x-SCP-TOM	SBE4x-SCP-TOM	SBE8x-SCP-TOM	SBE16x-SCP-TOM
0.00 ng/ul activin	1148	829	982	1283
0.01 ng/ul activin	1075	930	771	1262
0.10 ng/ul activin	1051	655	614	997
1.00 ng/ul activin	1385	956	634	1098
10.00 ng/ul activin	1177	942	936	1224
100.00 ng/ul activin	1430	654	1038	765

Figure 36 Average number of cells in TOM<sup>+</sup> gate. Number of cells in TOM<sup>+</sup> gate varied widely between constructs, however were relatively consistent between Activin treatment grounds within construct groups.



**Figure 37** Fluorescent microscopy images of NIH 3T3 cells transfected with SBE16x-SCP-TOM and treated with 1.00, 10.00 or 100.00 ng/ml activin. An increasing number of TOM fluorescing cells is seen with increasing concentrations of activin treatment.

### 3.4.7 Co-transfection of PmaxGFP and SBE0x-, 4x-, 8x- or 16x-SCP-TOM

To normalize geometric mean of TOM<sup>+</sup> cells and number of TOM<sup>+</sup> cells to transfectional efficiency, NIH 3T3 cells were co-transfected with a positive control for transfection, PmaxGFP (25% molar ratio), and either SBE0x-, 4x-, 8x- or 16-SCP-TOM (75% molar ratio). These ratios were chosen as PmaxGFP constitutively expresses GFP at very high levels whereas our experimental vectors express fluorescence in a Smad enhancer-dependent manner and thus expressed TOM at much lower levels. Therefore, a relatively smaller amount of positive control is needed to yield positive results. Cells that were positive for GFP were seen to in a linear relationship when FITC (GFP) was graphed against PE (TOM) as seen in Figure 38, *orange arrows*. This is due to the spectral overlap of GFP into the PE filter, as explained in 2.5 *Flow Cytometry* and Figure 15.

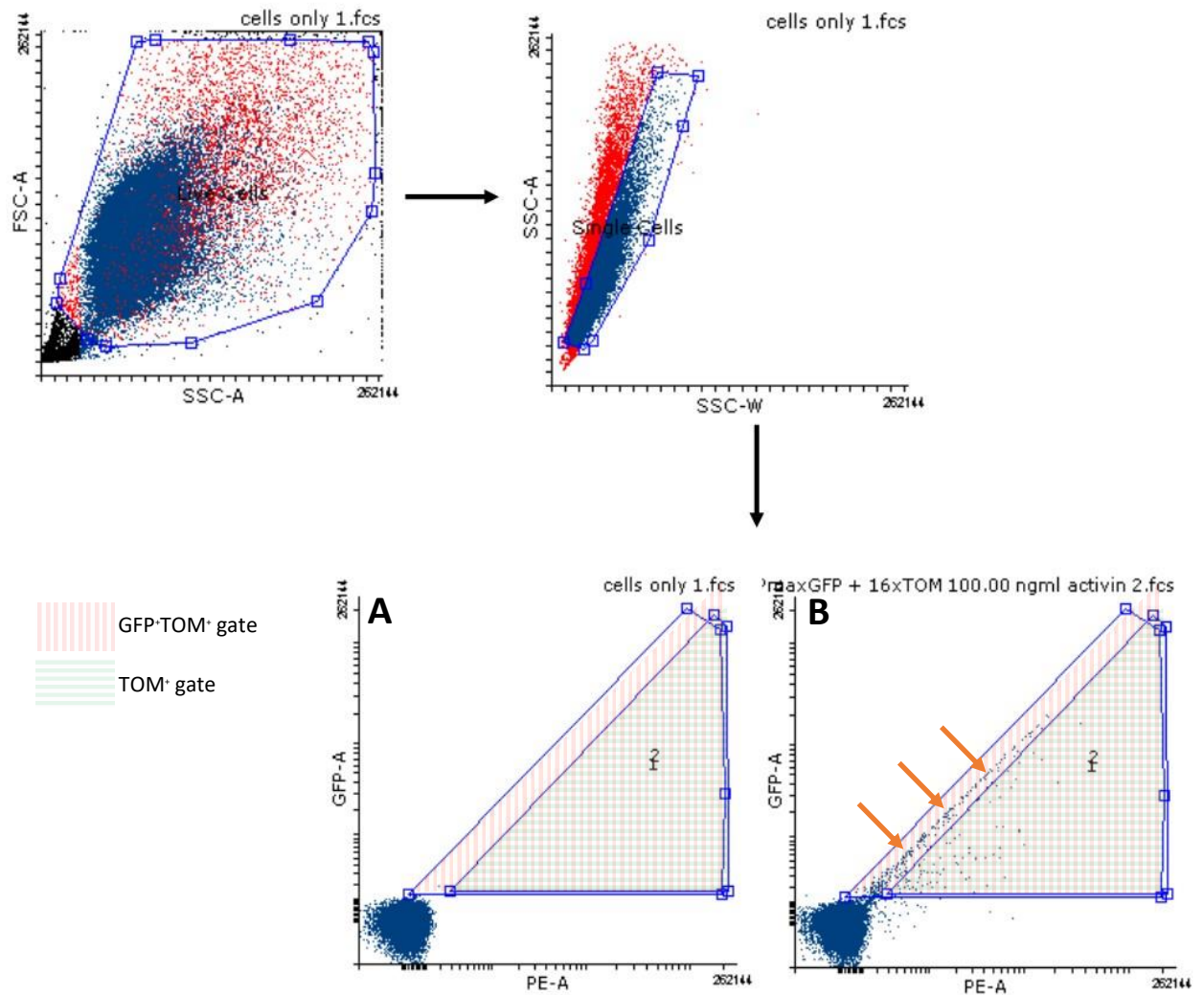
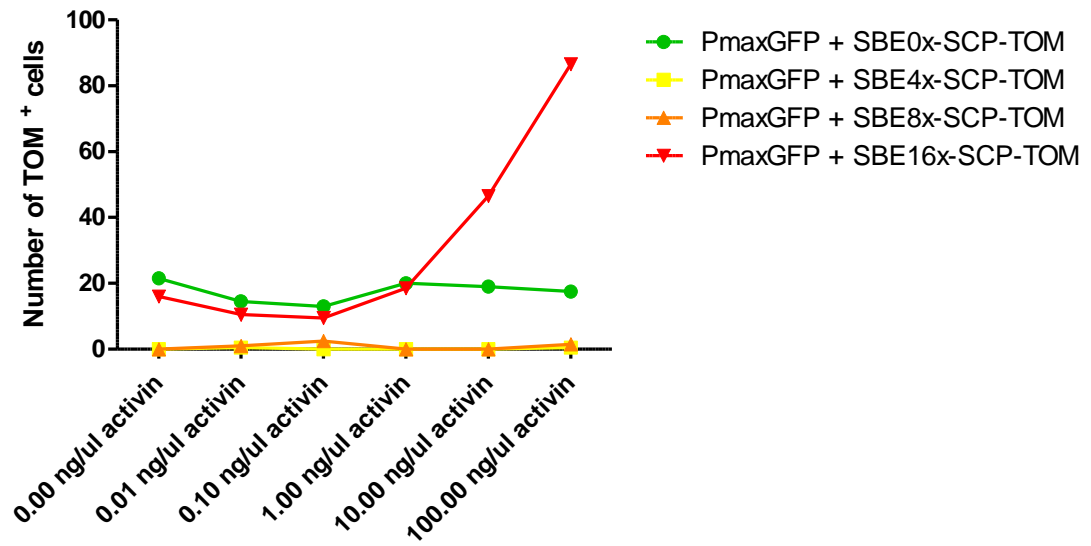


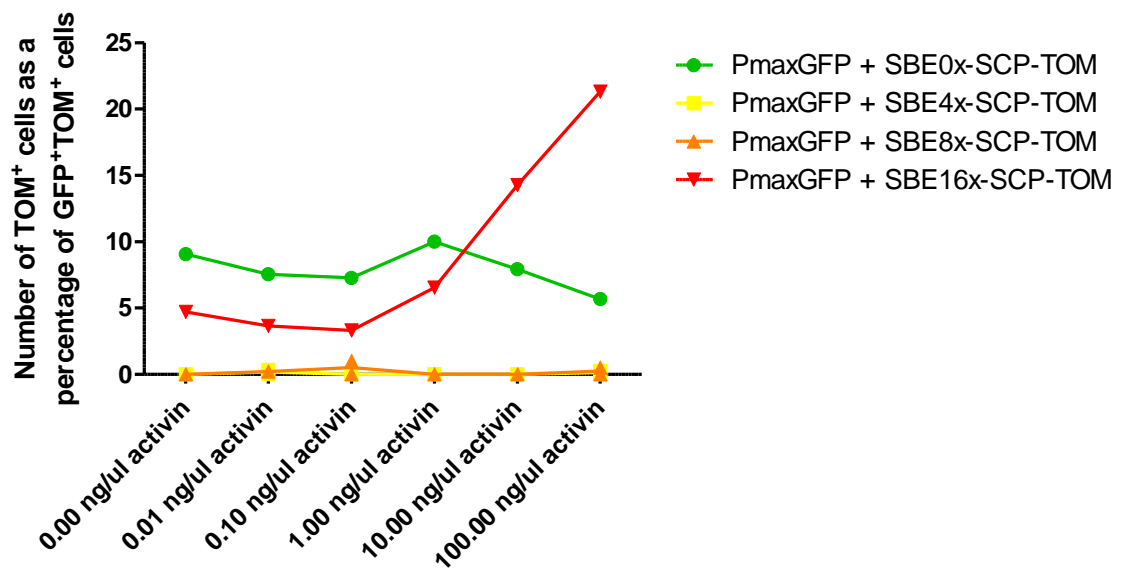
**Figure 38 Gating strategy for co-transfection of NIH 3T3 cells with both GFP and TOM containing vectors.** Live cells were first determined by a gate of cells plotted by forward scatter and side scatter area. Single cells were then determined by gating side scatter area against side scatter width to determine doublets. A double gate approach was used to determine which cells were expressing TOM (green horizontal stripes) and which were expressing GFP *and* TOM (red vertical stripes). These gates were applied to a sample of untransfected cells (A), and to one containing cells transfected with PmaxGFP *and* SBE16x-SCP-TOM and subsequently treated with 100 ng/ml Activin for 48 hours (B). A linear relationship of GFP<sup>+</sup> and TOM<sup>+</sup> cells is seen (orange arrows) this population reflects PmaxGFP GFP expression which is being recieved by the PE filter as a result of spectral overlap. A population of TOM<sup>+</sup> cells is seen to the right of this.

A dose dependent response of TOM florescence was seen when NIH 3T3 cells were co-transfected with PmaxGFP and SBE16x-SCP-TOM and treated with increasing concentrations of Activin (Figure 39 *A* and *B*). *Figure A* shows the number of cells present in the TOM<sup>+</sup> gate (green horizontal stripes in Figure 38), and *figure B* shows the number of TOM<sup>+</sup> cells as a percentage of GFP<sup>+</sup>TOM<sup>+</sup> cells (number of cells in green horizontal striped gate as a percentage of number of cells in red vertical stripe gate in Figure 38). This statistical representation indicates true response of SBE16x-SCP-TOM reporter to Activin treatment and confirms conclusions made previously regarding responsiveness of this construct. No fluorescent signal was generated by cells co-transfected with PmaxGFP and SBE0x-, 4x- or 8x-SCP-TOM. Figure 40 shows the increase in number of co-transfected (PmaxGFP and SBE16x-SCP-TOM) TOM<sup>+</sup> cells and migration of TOM<sup>+</sup> cells along the x-axis (representing an increase in TOM fluorescence). This movement is indicated by grey dashed arrows. These images reiterate both the increase in number of TOM<sup>+</sup> cells (Figure 39, *A*) and increase in number of TOM<sup>+</sup> cells as a percentage of GFP<sup>+</sup>TOM<sup>+</sup> cells shown in Figure 39, *B*.

**A**

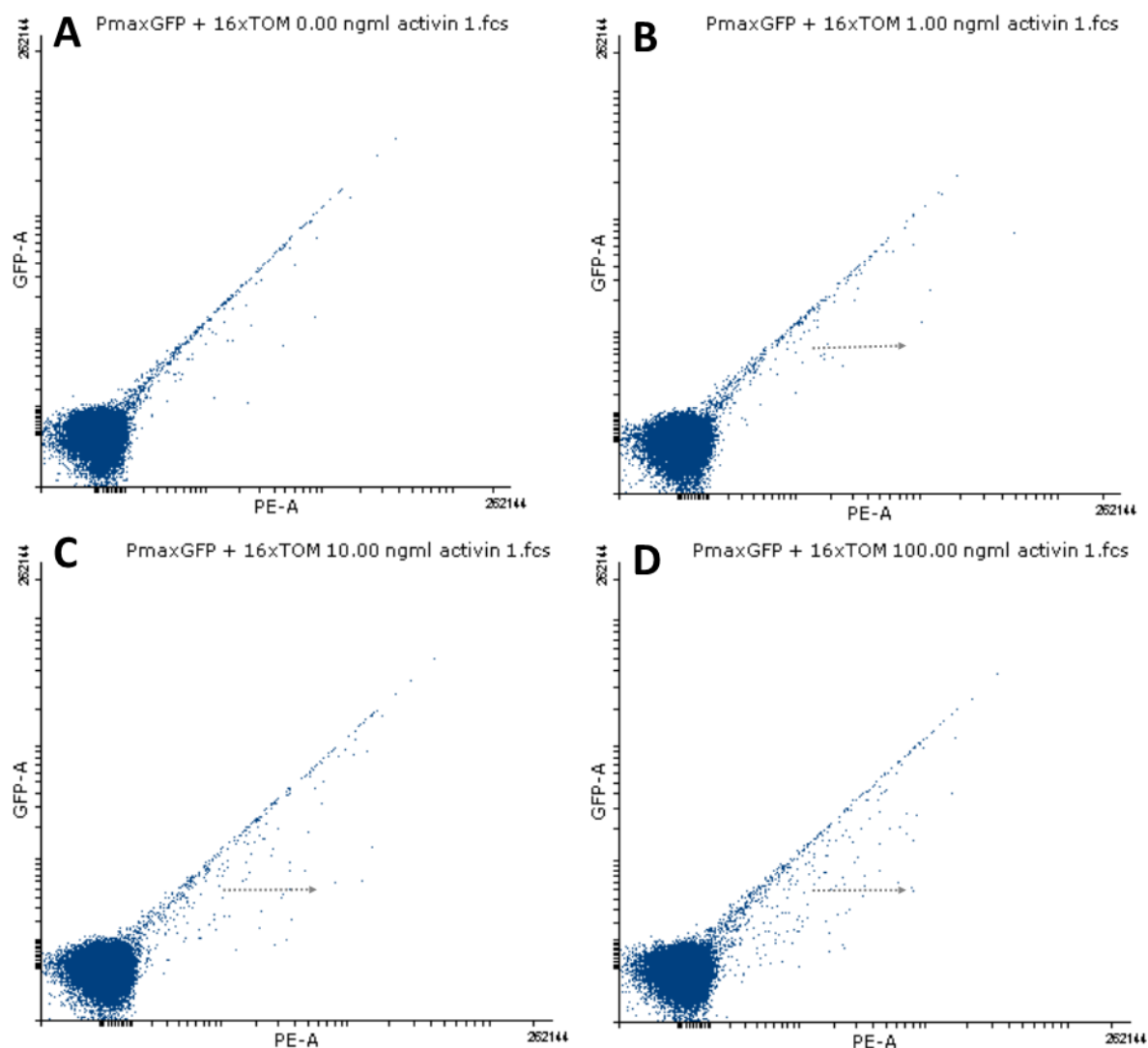


**B**



**Figure 39** Number of TOM<sup>+</sup> cells (A) and number of TOM<sup>+</sup> cells as a percentage of GFP<sup>+</sup>TOM<sup>+</sup> cells (B) co-transfected with PmaxGFP and SBE0x-, 4x-, 8x- and 16x-SCP-TOM and treated with varying concentrations of Activin. A dose dependent response of cells transfected with SBE16x-SCP-TOM and PmaxGFP which were subsequently treated with various concentrations of Activin is seen. This response is not seen in cells co transfected with PmaxGFP and SBE0x-, 4x- or 8x-SCP-TOM.

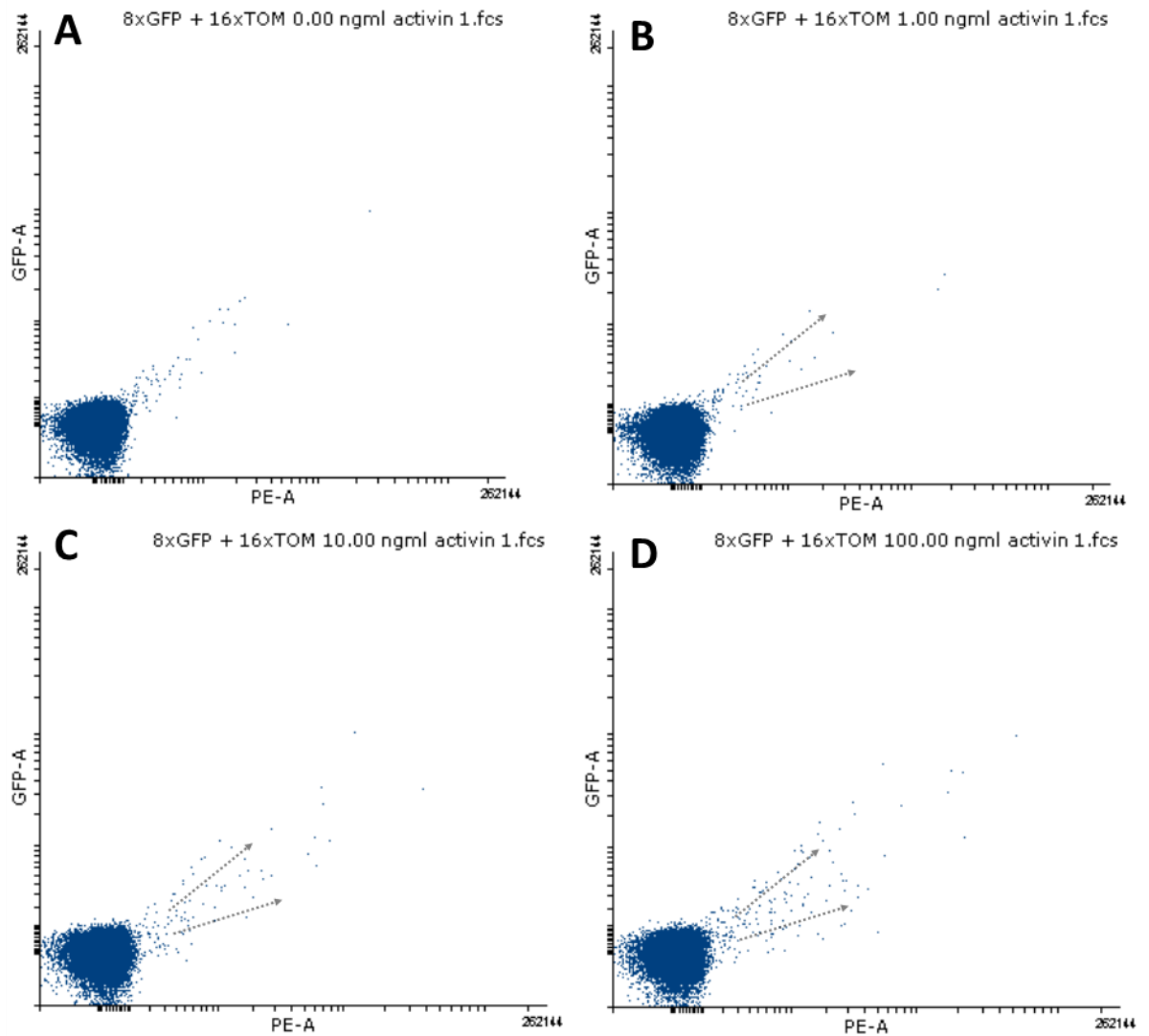




**Figure 40 Dot plots showing response of cells co-transfected with PmaxGFP and SBE16x-SCP-TOM to increasing concentrations of Activin treatment.**— At low Activin concentration, a population of GFP<sup>+</sup>TOM<sup>+</sup> cells are seen in a linear relationship, representing PmaxGFP expression received by both the GFP and PE filters (spectral overlap of GFP into the PE filter). (B, C and D) – with greater concentrations of Activin treatment, an increasing number of cells are seen moving right along the x-axis, and are therefore emitting more tdTomato fluorescence.

### 3.4.8 Co-transfection of SBE8x-SCP-GFP and SBE16x-SCP-TOM

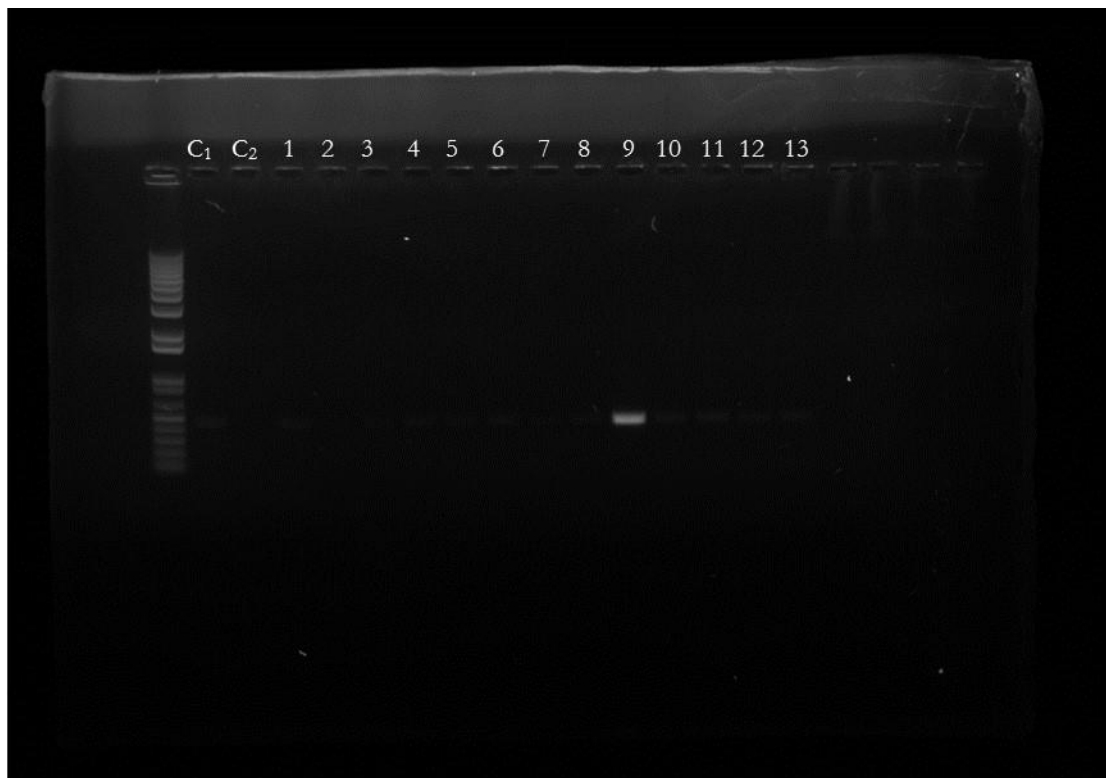
Next, we wanted to investigate the effect of co-transfection of two Smad reporter constructs of differing sensitivities as a long-term goal is to create a colour coded dose-response reporter system containing Smad binding elements of differing sensitivities driving transcription of different fluorescent proteins. SBE8x-SCP-GFP and SBE16x-SCP-TOM were co-transfected into NIH 3T3 cells in equi-molar ratios (Figure 41). Equal amounts of vectors were used to investigate relative expression of one vector to the other. No GFP response was seen in these cells, reflecting results of previous experiments which indicated that SBE8x-SCP-GFP does not respond to treatment of any experimental concentrations of Activin. A pronounced increase in number of TOM<sup>+</sup> cells is seen with increasing treatment concentrations of Activin (changes in cell population location represented by grey dotted arrows). This TOM response is very similar to that seen in cells co-transfected with PmaxGFP and SBE16x-SCP-TOM, reconfirming the ability of our SBE16x-SCP-TOM Smad activity reporter construct to respond to Smad signaling and illustrating reproducibility of our results.



**Figure 41** Dot plots showing response of cells co-transfected with SBE8x-SCP-GFP and SBE16x-SCP-TOM to increasing concentrations of Activin treatment. (A) at low concentrations, few cells express TOM. (C and D) at increasing concentrations of Activin treatment, greater numbers of cells express TOM. No GFP expressing cells are seen at any Activin treatment concentrations.

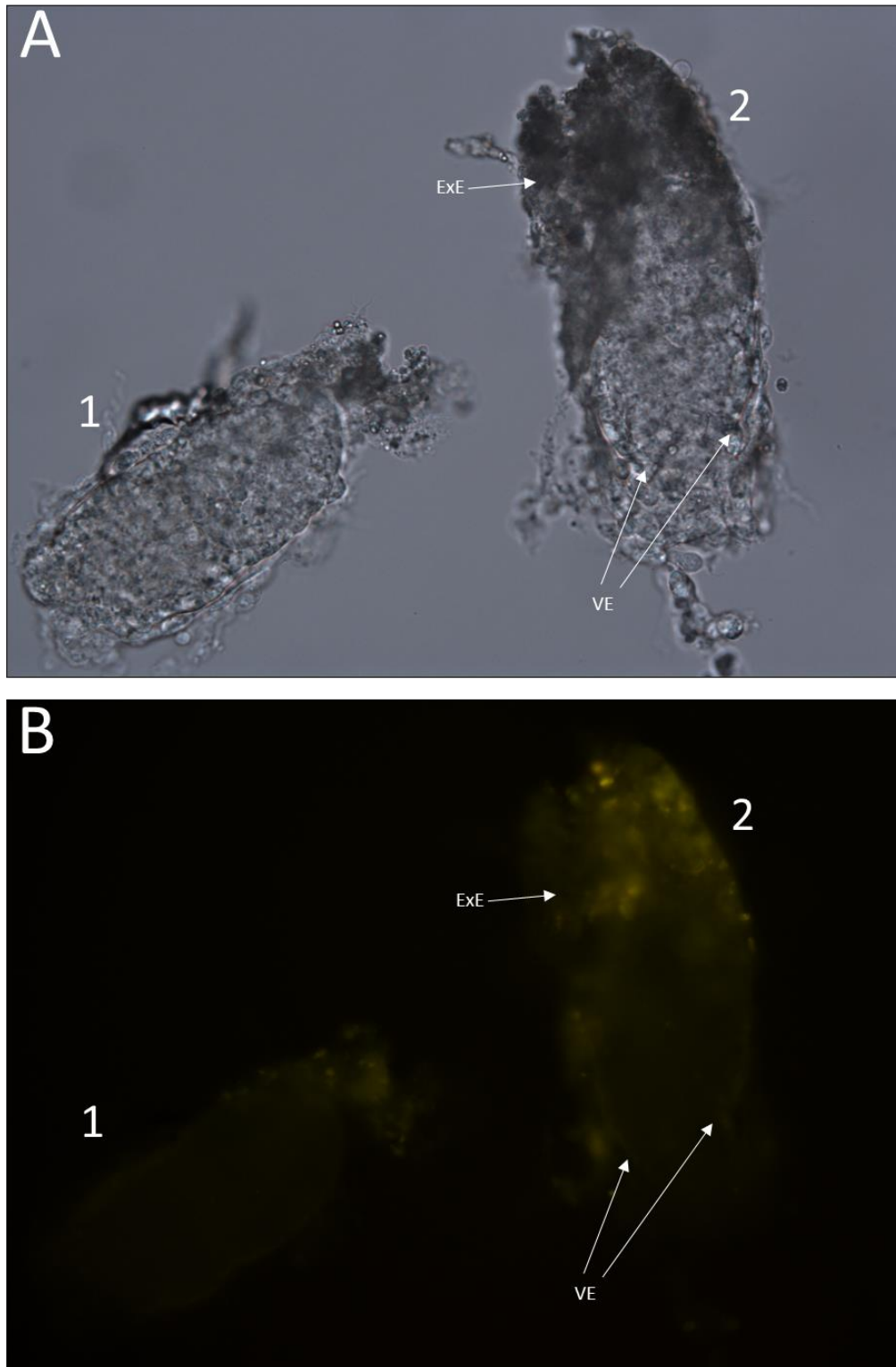
### 3.5 *In Vivo* results

A dose-dependent response of NIH 3T3 cells transfected with SBE16x-SCP-GFP to increasing concentration of Activin was seen (Figure 28). To investigate responsiveness of this reporter construct *in vivo*, a transgenic mouse line was created by pronuclear injection of a prepared sample of SBE16x-SCP-GFP (2.6 *Creation of transgenic mouse line containing SBE16x-SCP-GFP construct*). Genotyping of the offspring of pronuclear injection was performed (2.6.1 *Genotyping mice*) and results are illustrated in Figure 42, below. Mouse/sample number 9, a male, is positive for GFP, indicating that the individual is transgenic for the SBE16x-SCP-GFP reporter construct. Mouse number 9 was breed with wild type (wt) females. Females were culled at embryonic day 6 and 8.5. After photographing embryos under bright-field or FITC laser, embryos were genotyped for presence of SBE16x-SCP-GFP (genotyping results shown in Figure 46).



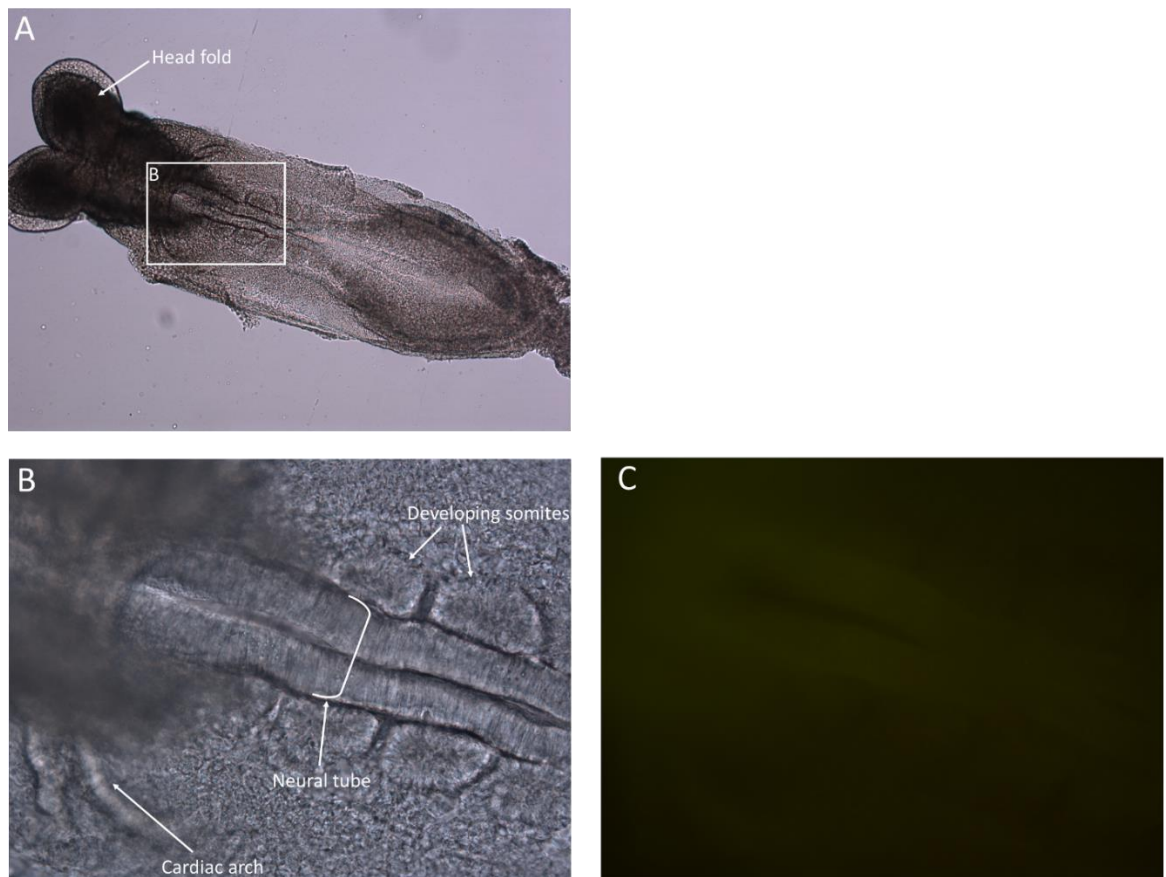
**Figure 42 Agarose gel of pronuclear injection offspring genotyping.** Lanes: ladder, C<sub>1</sub> water negative control, C<sub>2</sub> Proteinase K buffer negative control, 1- 13 genotyping samples. Sample number 9 is positive and therefore transgenic for SBE16x-SCP-GFP.

Figure 43 shows embryos 1 and 2 (embryonic day 6) photographed under bright-field (*A*) or FITC laser (*B*). Embryo 1 is wt and embryo 2 is transgenic for SBE16x-SCP-GFP (Figure 46). While embryo 1 shows a low level of background fluorescence, embryo 2 is seen to fluoresce dimly in the visceral endoderm (VE) or epiblast cells in close proximity to the VE. This fluorescence seen may in fact be ‘background’ fluorescence and our reporter construct may not be responding in this embryo. Fluorescence seen in the extraembryonic ectoderm (ExE) is most likely background fluorescence accumulated from a thicker section of the embryo. We expected to see fluorescence throughout the epiblast in day 6 embryos, reflecting known Nodal and Smad signaling in the embryo at this time (Alexander F. Schier 2003b). An additional wild type embryo is shown in *Supplementary figure 1: E6<sub>4</sub> wt embryo* which shows a similar fluorescence pattern to that of Figure 43, embryo 2 (tg), indicating fluorescence observed may indeed be ‘background’.



**Figure 43 Microscopy images of embryonic day 6 embryos 1 and 2.** BF (A) and FITC laser (B) images of embryos number 1 and 2 at 5x magnification. VE denotes visceral endoderm and ExE denotes extraembryonic ectoderm. Some reporter activity may be present in the VE or epiblast in close proximity to the VE of embryo number 2 (transgenic). No fluorescent activity is seen in embryo 1.

Figure 44 shows microscopy images of an embryonic day 8.5, SBE16x-SCP-GFP transgenic embryo (embryo number E8.5<sub>10</sub> in Figure 46). At this stage, primitive structures have begun to develop such as the headfold, neural tube, cardiac arch and some early developing somites. A small amount of fluorescence may be occurring in the neural tube; however, this may be background fluorescence as a result of imaging through a thicker area of the embryo. An additional transgenic E8.5 embryo is shown in *Supplementary figure 2: E8.5<sub>3</sub> transgenic embryo*. Figure 45, illustrating a wild type day 8.5 embryo, shows the extent of background fluorescence in embryos photographed with a FITC laser. It is important to consider background signal when gauging dull fluorescence responses.



**Figure 44 Microscopy images of embryo number 10 (tg) transgenic for SBE16x-SCP-GFP at embryonic day 8.5.** (A) 5x magnification of embryo number 10 (transgenic), bright-field, (B) 20x magnification, bright-field, (C) 20x magnification, FITC laser. Some fluorescence may be present in the neural tube (C).

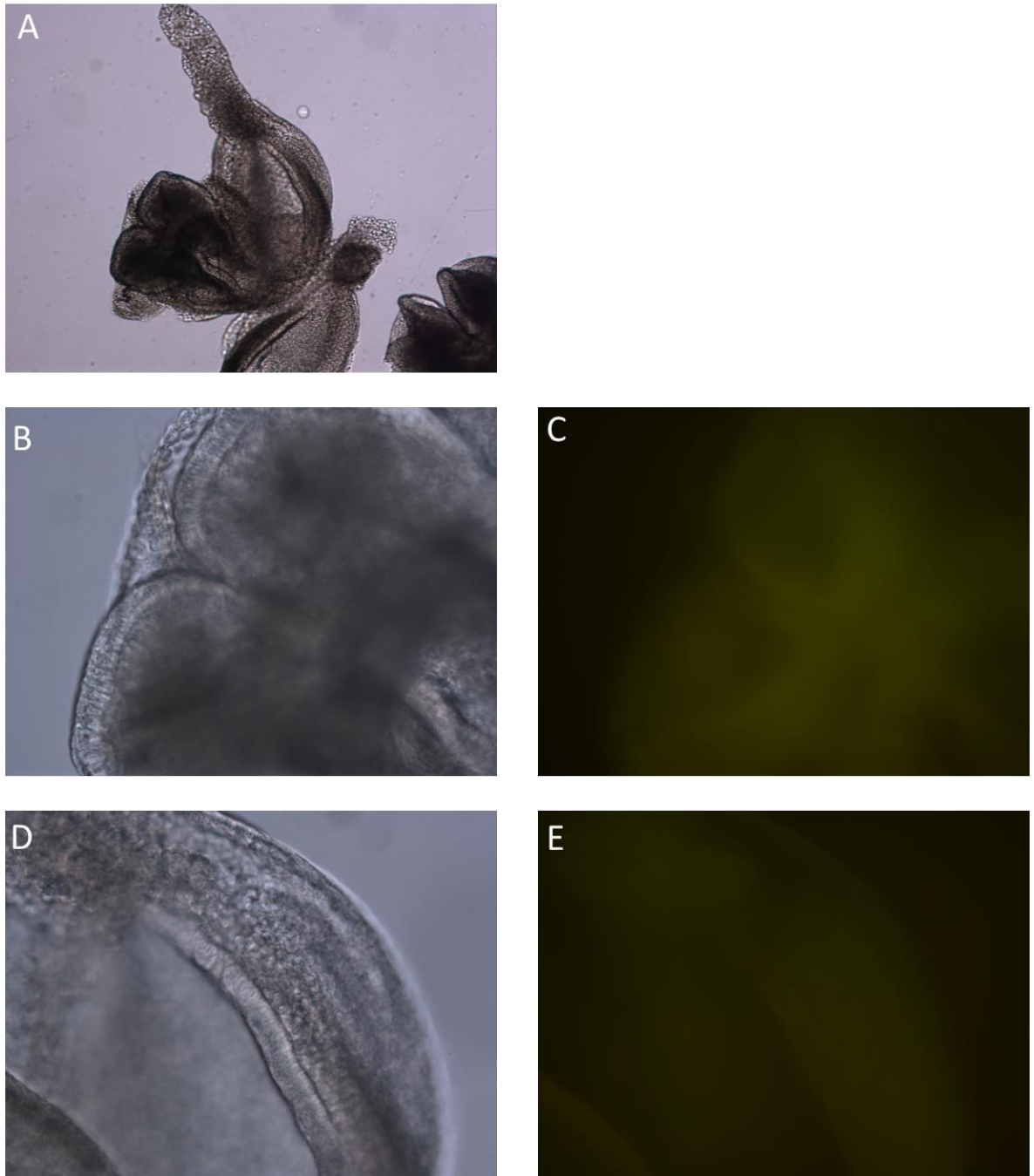


**Figure 45** Microscopy images of embryo number 12 (wt) at embryonic day 8.5. This wild type embryo indicates the extent of background fluorescence exhibited.



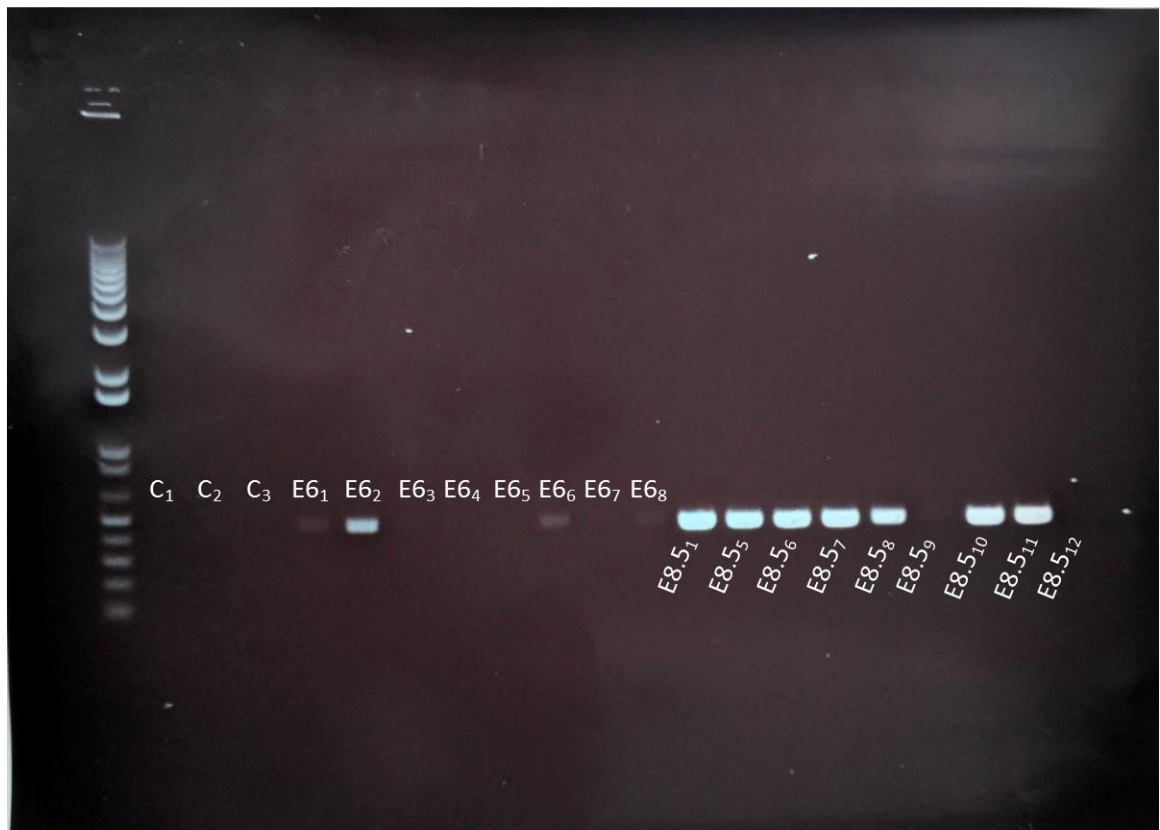


**Figure 46 Agarose gel image of embryo genotyping results.** Lanes: ladder, C<sub>1</sub> water negative control, C<sub>2</sub> Proteinase K buffer negative control, C<sub>3</sub> no sample, E<sub>6\_1</sub> to E<sub>6\_8</sub> day 6 embryo genotyping results, E8.5<sub>1</sub> to E8.5<sub>12</sub> day 8.5 embryo genotyping results. Embryos E<sub>6\_2</sub>, E8.5<sub>1</sub>, E8.5<sub>5</sub>, E8.5<sub>6</sub>, E8.5<sub>7</sub>, E8.5<sub>8</sub>, E8.5<sub>10</sub> and E8.5<sub>11</sub> are transgenic, containing SBE16x-SCP-GFP.

Microscopy images of embryos transgenic for SBE16x-SCP-GFP seem to show no or very little fluorescence activity in the epiblast at embryonic day 6. We expected to see fluorescence in this area as it has been previously shown that Nodal signals in a Smad2 dependent manner at embryonic day 6.5 (Brennan et al. 2001). In the embryonic day 8.5 embryo shown here, little fluorescence is seen. This is in accordance with the idea that Nodal is expressed in the epiblast at day 5.5, and is thereafter limited to the posterior side of the embryo as it becomes inhibited by lefty and cerebus-like signals from the anterior visceral endoderm (embryonic day 6.0) (Alexander F. Schier 2003b). It may therefore be that little Nodal signaling is occurring in day 8.5 embryos.

## 4 Discussion

In this body of work, we successfully created a collection of various sensitivity fluorescent genetic reporters of Activin signaling. While all constructs have been shown to be cloned correctly, without mistakes or mismatches when compared to reference clone charts (Figure 19, Figure 20, Figure 22 and Figure 23), our *in vitro* results show that only high sensitivity constructs containing 16 Smad binding elements were responsive to Activin ligand treatment (Figure 28, Figure 35 and Figure 39). Cells transfected with constructs containing 0, 4 and 8 repeats of the Smad binding elements did not respond to Activin treatment (Figure 26, Figure 27 and Figure 35). These results suggest that a high amount of phosphorylated Smad protein is required to bind to multiple SBEs in order for initiation of fluorescent protein transcription via a minimal promoter (SCP). A graded response of SBE16x-SCP-GFP and SBE16x-SCP-TOM to increasing Activin concentrations is seen: as greater number of cells and/or greater amount of fluorescence of GFP or TOM expressing cells is observed with greater ligand concentration. Cells transfected with both SBE16x-SCP-GFP and SBE16x-SCP-TOM showed 'background' levels of response to Activin treatment concentrations of 0.00, 0.01, 0.10 and 1.00 ng/ml. A stepwise increase in fluorescence response was seen when cells were treated with 10.00 and 100.00 ng/ml Activin.

The results shown here extend and refine work published by Dennler et al and Warmflash et al. In their work, *Direct binding of Smad3 and Smad4 to critical TGF $\beta$ -inducible elements in the promoter of human plasminogen activator inhibitor-type 1 gene*, Dennler et al showed that a Smad3/4 complex binds a CAGA sequence. This signal binding is essential and sufficient to confer TGF $\beta$  and Activin signaling to a luciferase reporter construct. The researchers went on to show that the CAGA box is responsive to Activin and TGF $\beta$ , but not to BMP signaling by transfecting Mv1Lu cells with Activin or BMP TGF $\beta$  receptors. The luciferase reporter response was seen in cells transfected with Activin receptors but not with BMP receptors. Additionally, Dennler et al showed that increasing the number of CAGA boxes from 9 repeats to 12 increased luciferase activity and that introduction of point mutations decreased activity. Here, we have expanded this idea by creating a construct based on Dennler's CAGA box which acts as an enhancer to a minimal super core promoter driving GFP or TOM transcription. In this way, we have created a reporter of Activin signaling which not only reflects the amount of activated TGF $\beta$  receptor and phosphorylated Smad proteins; but also

inhibitor, repressor and activator control of the Nodal/Activin signaling system. In addition, our reporter construct is specific for Activin and Nodal signaling, as investigated by both Dennler, explained above, and ourselves by showing that the Activin specific inhibitor SB431542 decreases activity of SBE16x-SCP-GFP.

By creating a clonal cell line of mouse myoblast C2C12 cells which stably expressed a RFP-Smad2 fusion protein and a GFP-nuclear localization signal, Warmflash et al were able to determine that Smad2/3 activation reflects the concentration of the ligand for which the cells were treated. Live cell imaging and western blotting experiments showed that phosphorylated Smad2/3 was continuously present in the nucleus with high levels of ligand stimulation. In this body of work, we have extended on these findings – our results show a dose dependent response of NIH 3T3 transfected cells with SBE16x-SCP-GFP and SBE16x-SCP-TOM to increasing concentrations of Activin. These complement Warmflash's findings that phosphorylated Smad2/3 is present in the nucleus after ligand stimulation, showing that not only are these factors present – but they actively bind to enhancer elements (SBEs) to induce transcription of reporter genes (GFP or TOM). Additionally, our results reflect the larger Smad signaling pathway activity, including that of co-receptors (Cripto), extracellular receptor inhibitors (Lefty and Cerebus-like), intracellular inhibitors (Smads6 and 7).

Our florescence genetic reporter system indicates the degree to which Smad3/4 signaling occurs upon stimulation by Activin treatment. To investigate the activity of Smad2, an additional FoxH1 binding site would need to be included upstream or downstream of the Smad binding sites in our reporter constructs. This is because Smad2 does not interact with DNA directly, rather through the co-factor FoxH1 and Smad4 (Derynck and Zhang 2003b; Y. Shi et al. 1998b; X. Chen et al. 1997b). However, work by Yagi et al indicates that a splice variant of Smad2 containing a deletion in exon 3 (Smad2 $\Delta$ exon3) acts in a similar manner to Smad3, binding the Activin-response element of the *Mix2* gene, known for its Smad3 and 4 binding capabilities (Yagi et al. 1999; C. Y. Yeo, Chen, and Whitman 1999b). Therefore, our Smad reporter constructs may confer signaling of both Smad3 and Smad2 $\Delta$ exon3.

The trend seen in our results - that high numbers of copies of the SBE are required for our reporter construct to transcribe GFP or TOM - could be investigated further by creation of a SBE24x construct by multimerization of the SBE8x element, or a SBE32x construct by multimerizing the SBE16x element. Experiments performed with these proposed vectors will increase understanding about the number of Smad binding elements required to confer Smad signaling and help to explain the graded response of our Smad reporter to increasing ligand concentrations. These results may illustrate that our Smad signaling reporter system is saturated with 16 SBE repeats, and no additional response is seen with an increase in Smad binding elements, or that fluorescent output of the system increases proportionately or logarithmically with increasing numbers of Smad binding elements. Dennler et al showed that by increasing the number of CAGA box repeats from 9 to 12, luciferase activity more than doubled. This kind of activity may result from further multimerisation of SBEs in our constructs. Additionally, point mutations could be introduced into the SBE in a bid to increase the affinity of the SBE enhancer region. Primers containing one or more point mutations would be designed and the enhancer region made by PCR. While Dennler et al showed that introduction of two point mutations significantly decreased reporter signal, alternative mutations may result in increased specificity of the SBE for Smad proteins.

Affinity of phosphorylated Smad proteins for the SBE enhancer region could also be increased by the addition of co-factor binding sites to the enhancer region. For example, the addition of FoxH1 or CBP/p300 proteins, which both bind both target DNA and phosphorylated Smad proteins to upregulate transcription, could increase the efficiency of the system. It is important to understand the limitations of adding co-factor binding sites to the reporter system – unless the co-factor is expressed in the experimental cells or embryonic region of interest at adequate concentrations, co-factors could limit activity and permissibility of the reporter system.

A less stringent promoter, the Heat Shock Promoter (HSP), was investigated as an alternative to the Super Core Promoter as we were inquisitive regarding whether the minimal components of the SCP were in fact limiting response in the SBE0x, 4x-, 8x- and 16x-SCP-GFP vectors. By replacing the SCP element with a HSP element, a SBE16x-HSP-GFP reporter construct was made. We saw that this promoter was indeed less stringent and that a higher level of background fluorescence was

being expressed in cells transfected with SBE16x-HSP-GFP and treated with increasing concentrations of Activin. High background fluorescence was seen at all Activin treatment concentrations, while a small increase in response was seen at 10 ng/ml and 100 ng/ml Activin treatment. As non-specific GFP transcription is not desired in our Smad signaling reporter system, we decided not to pursue the HSP experimentally.

As a dose-dependent response of NIH 3T3 cells transfected with SBE16x-SCP-GFP to increasing concentrations of Activin treatment was seen, we decided to create a line of mice transgenic for this reporter construct. Embryos transgenic for SBE16x-SCP-GFP would be used to experimentally demonstrate when, where and to what degree Nodal/Activin and Smad2/3 signaling occurs in early mouse embryonic development. In day 6 embryos transgenic for SBE16x-SCP-GFP, a small amount of GFP fluorescence is seen in the visceral endoderm area (Figure 43). Fluorescence in this region at this time point correlates to known Nodal activity in this area (Conlon et al. 1994). However, this signal is very dim and may be background fluorescence as a result of imaging through thick layers of the embryo. Indeed, an embryonic day 6, wild type embryo shown in *Supplementary figure 1* has a similar fluorescence profile to the transgenic embryo in Figure 43. To a similar degree, a dull fluorescent signal is seen in the neural tube of embryonic day 8.5 transgenic embryos (Figure 44). While it may be possible that low levels of fluorescence are occurring in the areas discussed, it is perhaps more likely that fluorescence visualized is background fluorescence, indicating that our SBE16x-SCP-GFP reporter construct is not functioning *in vivo*. This may be due to a few reasons; firstly, the ligand concentration *in vivo* may not be high enough to induce transcription of GFP via the SBE enhancer and Super Core Promoter. While response of SBE16x-SCP-GFP transfected NIH 3T3 cells was seen to Activin treatment concentrations of 10.00 and 100.00 ng/ml, *in vivo* ligand concentrations may be much lower, perhaps relative to *in vitro* 0.01, 0.10 or 1.00 ng/ml concentrations -at which we saw no SBE16x-SCP-GFP response - explaining lack of embryonic fluorescent signal. Secondly, we may be visualizing embryos at time points during which little to no ligand is present. However, studies by Conlon et al shows that Nodal mRNA is present in the epiblast at day 5.5 and work by Brennan et al shows that Nodal

signals from the epiblast at day 6.5, indicating that Nodal should indeed be present at embryonic day 6.

By increasing the sensitivity and affinity of the SBE constructs by the methods discussed above, we may generate a reporter system with adequate sensitivity to fluoresce in response to the relatively low levels of *in vivo* ligand. Once this is achieved, reporters containing different sensitivity or affinity Smad reporter elements driving different colour fluorescent proteins could be incorporated together to create a colour-coded ligand dose-dependent response system. This system would ultimately fluoresce one colour at low ligand concentration and another at high ligand concentration, creating a map of where and to what degree Nodal signaling is occurring.

Knowledge gained from these future experiments may be applied to bovine fertility studies, aiding agricultural research into the decline of New Zealand dairy cow fertility (CW 2001), or human fertility, expanding the little investigated field of human embryonic development.

## 5 Recipes



## 5.1 LB Broth and LB Agar

### 5.1.1 LB Broth

To make 1 L:

Yeast extract	5 g
---------------	-----

Bactro-tryptone	10 g
-----------------	------

NaCl	10 g
------	------

Up to 1 L ddH<sub>2</sub>O

### 5.1.2 LB Agar

Add 15 g of agar to 1 L of LB Broth and autoclave. Cool agar to 55°C and add antibiotic before pouring agar into petri dishes. Allow plates to set and dry either next to a Bunsen flame or in a laminar flow hood to keep plates free from debris.

## 5.2 Alkaline Lysis Solutions

Solution recipes were adapted from Molecular Cloning: A Laboratory Manual (Green and Sambrook 2012).

### 5.2.1 Alkaline Lysis Solution I

Tris-Cl (pH 8.0)	25 mM
------------------	-------

EDTA (pH 8.0)	10 mM
---------------	-------

Alkaline Lysis Solution I was prepared from standard stocks in batches of 100 ml, autoclaved on liquid cycle and stored at 4°C.

### 5.2.2 Alkaline Lysis Solution II

NaOH	0.2 M
SDS	1 % (w/w)

Alkaline Lysis Solution II was prepared from standard stocks and stored at room temperature.

### 5.2.3 Alkaline Lysis Solution III

Potassium acetate	60 ml
Glacial acetic acid	11.5 ml
dd-H <sub>2</sub> O	28.5 ml

Alkaline Lysis Solution III is 3 M with respect to potassium and 5 M with respect to acetate. Solution is stored at 4°C.

## 5.3 Injection buffer

Tris	8mM
EDTA	0.1mM

## 5.4 Proteinase K buffer

Tris, Ph 8	100 mM
EDTA	5 mM
SDS	0.1%
NaCl	200 mM

## 6 Supplementary material

## 6.1 Wizard SV Gel Clean-Up System protocol

### Wizard® SV Gel and PCR Clean-Up System

INSTRUCTIONS FOR USE OF PRODUCTS AS200, AS201, AS202, AND AS205.

**Quick  
PROTOCOL**

#### DNA Purification by Centrifugation

##### Gel Slice and PCR Product Preparation

###### A. Dissolving the Gel Slice

1. Following electrophoresis, excise DNA band from gel and place gel slice in a 1.5ml microcentrifuge tube.
2. Add 10µl Membrane Binding Solution per 10mg of gel slice. Vortex and incubate at 60–65°C until gel slice is completely dissolved.

###### B. Processing PCR Amplifications

1. Add an equal volume of Membrane Binding Solution to the PCR amplification.

##### Binding of DNA

1. Insert SV Minicolumn into Collection Tube.
2. Transfer dissolved gel mixture or prepared PCR product to the Minicolumn assembly. Incubate at room temperature for 1 minute.
3. Centrifuge at  $16,000 \times g$  for 1 minute. Discard flowthrough and reinsert Minicolumn into Collection Tube.

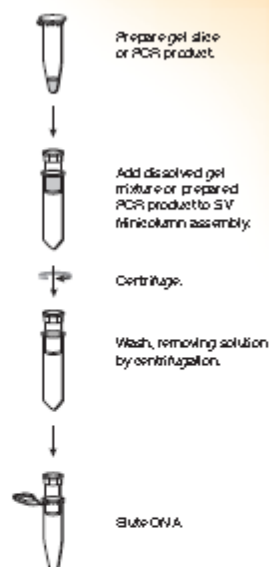
##### Washing

4. Add 700µl Membrane Wash Solution (ethanol added). Centrifuge at  $16,000 \times g$  for 1 minute. Discard flowthrough and reinsert Minicolumn into Collection Tube.
5. Repeat Step 4 with 500µl Membrane Wash Solution. Centrifuge at  $16,000 \times g$  for 5 minutes.
6. Empty the Collection Tube and recentrifuge the column assembly for 1 minute with the microcentrifuge lid open (or off) to allow evaporation of any residual ethanol.

##### Elution

7. Carefully transfer Minicolumn to a clean 1.5ml microcentrifuge tube.
8. Add 50µl of Nuclease-Free Water to the Minicolumn. Incubate at room temperature for 1 minute. Centrifuge at  $16,000 \times g$  for 1 minute.
9. Discard Minicolumn and store DNA at 4°C or –20°C.

Additional protocols are available for use with the Wizard System #T3300, available online at [www.promega.com](http://www.promega.com)



201004002-01

ORDERING/TECHNICAL INFORMATION:  
[www.promega.com](http://www.promega.com) • Phone 608-274-4330 or 800-356-0526 • Fax 608-277-2601

© 2002, 2004, 2005 and 2006 Promega Corporation. All Rights Reserved.



**Promega**

Printed in USA, Revised 11/03  
Part # T3300-01

## Wizard<sup>®</sup>SV Gel and PCR Clean-Up System

INSTRUCTIONS FOR USE OF PRODUCTS A1201, A1201A, A1202 AND A1205

**Quick  
PROTOCOL**

### DNA Purification by Vacuum

#### Gel Slice and PCR Product Preparation

##### A. Dissolving the Gel Slice

1. Following electrophoresis, excise DNA band from gel and place gel slice in a 1.5ml microcentrifuge tube.
2. Add 10µl Membrane Binding Solution per 10mg of gel slice. Vortex and incubate at 50–65°C until gel slice is completely dissolved.

##### B. Processing PCR Amplifications

1. Add an equal volume of Membrane Binding Solution to the PCR amplification.

#### Binding of DNA

1. Attach Vacuum Adapter to manifold port and insert SV Minicolumn into Adapter.
2. Transfer dissolved gel mixture or prepared PCR product to the Minicolumn. Incubate at room temperature for 1 minute.
3. Apply vacuum to pull liquid through Minicolumn. Release vacuum when all liquid has passed through Minicolumn.

#### Washing

4. Add 700µl Membrane Wash Solution (ethanol added). Apply a vacuum to pull solution through Minicolumn.
5. Turn off vacuum and repeat Step 4 with 500µl Membrane Wash Solution. Apply a vacuum to pull solution through Minicolumn.
6. Transfer Minicolumn to a Collection Tube. Centrifuge at 16,000 × g for 5 minutes.
7. Empty the Collection Tube and recentrifuge the column assembly for 1 minute with the microcentrifuge lid open (or off) to allow evaporation of any residual ethanol.

#### Elution

8. Carefully transfer Minicolumn to a clean 1.5ml microcentrifuge tube.
9. Add 50µl of Nuclease-Free Water to the Minicolumn. Incubate at room temperature for 1 minute. Centrifuge at 16,000 × g for 1 minute.
10. Discard Minicolumn and store DNA at 4°C or –20°C.

A detailed protocol is form that is available in Technical Bulletin #T9204, available online at [www.promega.com](http://www.promega.com)



5012041.00\_01

ORDERING/TECHNICAL INFORMATION:  
[www.promega.com](http://www.promega.com) • Phone 608-274-4330 or 800-356-0526 • Fax 608-277-2001



**Promega**

Printed in the United States  
Part #104-20

© 2002, 2004, 2005 and 2006 Promega Corporation. All Rights Reserved.

## 6.2 Takara Mighty Mix Protocol-at-a-Glance.

DNA Ligation Kit, Mighty Mix (Cat.# 6023)

### Protocol-at-a-Glance: DNA Ligation Kit, Mighty Mix

Takara's DNA Ligation Kit, Mighty Mix (Cat. # 6023), is a premixed ligation solution that enables highly efficient ligation. It can be used for many types of applications including standard cloning (sticky and blunt end), T-vector cloning, self-circularization, linker ligation, and preparation of  $\lambda$  phage library.

The following Protocols-At-A-Glance provide brief instructions for ligations commonly performed with this product. For more information, refer to the product User Manual.

#### Protocol 1: Insertion of DNA fragments into plasmid vectors

The Standard Protocol should be used for general ligation reactions. When performing sticky-end DNA ligations or when the highest efficiency is not required, the Rapid Protocol offers good efficiency in a shorter period of time.

##### [Standard Protocol]

1. Combine the digested plasmid vector DNA and the DNA insert in a total volume of 5 - 10  $\mu$ l. We recommend using TE buffer (10 mM Tris-HCl, pH 8.0, 1 mM EDTA) for dissolving DNA. The recommended vector : insert ratio is 25 fmol vector : 25 - 250 fmol insert. (Note : 25 fmol of pUC118 DNA (3,162 bp) corresponds to approx. 50 ng).

2. Add one volume of Ligation Mix (5 - 10  $\mu$ l) to the DNA solution and mix thoroughly.

3. Incubate at 16°C for 30 minutes\*1.

4. The ligation reaction mixture can be used directly for transformation of *E. coli* competent cells. When performing transformation immediately following ligation, add 10  $\mu$ l of the ligation mixture to 100  $\mu$ l of competent cells\*2.

\*1: This incubation may be performed overnight.

\*2: If more than 10  $\mu$ l of the ligation reaction mixture must be used for transformation, then the ligated DNA should be ethanol precipitated prior to use.

NOTE: The ligation reaction mixture should not be used directly in electroporation. Instead, ligated DNA should be ethanol precipitated and dissolved in a low salt buffer, such as TE buffer, prior to use for electroporation.

##### [Rapid Protocol]

1. Combine the digested plasmid vector and the DNA insert in a total volume of 5 - 10  $\mu$ l. We recommend using TE buffer (10 mM Tris-HCl, pH 8.0, 1 mM EDTA) for dissolving DNA. Recommended vector : insert ratio is 25 fmol vector : 25 - 250 fmol insert (Note : 25 fmol of pUC118 DNA (3,162 bp) corresponds to approx. 50 ng).

2. Add one volume of Ligation Mix (5 - 10  $\mu$ l) to the DNA solution and mix thoroughly.

3. Incubate at 25°C for 5 minutes\*1.

4. The ligation reaction mixture can be used directly for transformation of *E. coli* competent cells. When performing transformation immediately after ligation, add 10  $\mu$ l of the ligation mixture to 100  $\mu$ l of competent cells\*2.

\*1: Higher temperatures (>26°C) will inhibit the formation of circular DNA. When performing the Rapid Protocol, maintain the reaction temperature at 25°C.

\*2: If more than 10  $\mu$ l of the ligation reaction mixture must be used for transformation, then the ligated DNA should be ethanol precipitated prior to use.

NOTE: The ligation reaction mixture should not be used directly in electroporation. Instead, ligated DNA should be ethanol precipitated and dissolved in a low salt buffer, such as TE buffer, prior to use for electroporation.

- Continued -

**Takara**

TAKARA BIO INC.  
800-862-2566

©2010 Takara Bio Inc. All rights reserved. This product is sold as a research tool and is not intended for clinical use. The product is sold as a research tool and is not intended for clinical use. The product is sold as a research tool and is not intended for clinical use. The product is sold as a research tool and is not intended for clinical use.

[www.clontech.com/takara](http://www.clontech.com/takara)

## 6.3 Invitrogen Max Efficiency DH5 $\alpha$ transformation protocol.



### MAX Efficiency<sup>®</sup> DH5 $\alpha$ <sup>™</sup> Competent Cells

Cat. No. 18258-012

Size: 1 ml

Store at -70°C.

Do not store in liquid nitrogen.

#### Description:

MAX Efficiency<sup>®</sup> DH5 $\alpha$ <sup>™</sup> Competent Cells have been prepared by a patented modification of the procedure of Hanahan (1). These cells are suitable for the construction of gene banks or for the generation of cDNA libraries using plasmid-derived vectors. The  $\phi$ 80d*lacZ* $\Delta$ M15 marker provides  $\alpha$ -complementation of the  $\beta$ -galactosidase gene from pUC or similar vectors and, therefore, can be used for blue/white screening of colonies on bacterial plates containing Blue-gal or X-gal. DH5 $\alpha$ <sup>™</sup> is capable of being transformed efficiently with large plasmids, and can also serve as a host for the M13mp cloning vectors if a lawn of DH5 $\alpha$ -FT<sup>™</sup>, DH5 $\alpha$ F<sup>™</sup>, DH5 $\alpha$ FIQ<sup>™</sup>, JM101 or JM107 is provided to allow plaque formation.

#### Genotype

F-  $\phi$ 80*lacZ* $\Delta$ M15  $\Delta$ (*lacZYA-argF*) U169 *recA1 endA1 hsdR17* ( $r_k^-$ ,  $m_k^+$ ) *phoA supE44*  $\lambda^-$  *thi-1 gyrA96 relA1*

Component	Amount per Vial
DH5 $\alpha$ <sup>™</sup> Competent Cells	200 $\mu$ l
pUC19 DNA (0.01 $\mu$ g/ml)	100 $\mu$ l

**Quality Control:** MAX Efficiency<sup>®</sup> DH5 $\alpha$ <sup>™</sup> Competent Cells consistently yield  $> 1.0 \times 10^9$  transformants/ $\mu$ g pUC19 with non-saturating amounts (50 pg) of DNA. Saturating amounts of pUC19 (25 ng) generate  $> 1 \times 10^6$  ampicillin-resistant colonies in a 100- $\mu$ l reaction.

Part No. 18258012 pps

Rev. Date: 26 October 2006



#### Transformation Procedure:

A stock pUC19 solution (0.01 µg/ml) is provided as a control to determine the transformation efficiency. The stock solution of pFastBac™-gus (0.2 µg/ml), provided with pFastBac™1 Expression Vector (Cat. No. 10360-014), can be used as a control for the transposition frequency. To obtain maximum transformation efficiency, the experimental DNA must be free of phenol, ethanol, protein and detergents.

1. Thaw competent cells on wet ice. Place required number of 17 × 100 mm polypropylene tubes (Falcon® 2059) on ice.
2. Gently mix cells, then aliquot 100 µl of competent cells into chilled polypropylene tubes.
3. Refreeze any unused cells in the dry ice/ethanol bath for 5 minutes before returning to the -70°C freezer. Do not use liquid nitrogen.
4. To determine the transformation efficiency, add 5 µl (50 pg) pUC19 control DNA to one tube containing 100 µl competent cells. Move the pipette through the cells while dispensing. Gently tap tube to mix.
5. For DNA from ligation reactions, dilute the reactions 5-fold in 10 mM Tris-HCl (pH 7.5) and 1 mM EDTA. Add 1 µl of the dilution to the cells (1 to 10 ng DNA), moving the pipette through the cells while dispensing. Gently tap tubes to mix.
6. Incubate cells on ice to 30 minutes.
7. Heat-shock cells 45 seconds in a 42°C water bath; do not shake.
8. Place on ice for 2 minutes.
9. Add 0.9 ml room temperature S.O.C. Medium (Cat. No. 15544-034).
10. Shake at 225 rpm (37°C) for 1 hour.
11. Dilute the reaction containing the control plasmid DNA 1:100 with S.O.C. Medium. Spread 100 µl of this dilution on LB or YT plates with 100 µg/ml ampicillin.
12. Dilute the experimental reactions as necessary and spread 100 to 200 µl of this dilution as described in Step 11.
13. Incubate overnight at 37°C.

#### Growth of Transformants for Plasmid Preparations:

DH5α™ Competent Cells which have been transformed with pUC-based plasmids should be grown at 37°C overnight in TB(2). A 100-ml growth in a 500-ml baffled shake flask will yield approximately 1 mg of pUC19 DNA.

#### Notes:

1. For best results, each vial of cells should be thawed only once. Although the cells are refreezable, subsequent freeze-thaw cycles will lower transformation frequencies by approximately two-fold.
2. Media other than S.O.C. Medium can be used, but the transformation efficiency will be reduced. Expression in Luria Broth reduces transformation efficiency a minimum of two- to three-fold (4).
3. Transformation efficiencies will be approximately 10-fold lower for ligation of inserts to vectors than for an intact control plasmid. Ligation reactions should be diluted 5-fold prior to using the DNA in a transformation. Only 1 µl of this dilution should be used. A standard ligation reaction (20 µl) normally contains 100-1000 ng of DNA. Therefore, the addition of 1 µl of diluted DNA will result in adding 1 to 10 ng of ligated DNA to the cells. We have observed that the cells begin to saturate with 10-50 ng of DNA (3). Also our data show that the 5-fold dilution of ligation mixtures results in more efficient transformation (3,4).
4. MAX Efficiency® DH5α™ can support the replication of M13mp vectors. However, DH5α™ is F and cannot support plaque formation. Therefore, log phase DH5α-F™, DH5α-F'™, DH5α-F'IQ™, JM101 or JM107 cells must be added to the top agar which should contain X-gal (Cat. No. 15520-034) or Blue-gal, final concentration 50 µg/ml, and IPTG (Cat. No. 15529-019), final concentration 1 mM. The competent cells should be added to top agar after lawn cells, IPTG and Blue-gal or X-gal have been added. Incubation at 37°C for 1 hour is not required after addition of S.O.C. Medium.

5. Generally, transformation efficiencies will be 10- to 100-fold lower for cDNA than for an intact control plasmid such as pUC19. Approximately 50,000 transformants/5 ng cDNA may be obtained. The amount of cDNA used in a 100 µl transformation should be 1-5 ng in 5 µl or less.

6. Transformation efficiency (CFU/µg):

$$\frac{\text{CFU in control plate}}{\text{pg pUC19 used in transformation}} \times \frac{1 \times 10^4 \text{ pg}}{\mu\text{g}} \times \text{dilution factor(s)}$$

For example, if 50 pg pUC19 yields 100 colonies when 100 µl of a 1:100 dilution is plated, then:

$$\text{CFU}/\mu\text{g} = \frac{100 \text{ CFU}}{50 \text{ pg}} \times \frac{1 \times 10^4 \text{ pg}}{\mu\text{g}} \times \frac{1 \text{ ml}}{0.1 \text{ ml plated}} \times 10^2 = 2 \times 10^9$$

#### References:

1. Hanahan, D. (1983) *J. Mol. Biol.* 166, 557.
2. Tartof, K. D. and Hobbs, C. A. (1987) *Focus*<sup>®</sup> 9:2, 12.
3. Jessee, J. (1984) *Focus* 6:4, 5.
4. King, P. V. and Blakesley, R. (1986) *Focus*<sup>®</sup> 8:1, 1.

Falcon<sup>®</sup> is a registered trademark of Becton Dickinson.

2004-2006 Invitrogen Corporation. All rights reserved. For research use only.  
Not intended for any animal or human therapeutic or diagnostic use.

## 6.4 Qiagen Miniprep protocol

### Quick-Start Protocol

#### QIAGEN® Plasmid Mini, Midi, and Maxi Kits

The QIAGEN Plasmid Mini Kit (cat. nos. 12123 and 12125), the QIAGEN Plasmid Midi Kit (cat. nos. 12143 and 12145), the QIAGEN Plasmid Maxi Kit (cat. nos. 12162, 12163, and 12165), and the Plasmid Buffer Set (cat. no. 19046) can be stored at room temperature (15–25°C) for up to 2 years.

For more information, especially on the purification of cosmids and very low-copy plasmids, please refer to the *QIAGEN Plasmid Purification Handbook*, which can be found at [www.qiagen.com/handbooks](http://www.qiagen.com/handbooks).

For technical assistance, please call toll-free 00800-22-44-6000, or find regional phone numbers at [www.qiagen.com/contact](http://www.qiagen.com/contact).

#### Notes before starting

- Add RNase A solution to Buffer P1, mix, and store at 2–8°C.
- **Optional:** Add LyseBlue® reagent to Buffer P1 at a ratio of 1:1000.
- Prechill Buffer P3 at 4°C. Check Buffer P2 for SDS precipitation.
- Isopropanol and 70% ethanol are required.
- Symbols: ● QIAGEN Plasmid Mini Kit; ▲ QIAGEN Plasmid Midi Kit; and ■ QIAGEN Plasmid Maxi Kit.

Table 1. Recommended LB culture volumes

Kit	High-copy plasmid	Low-copy plasmid
QIAGEN Plasmid Mini	3 ml	Not recommended
QIAGEN Plasmid Midi	25 ml	100 ml
QIAGEN Plasmid Maxi	100 ml	500 ml

1. Harvest overnight bacterial culture by centrifuging at 6000 × g for 15 min at 4°C.
2. Resuspend the bacterial pellet in ● 0.3 ml, ▲ 4 ml, or ■ 10 ml Buffer P1.

January 2011



## Quick-Start Protocol

---

3. Add ● 0.3 ml, ▲ 4 ml, or ■ 10 ml Buffer P2, mix thoroughly by vigorously inverting 4–6 times, and incubate at room temperature (15–25°C) for 5 min. If using LyseBlue reagent, the solution will turn blue.
4. Add ● 0.3 ml, ▲ 4 ml, or ■ 10 ml prechilled Buffer P3, mix thoroughly by vigorously inverting 4–6 times. Incubate on ice for ● 5 min, ▲ 15 min, or ■ 20 min. If using LyseBlue reagent, mix the solution until it is colorless.
5. ●: Centrifuge at 14,000–18,000 x g for 10 min at 4°C. Re-centrifuge if the supernatant is not clear.  
▲ and ■: Centrifuge at ≥20,000 x g for 30 min at 4°C. Re-centrifuge the supernatant at ≥20,000 x g for 15 min at 4°C.
6. Equilibrate a QIAGEN-tip ● 20, ▲ 100, or ■ 500 by applying ● 1 ml, ▲ 4 ml, or ■ 10 ml Buffer QBT, and allow column to empty by gravity flow.
7. Apply the supernatant from step 5 to the QIAGEN-tip and allow it to enter the resin by gravity flow.
8. Wash the QIAGEN-tip with ● 2 x 2 ml, ▲ 2 x 10 ml, or ■ 2 x 30 ml Buffer QC. Allow Buffer QC to move through the QIAGEN-tip by gravity flow.
9. Elute DNA with ● 0.8 ml, ▲ 5 ml, or ■ 15 ml Buffer QF into a clean ● 2 ml, ▲ 15 ml, or ■ 50 ml vessel. For constructs larger than 45 kb, prewarming the elution buffer to 65°C may help to increase the yield.
10. Precipitate DNA by adding ● 0.56 ml, ▲ 3.5 ml, or ■ 10.5 ml (0.7 volumes) room-temperature isopropanol to the eluted DNA and mix. Centrifuge at ≥15,000 x g for 30 min at 4°C. Carefully decant the supernatant.
11. Wash the DNA pellet with ● 1 ml, ▲ 2 ml, or ■ 5 ml room-temperature 70% ethanol and centrifuge at ≥15,000 x g for 10 min. Carefully decant supernatant.
12. Air-dry pellet for 5–10 min and redissolve DNA in a suitable volume of appropriate buffer (e.g., TE buffer, pH 8.0, or 10 mM Tris-Cl, pH 8.5).

For up-to-date licensing information and product-specific disclaimers, see the respective QIAGEN kit handbook or user manual.

Trademarks: QIAGEN®, LyseBlue® (QIAGEN Group). 1066960 01/2011  
© 2011 QIAGEN, all rights reserved.



## 6.4 NIH 3T3 Culture method

### NIH/3T3 (ATCC® CRL-1658™)

Organism: *Mus musculus neovius* | Cell Type: *fibroblast* | Format: *unifrac* |

GENERAL INFORMATION	CHARACTERISTICS	CULTURE METHOD	HISTORY	DOCUMENTATION	LINE	DATE	PERF
Complete Growth Medium	The base medium for this cell line is ATCC formulated Dulbecco Modified Eagle's Medium, Catalog No. 90-2002. To make the complete growth medium, add the following components to the base medium, bovine calf serum to a final concentration of 10%.						
Subculturing	<p>Volumes as given in a 75 cm<sup>2</sup> flask. Increase or decrease the amount of dissociation medium needed proportionally to culture vessels of other sizes. Corning® T-75 flasks (catalog #430041) are recommended for subculturing this product.</p> <ol style="list-style-type: none"> <li>1. Remove and discard culture medium.</li> <li>2. Reify/erase the cell layer with 0.25% (w/v) trypsin - 0.50 mM EDTA solution to remove all traces of serum which contains trypsin inhibitors.</li> <li>3. Add 2.0 to 3.0 mL of trypsin/EDTA solution to flask and observe cells under an inverted microscope until cell layer is disengaged (usually within 5 to 15 minutes). Note: To avoid clumping do not agitate the cells by hitting or shaking the flask while waiting for the cells to detach. Cells that seek to pull to detach may be placed at 37°C to facilitate disengagement.</li> <li>4. Add 8.0 to 9.0 mL of complete growth medium and agitate cells by gently pipetting.</li> <li>5. Add appropriate aliquots of the cell suspension to new culture vessels.</li> <li>6. Inoculate cultures at 37°C.</li> </ol> <p>DO NOT ALLOW THE CELLS TO BECOME CONFLUENT Subculture at least twice per week at 80% confluence or less. Subculture when 1 flask inoculate 2 to 5 x 10<sup>5</sup> cells/cm<sup>2</sup> Medium: 14 mL / 1 passage / week</p>						
Cryopreservation	<p>Inoculation medium: Complete growth medium supplemented with 5% (v/v) DMSO Storage temperature: liquid nitrogen vapor phase</p>						
Culture Conditions	<p>Atmosphere: air, 95%, carbon dioxide (CO<sub>2</sub>), 5% Temperature: 37°C Growth Conditions: The serum used as ingredient in culturing this line, Calf serum is recommended and not fetal bovine serum. The calf serum initially employed and found to be satisfactory was from the Colorado Serum Co., Denver.</p>						


## 6.5 Lipofectamine Transfection Protocols

### 6.5.1 Lipofectamine 2000 Protocol

Protocol Pub. No. MAN0007824 Rev.1.0


## Lipofectamine® 2000 Reagent

[Learn More](#)


**Package Contents**

Catalog Number      Size


- 11668-030 [Buy Now](#) 0.3 mL vial
- 11668-027 [Buy Now](#) 0.75 mL vial
- 11668-019 [Buy Now](#) 1.5 mL vial
- 11668-500 [Buy Now](#) 15 mL vial

**Storage Conditions**


Store at 4°C (do not freeze).

**Required Materials**


- Plasmid DNA (0.5–5 µg/µL stock)
- Opti-MEM® Reduced Serum Medium
- Eppendorf tubes

**Timing**


Preparation: 10 minutes  
Incubation: 5 minutes  
Final Incubation: 1–3 days

**Selection Guide**


[Lipofectamine® Reagents](#)  
Go online to view related products.

**Product Description**

- Lipofectamine® 2000 Reagent is a proprietary formulation for transfecting nucleic acids into a wide range of eukaryotic cells.


**Important Guidelines**


- DNA-Lipofectamine® 2000 complexes must be made in serum-free medium such as Opti-MEM® Reduced Serum Medium and can be added directly to cells in culture medium, in the presence or absence of serum/antibiotic.
- It is not necessary to remove complexes or change/add medium after transfection.
- The amount of Lipofectamine® 2000 Reagent required for successful transfection varies depending on the cell type and passage number. Start any new transfection by testing the recommended four concentrations of Lipofectamine® 2000 Reagent to determine an optimum amount.

**Online Resources**

Visit our [product page](#) for additional information and protocols. For support, visit [www.lifetechnologies.com/support](http://www.lifetechnologies.com/support).

For Research Use Only. Not for use in diagnostic procedures.





### Protocol Outline

- Plate cells so they will be 70–90% confluent at the time of transfection.
- Prepare plasmid DNA-lipid complexes.
- Add DNA-lipid complexes to cells.

### Lipofectamine® 2000 DNA Transfection Reagent Protocol

See page 2 to view a typical DNA transfection procedure.


Component	96-well	24-well	6-well
Final DNA per well	100 ng	500 ng	2500 ng
Final Lipofectamine® 2000 Reagent per well	0.2–0.5 µL	1.0–2.5 µL	5.0–12.5 µL


### Co-Transfection of Plasmid DNA and siRNA


Transfect plasmid DNA and siRNA at the same time using Lipofectamine® 2000 Reagent by adding 30 pmol (~0.6 µg) of siRNA per 1 µg of DNA.


### mRNA Transfection

mRNA can be transfected in a 24-well plate using Lipofectamine® 2000 Reagent by adding 0.5–1 µg of mRNA per well.

**Photograph of Expected Results**








**Scaling Up or Down Transfections**

**Limited Product Warranty and Disclaimer Details**



### Lipofectamine® 2000 DNA Transfection Reagent Protocol

Transfect cells according to the following chart. Volumes are given on a per-well basis. Each reaction mix is sufficient for triplicate (96-well), duplicate (24-well), and single well (6-well) transfections, and accounts for pipetting variations. Adjust the amounts of components according to your tissue culture format. For additional information on scaling your transfection reaction, see page 1.

Timeline		Steps	Procedure Details				
Day 0	1		Seed cells to be 70–90% confluent at transfection	Component	96-well	24-well	6-well
	2		Dilute four amounts of Lipofectamine® Reagent in Opti-MEM® Medium	Adherent cells	1–4 × 10 <sup>4</sup>	0.5–2 × 10 <sup>5</sup>	0.25–1 × 10 <sup>6</sup>
	3		Dilute DNA in Opti-MEM® Medium	Opti-MEM® Medium	25 µL × 4	50 µL × 4	150 µL × 4
Day 1	4		Add diluted DNA to diluted Lipofectamine® 2000 Reagent (1:1 ratio)	Lipofectamine® 2000 Reagent	<b>i</b> 1, 1.5, 2, 2.5 µL	<b>i</b> 2, 3, 4, 5 µL	<b>i</b> 6, 9, 12, 15 µL
	5		Incubate	Opti-MEM® Medium	125 µL	250 µL	700 µL
	6		Add DNA-lipid complex to cells	DNA (0.5–5 µg/µL)	2.5 µg	5 µg	14 µg
Day 2–4	7		Visualize/analyze transfected cells	Diluted DNA Total	25 µL	50 µL	150 µL
				Diluted Lipofectamine® 2000 Reagent	25 µL	50 µL	150 µL
				Incubate for 5 minutes at room temperature.			
			Component	96-well	24-well	6-well	
			DNA-lipid complex per well	10 µL	50 µL	250 µL	
			Final DNA used per well	100 ng	500 ng	2500 ng	
			Final Lipofectamine® 2000 Reagent used per well	0.2–0.5 µL	1.0–2.5 µL	5.0–12.5 µL	
			Incubate cells for 1–3 days at 37°C. Then analyze transfected cells.				









12 June 2013

## 6.5.2 Lipofectamine 3000 Protocol

### Lipofectamine™ 3000 Reagent

#### USER GUIDE

Document Part No. 100022234 Publication No. MAN0009872 Rev C.0

	<b>Package Contents</b>	<b>Catalog Numbers</b>	<b>Size:</b>
		L3000001 L3000008 L3000015 L3000075 L3000150	0.1 mL 0.75 mL 1.5 mL 5 × 1.5 mL 15 mL
	<b>Storage Conditions</b>	Store at 4°C (do not freeze).	
	<b>Required Materials</b>	<ul style="list-style-type: none"> <li>Plasmid DNA (0.5–5 µg/µL stock)</li> <li>Opti-MEM™ Reduced Serum Medium</li> <li>Microcentrifuge tubes</li> </ul>	
	<b>Timing</b>	Preparation: 10 minutes Incubation: 10–15 minutes Final Incubation: 1–3 days	
	<b>Selection Guide</b>	Lipofectamine™ Reagents Go online to view related products.	
	<b>Product Description</b>	<ul style="list-style-type: none"> <li>Lipofectamine™ 3000 Reagent is a proprietary formulation for transfecting nucleic acids into a wide range of eukaryotic cells and especially designed for hard to transfect cells</li> <li>Make DNA-Lipofectamine™ 3000 complexes in serum-free medium such as Opti-MEM™ Reduced Serum Medium and add directly to cells in culture medium, in the presence or absence of serum/antibiotic.</li> <li>It is not necessary to remove complexes or change/add medium after transfection.</li> <li>The amount of Lipofectamine™ 3000 Reagent for successful transfection varies. Start any new transfection by testing the recommended two concentrations of Lipofectamine™ 3000 Reagent to determine an optimum amount.</li> </ul>	
	<b>Important Guidelines</b>		
	<b>Online Resources</b>	Visit our product page for additional information and protocols. For support visit <a href="http://thermofisher.com/support">thermofisher.com/support</a>	

For Research Use Only. Not for use in diagnostic procedures.

invitrogen

### Lipofectamine™ 3000 Reagent Protocol

#### Protocol Outline

- Plate cells so they will be 70–90% confluent at the time of transfection.
- Prepare plasmid DNA-lipid complexes (recommend 2 doses of lipid).
- Add DNA-lipid complexes to cells.

#### Transfection Amounts

Component	96-well	24-well	6-well
DNA per well	100 ng	500 ng	2500 ng
P3000™ Reagent per well	0.2 µL	1 µL	5 µL
Lipofectamine™ 3000 Reagent per well	0.15 and 0.3 µL	0.75 and 1.5 µL	3.75 and 7.5 µL

#### Transfection of siRNA

To transfect cells with siRNA, follow the protocol as described for DNA but do not add P3000™ Reagent when diluting the siRNA (step 3).

#### Limited Product Warranty

Life Technologies Corporation and/or its affiliate(s) warrant their products as set forth in the Life Technologies' General Terms and Conditions of Sale found on Life Technologies' website at [www.lifetechnologies.com/termsandconditions](http://www.lifetechnologies.com/termsandconditions). If you have any questions, please contact Life Technologies at [www.lifetechnologies.com/support](http://www.lifetechnologies.com/support).

#### Important Licensing Information

These products may be covered by one or more Limited Use Label Licenses. By use of these products, you accept the terms and conditions of all applicable Limited Use Label Licenses.

#### Disclaimer

LIFE TECHNOLOGIES CORPORATION AND/OR ITS AFFILIATE(S) DISCLAIM ALL WARRANTIES WITH RESPECT TO THIS DOCUMENT, EXPRESSED OR IMPLIED, INCLUDING BUT NOT LIMITED TO THOSE OF MERCHANTABILITY, FITNESS FOR A PARTICULAR PURPOSE, OR NON-INFRINGEMENT TO THE EXTENT ALLOWED BY LAW. IN NO EVENT SHALL LIFE TECHNOLOGIES AND/OR ITS AFFILIATES BE LIABLE, WHETHER IN CONTRACT, TORT, WARRANTY OR UNDER ANY STATUTE OR ON ANY OTHER BASIS FOR SPECIAL, INCIDENTAL, INDIRECT, PUNITIVE, MULTIPLE OR CONSEQUENTIAL DAMAGES IN CONNECTION WITH OR ARISING FROM THIS DOCUMENT, INCLUDING BUT NOT LIMITED TO THE USE THEREOF. Corporate Entity: Life Technologies | Carlsbad, CA 92008 USA | Toll free in USA 1.800.955.6288 © 2016 Thermo Fisher Scientific Inc. All rights reserved. All trademarks are the property of Thermo Fisher Scientific and its subsidiaries unless otherwise specified.








**ThermoFisher**  
SCIENTIFIC

10 February 2016

For support visit [thermofisher.com/support](http://thermofisher.com/support)

### Lipofectamine™ 3000 Reagent Protocol

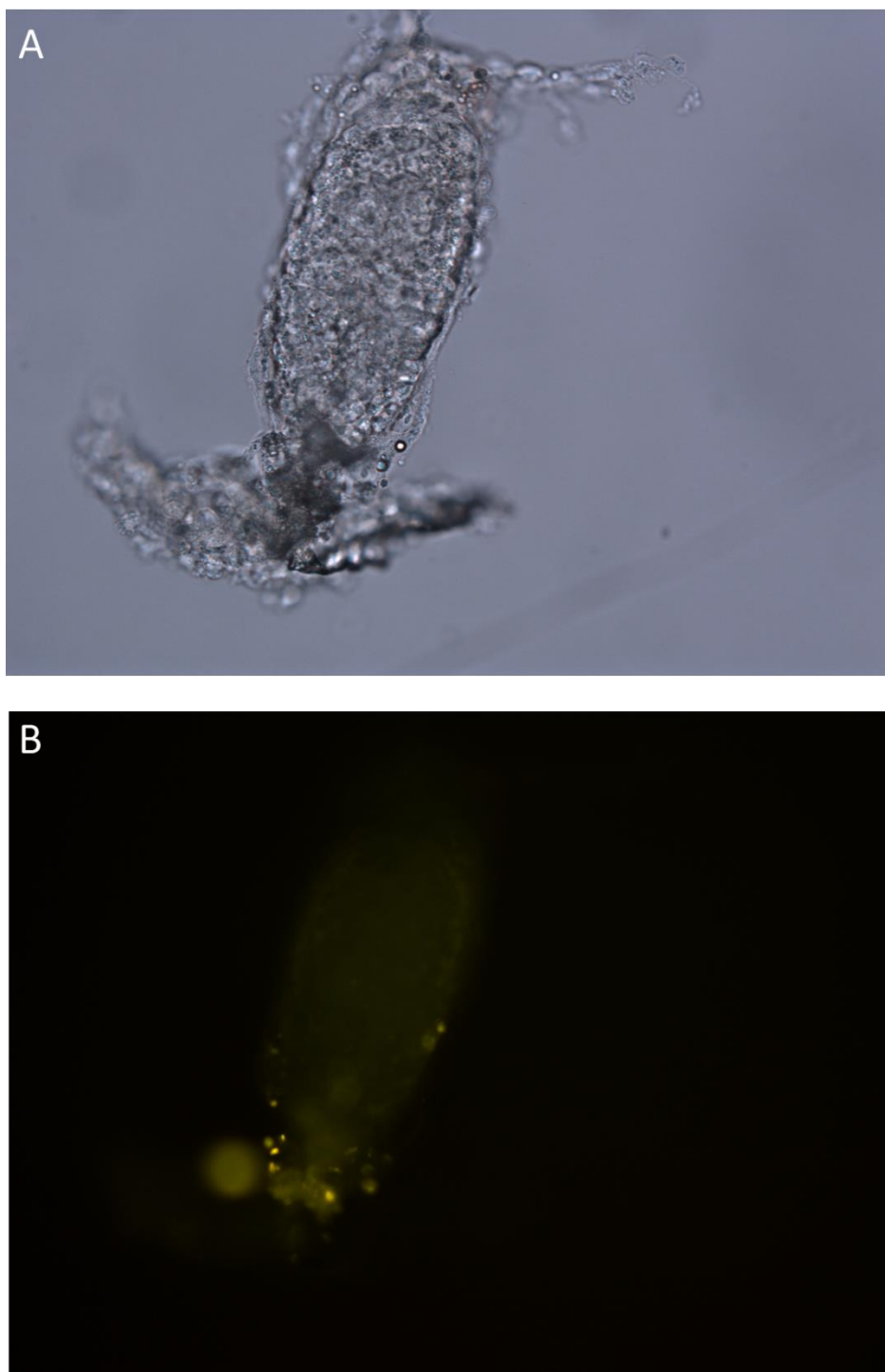
Transfect cells according to the following table. Use the indicated volume of DNA and P3000™ Reagent with each of the two volumes of Lipofectamine™ 3000 (when performing optimization). Each reaction mix volume is for one well and accounts for pipetting variations. Scale volumes proportionally for additional wells.

Timeline		Steps	Procedure Details (Two Reaction Optimization)			
			Component	96-well	24-well	6-well
Day 0	1	 Seed cells to be 70–90% confluent at transfection	Adherent cells	1–4 × 10 <sup>4</sup>	0.5–2 × 10 <sup>5</sup>	0.25–1 × 10 <sup>6</sup>
	2	 Dilute Lipofectamine™ 3000 Reagent in Opti-MEM™ Medium (2 tubes) – Mix well	Opti-MEM™ Medium	5 µL × 2	25 µL × 2	125 µL × 2
			Lipofectamine™ 3000 Reagent	0.15 and 0.3 µL	0.75 and 1.5 µL	3.75 and 7.5 µL
Day 1	3	 Prepare master mix of DNA by diluting DNA in Opti-MEM™ Medium, then add P3000™ Reagent – Mix well	Opti-MEM™ Medium	10 µL	50 µL	250 µL
			DNA (0.5–5 µg/µL)	0.2 µg	1 µg	5 µg
			P3000™ Reagent (2 µL/µg DNA)	0.4 µL	2 µL	10 µL
	4	 Add Diluted DNA to each tube of Diluted Lipofectamine™ 3000 Reagent (1:1 ratio)	Diluted DNA (with P3000™ Reagent)	5 µL	25 µL	125 µL
Day 2–4	5	 Incubate	Diluted Lipofectamine™ 3000 Reagent	5 µL	25 µL	125 µL
			Incubate for 10–15 minutes at room temperature.			
	6	 Add DNA-lipid complex to cells	Component (per well)	96-well	24-well	6-well
Day 2–4			DNA-lipid complex	10 µL	50 µL	250 µL
			DNA amount	100 ng	500 ng	2500 ng
			P3000™ Reagent	0.2 µL	1 µL	5 µL
			Lipofectamine™ 3000 Reagent used	0.15 and 0.3 µL	0.75 and 1.5 µL	3.75 and 7.5 µL
Day 2–4	7	 Visualize/analyze transfected cells	Incubate cells for 2–4 days at 37°C. Then, analyze transfected cells.			

For support visit [thermofisher.com/support](http://thermofisher.com/support)

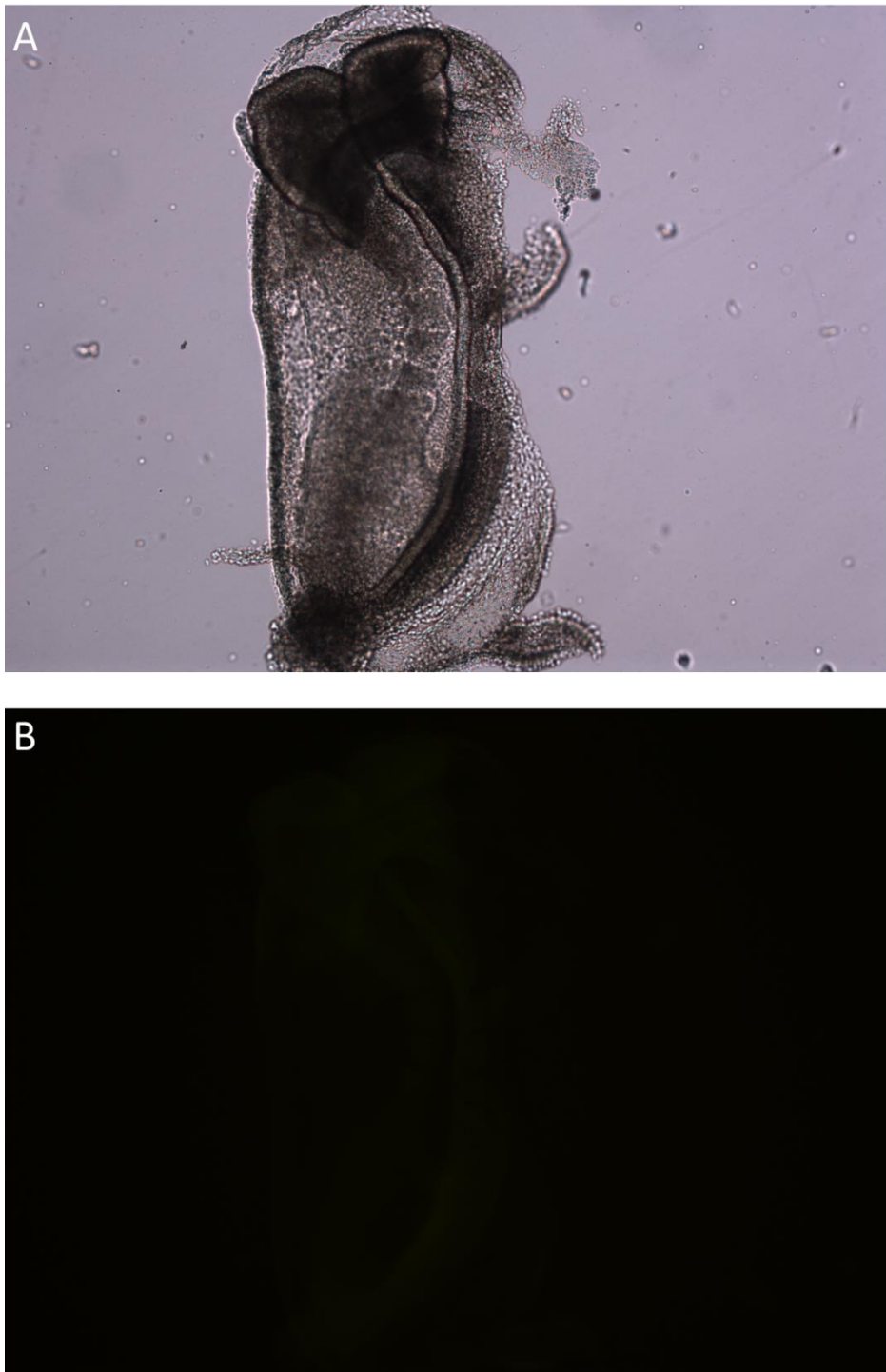


## 6.6 Supplementary embryo microscopy images



**Supplementary Figure 1 E6<sub>4</sub> wt embryo.** Background fluorescence is seen in this wt, day 6 embryo.

Embryo photographed with both bright-field (A) and FITC laser (B) at 5x magnification.



**Supplementary Figure 2 E8.5<sub>3</sub> transgenic embryo.** Background fluorescence, and possibly a low amount of signal in the neural tube is seen in this transgenic, day 8.5 embryo. Embryo photographed with both bright-field (A) and FITC laser (B) at 5x magnification.

## 7 References

- Agathon, Antoine, Bernard Thisse, and Christine Thisse. 2001. "Morpholino Knock-down of *antivin1* and *antivin2* Upregulates Nodal Signaling." *Genesis* 30 (3): 178–82. doi:10.1002/gene.1059.
- Amin, J, J Ananthan, and R Voellmy. 1988. "Key Features of Heat Shock Regulatory Elements." *Molecular and Cellular Biology* 8 (9): 3761–69.
- Beck, Séverine, J. Ann Le Good, Marcela Guzman, Nadav Ben Haim, Karine Roy, Friedrich Beermann, and Daniel B. Constam. 2002. "Extraembryonic Proteases Regulate Nodal Signalling during Gastrulation." *Nature Cell Biology* 4 (12): 981–85. doi:10.1038/ncb890.
- Beddington, Rosa S. P, and Elizabeth J Robertson. 1999. "Axis Development and Early Asymmetry in Mammals." *Cell* 96 (2): 195–209. doi:10.1016/S0092-8674(00)80560-7.
- Bellairs, R. 1986. "The Primitive Streak." *Anatomy and Embryology* 174 (1): 1–14.
- Belo, José António, D. Bachiller, E. Agius, C. Kemp, A.c. Borges, S. Marques, S. Piccolo, and Eddy M. De Robertis. 2000. "Cerberus-like Is a Secreted BMP and Nodal Antagonist Not Essential for Mouse Development." *Genesis* 26 (4): 265–70. doi:10.1002/(SICI)1526-968X(200004)26:4<265::AID-GENE80>3.0.CO;2-4.
- Ben-Haim, Nadav, Cindy Lu, Marcela Guzman-Ayala, Luca Pescatore, Daniel Mesnard, Mirko Bischofberger, Felix Naef, Elizabeth J. Robertson, and Daniel B. Constam. 2006. "The Nodal Precursor Acting via Activin Receptors Induces Mesoderm by Maintaining a Source of Its Convertases and BMP4." *Developmental Cell* 11 (3): 313–23. doi:10.1016/j.devcel.2006.07.005.
- Brennan, J., C. C. Lu, D. P. Norris, T. A. Rodriguez, R. S. Beddington, and E. J. Robertson. 2001. "Nodal Signalling in the Epiblast Patterns the Early Mouse Embryo." *Nature* 411 (6840): 965–69. doi:10.1038/35082103.

- Burt, D. W. 1992. "Evolutionary Grouping of the Transforming Growth Factor-Beta Superfamily." *Biochemical and Biophysical Research Communications* 184 (2): 590–95.
- Chen, Di, Ming Zhao, and Gregory R. Mundy. 2004. "Bone Morphogenetic Proteins." *Growth Factors (Chur, Switzerland)* 22 (4): 233–41.  
doi:10.1080/08977190412331279890.
- Cheng, Simon K., Felix Olale, Ali H. Brivanlou, and Alexander F. Schier. 2004. "Lefty Blocks a Subset of TGF $\beta$  Signals by Antagonizing EGF-CFC Coreceptors." *PLOS Biol* 2 (2): e30. doi:10.1371/journal.pbio.0020030.
- Chen, X., E. Weisberg, V. Fridmacher, M. Watanabe, G. Naco, and M. Whitman. 1997a. "Smad4 and FAST-1 in the Assembly of Activin-Responsive Factor." *Nature* 389 (6646): 85–89. doi:10.1038/38008.
- . 1997b. "Smad4 and FAST-1 in the Assembly of Activin-Responsive Factor." *Nature* 389 (6646): 85–89. doi:10.1038/38008.
- Chen, Y. G., A. Hata, R. S. Lo, D. Wotton, Y. Shi, N. Pavletich, and J. Massagué. 1998. "Determinants of Specificity in TGF-Beta Signal Transduction." *Genes & Development* 12 (14): 2144–52.
- Conlon, F. L., K. M. Lyons, N. Takaesu, K. S. Barth, A. Kispert, B. Herrmann, and E. J. Robertson. 1994. "A Primary Requirement for Nodal in the Formation and Maintenance of the Primitive Streak in the Mouse." *Development (Cambridge, England)* 120 (7): 1919–28.
- CW, Holmes. 2001. "Managing Fertility in the New Zealand Dairy Herd." *Proceedings of the New Zealand Society of Animal Production* 61 (January): 135–40.
- Dennler, S., S. Itoh, D. Vivien, P. ten Dijke, S. Huet, and J. M. Gauthier. 1998a. "Direct Binding of Smad3 and Smad4 to Critical TGF Beta-Inducible Elements in the Promoter of Human Plasminogen Activator Inhibitor-Type 1 Gene." *The EMBO Journal* 17 (11): 3091–3100. doi:10.1093/emboj/17.11.3091.

- Dennler, S, S Itoh, D Vivien, P ten Dijke, S Huet, and J M Gauthier. 1998b. "Direct Binding of Smad3 and Smad4 to Critical TGF Beta-Inducible Elements in the Promoter of Human Plasminogen Activator Inhibitor-Type 1 Gene." *The EMBO Journal* 17 (11): 3091–3100. doi:10.1093/emboj/17.11.3091.
- Derynck, Rik, and Ying E. Zhang. 2003a. "Smad-Dependent and Smad-Independent Pathways in TGF-Beta Family Signalling." *Nature* 425 (6958): 577–84. doi:10.1038/nature02006.
- . 2003b. "Smad-Dependent and Smad-Independent Pathways in TGF-Beta Family Signalling." *Nature* 425 (6958): 577–84. doi:10.1038/nature02006.
- Ding, J., L. Yang, Y. T. Yan, A. Chen, N. Desai, A. Wynshaw-Boris, and M. M. Shen. 1998. "Cripto Is Required for Correct Orientation of the Anterior-Posterior Axis in the Mouse Embryo." *Nature* 395 (6703): 702–7. doi:10.1038/27215.
- Ebisawa, T., M. Fukuchi, G. Murakami, T. Chiba, K. Tanaka, T. Imamura, and K. Miyazono. 2001. "Smurf1 Interacts with Transforming Growth Factor-Beta Type I Receptor through Smad7 and Induces Receptor Degradation." *The Journal of Biological Chemistry* 276 (16): 12477–80. doi:10.1074/jbc.C100008200.
- Feng, Xin-Hua, and Rik Derynck. 2005. "Specificity and Versatility in Tgf-Beta Signaling through Smads." *Annual Review of Cell and Developmental Biology* 21: 659–93. doi:10.1146/annurev.cellbio.21.022404.142018.
- Feng, Xin-Hua, Ying Zhang, Rui-Yun Wu, and Rik Derynck. 1998. "The Tumor Suppressor Smad4/DPC4 and Transcriptional Adaptor CBP/p300 Are Coactivators for Smad3 in TGF- $\beta$ -Induced Transcriptional Activation." *Genes & Development* 12 (14): 2153–63.
- Gardner, R.L. 1983. "Origin and Differentiation of Extraembryonic Tissues in the Mouse." *International Review of Experimental Pathology* Vol. 24: 63–133.

- Green, Michael R., and Joseph Sambrook. 2012. *Molecular Cloning: A Laboratory Manual (Fourth Edition): Three-Volume Set*. 4th edition. Cold Spring Harbor, N.Y: Cold Spring Harbor Laboratory Press.
- Hamada, Hiroshi, Chikara Meno, Daisuke Watanabe, and Yukio Saijoh. 2002. “Establishment of Vertebrate Left–right Asymmetry.” *Nature Reviews Genetics* 3 (2): 103–13. doi:10.1038/nrg732.
- Hayashi, H., S. Abdollah, Y. Qiu, J. Cai, Y. Y. Xu, B. W. Grinnell, M. A. Richardson, et al. 1997. “The MAD-Related Protein Smad7 Associates with the TGFbeta Receptor and Functions as an Antagonist of TGFbeta Signaling.” *Cell* 89 (7): 1165–73.
- Herpin, Amaury, Christophe Lelong, and Pascal Favrel. 2004. “Transforming Growth Factor-Beta-Related Proteins: An Ancestral and Widespread Superfamily of Cytokines in Metazoans.” *Developmental and Comparative Immunology* 28 (5): 461–85. doi:10.1016/j.dci.2003.09.007.
- Hocevar, Barbara A., Abdelkrim Smine, Xiang-Xi Xu, and Philip H. Howe. 2001. “The Adaptor Molecule Disabled-2 Links the Transforming Growth Factor  $\beta$  Receptors to the Smad Pathway.” *The EMBO Journal* 20 (11): 2789–2801. doi:10.1093/emboj/20.11.2789.
- Hoodless, P. A., M. Pye, C. Chazaud, E. Labbé, L. Attisano, J. Rossant, and J. L. Wrana. 2001. “FoxH1 (Fast) Functions to Specify the Anterior Primitive Streak in the Mouse.” *Genes & Development* 15 (10): 1257–71. doi:10.1101/gad.881501.
- Inman, Gareth J., Francisco J. Nicolás, James F. Callahan, John D. Harling, Laramie M. Gaster, Alastair D. Reith, Nicholas J. Laping, and Caroline S. Hill. 2002. “SB-431542 Is a Potent and Specific Inhibitor of Transforming Growth Factor- $\beta$  Superfamily Type I Activin Receptor-Like Kinase (ALK) Receptors ALK4, ALK5, and ALK7.” *Molecular Pharmacology* 62 (1): 65–74. doi:10.1124/mol.62.1.65.

- Inman, G. J., F. J. Nicolas, and C. S. Hill. 2002. "Nucleocytoplasmic Shuttling of Smads 2, 3, and 4 Permits Sensing of TGF-Beta Receptor Activity." *Molecular Cell* 10 (2): 283–94. doi:10.1016/S1097-2765(02)00585-3.
- Itoh, Fumiko, Hironobu Asao, Kazuo Sugamura, Carl-Henrik Heldin, Peter ten Dijke, and Susumu Itoh. 2001. "Promoting Bone Morphogenetic Protein Signaling through Negative Regulation of Inhibitory Smads." *The EMBO Journal* 20 (15): 4132–42. doi:10.1093/emboj/20.15.4132.
- Janknecht, Ralf, Nicholas J. Wells, and Tony Hunter. 1998. "TGF- $\beta$ -Stimulated Cooperation of Smad Proteins with the Coactivators CBP/p300." *Genes & Development* 12 (14): 2114–19. doi:10.1101/gad.12.14.2114.
- Johnson, M.H., and C.A. Ziomek. 1981. "The Foundation of Two Distinct Cell Lineages within the Mouse Morula." *Cell* 24 (1): 71–80. doi:10.1016/0092-8674(81)90502-X.
- Juven-Gershon, Tamar, Susan Cheng, and James T. Kadonaga. 2006. "Rational Design of a Super Core Promoter That Enhances Gene Expression." *Nature Methods* 3 (11): 917–22. doi:10.1038/nmeth937.
- Keeton, M. R., S. A. Curriden, A. J. van Zonneveld, and D. J. Loskutoff. 1991. "Identification of Regulatory Sequences in the Type 1 Plasminogen Activator Inhibitor Gene Responsive to Transforming Growth Factor Beta." *The Journal of Biological Chemistry* 266 (34): 23048–52.
- Labbé, E., C. Silvestri, P. A. Hoodless, J. L. Wrana, and L. Attisano. 1998. "Smad2 and Smad3 Positively and Negatively Regulate TGF Beta-Dependent Transcription through the Forkhead DNA-Binding Protein FAST2." *Molecular Cell* 2 (1): 109–20.



- Lawson, K. A., J. J. Meneses, and R. A. Pedersen. 1991. "Clonal Analysis of Epiblast Fate during Germ Layer Formation in the Mouse Embryo." *Development (Cambridge, England)* 113 (3): 891–911.
- Lee, M. M., and P. K. Donahoe. 1993. "Mullerian Inhibiting Substance: A Gonadal Hormone with Multiple Functions." *Endocrine Reviews* 14 (2): 152–64.  
doi:10.1210/edrv-14-2-152.
- Lin, Xia, Xueyan Duan, Yao-Yun Liang, Ying Su, Katharine H. Wrighton, Jianyin Long, Min Hu, et al. 2006. "PPM1A Functions as a Smad Phosphatase to Terminate TGF $\beta$  Signaling." *Cell* 125 (5): 915–28. doi:10.1016/j.cell.2006.03.044.
- Lo, R. S., Y. G. Chen, Y. Shi, N. P. Pavletich, and J. Massagué. 1998. "The L3 Loop: A Structural Motif Determining Specific Interactions between SMAD Proteins and TGF-Beta Receptors." *The EMBO Journal* 17 (4): 996–1005.  
doi:10.1093/emboj/17.4.996.
- Massagué, J. 1998. "TGF-Beta Signal Transduction." *Annual Review of Biochemistry* 67: 753–91. doi:10.1146/annurev.biochem.67.1.753.
- Massagué, Joan, Joan Seoane, and David Wotton. 2005. "Smad Transcription Factors." *Genes & Development* 19 (23): 2783–2810. doi:10.1101/gad.1350705.
- Menger, Gus J., Gregg C. Allen, Nichole Neuendorff, Sang-Soep Nahm, Terry L. Thomas, Vincent M. Cassone, and David J. Earnest. 2007. "Circadian Profiling of the Transcriptome in NIH/3T3 Fibroblasts: Comparison with Rhythmic Gene Expression in SCN2.2 Cells and the Rat SCN." *Physiological Genomics* 29 (3): 280–89. doi:10.1152/physiolgenomics.00199.2006.
- Ogryzko, V. V., R. L. Schiltz, V. Russanova, B. H. Howard, and Y. Nakatani. 1996. "The Transcriptional Coactivators p300 and CBP Are Histone Acetyltransferases." *Cell* 87 (5): 953–59.

- Perea-Gomez, Aitana, Francis D. J. Vella, William Shawlot, Mustapha Oulad-Abdelghani, Claire Chazaud, Chikara Meno, Veronique Pfister, et al. 2002. "Nodal Antagonists in the Anterior Visceral Endoderm Prevent the Formation of Multiple Primitive Streaks." *Developmental Cell* 3 (5): 745–56.
- Piccolo, S., E. Agius, L. Leyns, S. Bhattacharyya, H. Grunz, T. Bouwmeester, and E. M. De Robertis. 1999. "The Head Inducer Cerberus Is a Multifunctional Antagonist of Nodal, BMP and Wnt Signals." *Nature* 397 (6721): 707–10. doi:10.1038/17820.
- Randall, Rebecca A., Michael Howell, Christopher S. Page, Amanda Daly, Paul A. Bates, and Caroline S. Hill. 2004. "Recognition of Phosphorylated-Smad2-Containing Complexes by a Novel Smad Interaction Motif." *Molecular and Cellular Biology* 24 (3): 1106–21.
- Reissmann, E., H. Jörnvall, A. Blokzijl, O. Andersson, C. Chang, G. Minchiotti, M. G. Persico, C. F. Ibáñez, and A. H. Brivanlou. 2001. "The Orphan Receptor ALK7 and the Activin Receptor ALK4 Mediate Signaling by Nodal Proteins during Vertebrate Development." *Genes & Development* 15 (15): 2010–22. doi:10.1101/gad.201801.
- Rodriguez, Tristan A., Shankar Srinivas, Melanie P. Clements, James C. Smith, and Rosa S. P. Beddington. 2005. "Induction and Migration of the Anterior Visceral Endoderm Is Regulated by the Extra-Embryonic Ectoderm." *Development* 132 (11): 2513–20. doi:10.1242/dev.01847.
- Sakuma, Rui, Yu-ichiro Ohnishi, Chikara Meno, Hideta Fujii, Hou Juan, Jun Takeuchi, Toshihiko Ogura, En Li, Kohei Miyazono, and Hiroshi Hamada. 2002. "Inhibition of Nodal Signalling by Lefty Mediated through Interaction with Common Receptors and Efficient Diffusion." *Genes to Cells* 7 (4): 401–12. doi:10.1046/j.1365-2443.2002.00528.x.

- Schier, A. F., and M. M. Shen. 2000. "Nodal Signalling in Vertebrate Development." *Nature* 403 (6768): 385–89. doi:10.1038/35000126.
- Schier, Alexander F. 2003a. "Nodal Signaling in Vertebrate Development." *Annual Review of Cell and Developmental Biology* 19: 589–621. doi:10.1146/annurev.cellbio.19.041603.094522.
- . 2003b. "Nodal Signaling in Vertebrate Development." *Annual Review of Cell and Developmental Biology* 19: 589–621. doi:10.1146/annurev.cellbio.19.041603.094522.
- Schmierer, Bernhard, and Caroline S. Hill. 2005. "Kinetic Analysis of Smad Nucleocytoplasmic Shuttling Reveals a Mechanism for Transforming Growth Factor Beta-Dependent Nuclear Accumulation of Smads." *Molecular and Cellular Biology* 25 (22): 9845–58. doi:10.1128/MCB.25.22.9845-9858.2005.
- Shaner, Nathan C., Paul A. Steinbach, and Roger Y. Tsien. 2005. "A Guide to Choosing Fluorescent Proteins." *Nature Methods* 2 (12): 905–9. doi:10.1038/nmeth819.
- Shawlot, W., J. M. Deng, and R. R. Behringer. 1998. "Expression of the Mouse Cerberus-Related Gene, Cerr1, Suggests a Role in Anterior Neural Induction and Somatogenesis." *Proceedings of the National Academy of Sciences of the United States of America* 95 (11): 6198–6203.
- Shen, M. M., and A. F. Schier. 2000. "The EGF-CFC Gene Family in Vertebrate Development." *Trends in Genetics: TIG* 16 (7): 303–9.
- Shi, Y., A. Hata, R. S. Lo, J. Massagué, and N. P. Pavletich. 1997. "A Structural Basis for Mutational Inactivation of the Tumour Suppressor Smad4." *Nature* 388 (6637): 87–93. doi:10.1038/40431.
- Shi, Yigong, and Joan Massagué. 2003. "Mechanisms of TGF-Beta Signaling from Cell Membrane to the Nucleus." *Cell* 113 (6): 685–700.

- Shi, Y., Y. F. Wang, L. Jayaraman, H. Yang, J. Massagué, and N. P. Pavletich. 1998a. "Crystal Structure of a Smad MH1 Domain Bound to DNA: Insights on DNA Binding in TGF-Beta Signaling." *Cell* 94 (5): 585–94.
- . 1998b. "Crystal Structure of a Smad MH1 Domain Bound to DNA: Insights on DNA Binding in TGF-Beta Signaling." *Cell* 94 (5): 585–94.
- Stanley, E., C. Biben, S. Kotecha, L. Fabri, S. Tajbakhsh, C. C. Wang, T. Hatzistavrou, et al. 1998. "DAN Is a Secreted Glycoprotein Related to *Xenopus* Cerberus." *Mechanisms of Development* 77 (2): 173–84.
- Sutherland, A. E., T. P. Speed, and P. G. Calarco. 1990. "Inner Cell Allocation in the Mouse Morula: The Role of Oriented Division during Fourth Cleavage." *Developmental Biology* 137 (1): 13–25.
- Tam, P. P., and R. S. Beddington. 1987. "The Formation of Mesodermal Tissues in the Mouse Embryo during Gastrulation and Early Organogenesis." *Development (Cambridge, England)* 99 (1): 109–26.
- Topper, James N., Maria R. DiChiara, Jonathan D. Brown, Amy J. Williams, Dean Falb, Tucker Collins, and Michael A. Gimbrone. 1998. "CREB Binding Protein Is a Required Coactivator for Smad-Dependent, Transforming Growth Factor  $\beta$  Transcriptional Responses in Endothelial Cells." *Proceedings of the National Academy of Sciences of the United States of America* 95 (16): 9506–11.
- Tsukazaki, T., T. A. Chiang, A. F. Davison, L. Attisano, and J. L. Wrana. 1998. "SARA, a FYVE Domain Protein That Recruits Smad2 to the TGFbeta Receptor." *Cell* 95 (6): 779–91.
- Warmflash, Aryeh, Qixiang Zhang, Benoit Sorre, Alin Vonica, Eric D. Siggia, and Ali H. Brivanlou. 2012. "Dynamics of TGF- $\beta$  Signaling Reveal Adaptive and Pulsatile Behaviors Reflected in the Nuclear Localization of Transcription Factor Smad4."

- Proceedings of the National Academy of Sciences of the United States of America* 109 (28): E1947–56. doi:10.1073/pnas.1207607109.
- Weiss, Alexander, and Liliana Attisano. 2013. “The TGFbeta Superfamily Signaling Pathway.” *Wiley Interdisciplinary Reviews. Developmental Biology* 2 (1): 47–63. doi:10.1002/wdev.86.
- Westerhausen, D. R., W. E. Hopkins, and J. J. Billadello. 1991. “Multiple Transforming Growth Factor-Beta-Inducible Elements Regulate Expression of the Plasminogen Activator Inhibitor Type-1 Gene in Hep G2 Cells.” *The Journal of Biological Chemistry* 266 (2): 1092–1100.
- Wu, Jia-Wei, Min Hu, Jijie Chai, Joan Seoane, Morgan Huse, Carey Li, Daniel J. Rigotti, et al. 2001. “Crystal Structure of a Phosphorylated Smad2.” *Molecular Cell* 8 (6): 1277–89. doi:10.1016/S1097-2765(01)00421-X.
- Wu, J. W., A. R. Krawitz, J. J. Chai, W. Y. Li, F. J. Zhang, K. X. Luo, and Y. G. Shi. 2002. “Structural Mechanism of Smad4 Recognition by the Nuclear Oncoprotein Ski: Insights on Ski-Mediated Repression of TGF-Beta Signaling.” *Cell* 111 (3): 357–67. doi:10.1016/S0092-8674(02)01006-1.
- Xu, L., and A. Massague. 2004. “Nucleocytoplasmic Shuttling of Signal Transducers.” *Nature Reviews Molecular Cell Biology* 5 (3): 209–19. doi:10.1038/nrm1331.
- Yagi, Ken, Daisuke Goto, Toshiaki Hamamoto, Seiichi Takenoshita, Mitsuyasu Kato, and Kohei Miyazono. 1999. “Alternatively Spliced Variant of Smad2 Lacking Exon 3 COMPARISON WITH WILD-TYPE Smad2 AND Smad3.” *Journal of Biological Chemistry* 274 (2): 703–9. doi:10.1074/jbc.274.2.703.
- Yamamoto, M., C. Meno, Y. Sakai, H. Shiratori, K. Mochida, Y. Ikawa, Y. Saijoh, and H. Hamada. 2001. “The Transcription Factor FoxH1 (FAST) Mediates Nodal Signaling during Anterior-Posterior Patterning and Node Formation in the Mouse.” *Genes & Development* 15 (10): 1242–56. doi:10.1101/gad. 883901.

- Yeo, Chang-Yeol, and Malcolm Whitman. 2001. "Nodal Signals to Smads through Cripto-Dependent and Cripto-Independent Mechanisms." *Molecular Cell* 7 (5): 949–57. doi:10.1016/S1097-2765(01)00249-0.
- Yeo, C. Y., X. Chen, and M. Whitman. 1999a. "The Role of FAST-1 and Smads in Transcriptional Regulation by Activin during Early *Xenopus* Embryogenesis." *The Journal of Biological Chemistry* 274 (37): 26584–90.
- . 1999b. "The Role of FAST-1 and Smads in Transcriptional Regulation by Activin during Early *Xenopus* Embryogenesis." *The Journal of Biological Chemistry* 274 (37): 26584–90.